IN-02
78062
P- 171

NASA Contractor Report 4432

Improvements to the Missile Aerodynamic Prediction Code DEMON3

Marnix F. E. Dillenius, David L. Johnson, and Daniel J. Lesieutre

NASA

NASA Contractor Report 4432

Improvements to the Missile Aerodynamic Prediction Code DEMON3

Marnix F. E. Dillenius, David L. Johnson, and Daniel J. Lesieutre
Nielsen Engineering & Research, Inc.
Mountain View, California

NASA

National Aeronautics and
Space Administration

Office of Management

Scientific and Technical
Information Program

1992

TABLE OF CONTENTS

IMPROVEMENTS TO THE MISSILE AERODYNAMICS
PREDICTION CODE DEMON3

Marnix F. E. Dillenius
David L. Johnson
Daniel J. Lesieutre

Nielsen Engineering & Research, Inc.

SUMMARY

Computer program DEMON3 was developed for the aerodynamic analysis of nonconventional supersonic configurations comprising a body with noncircular cross section and up to two wing or fin sections. Within a wing or fin section, the lifting surfaces may be in cruciform, triform, planar, or low profile layouts, and the planforms of the lifting surfaces allow for breaks in sweep. The body and the fin sections are modeled by triplet and constant u-velocity panels, respectively, accounting for mutual body-fin interference. Fin thickness effects are included through the use of supersonic planar source panels. One of the unique features of DEMON3 is the modeling of high angle of attack vortical effects associated with the lifting surfaces and the body. In addition, shock expansion and Newtonian pressure calculation methods can be optionally engaged. These two-dimensional nonlinear methods are augmented by aerodynamic interference determined from the linear panel methods. Depending on geometric details of the body, the DEMON3 program can be used to analyze nonconventional configurations at angles of attack up to 25 deg for Mach numbers from 1.1 to 6. Calculative results and comparisons with experimental data demonstrate the capabilities of DEMON3. Limitations and deficiencies are listed.

INTRODUCTION

This final technical report describes the work performed in accordance with Tasks 1, 2, 6, 7, and 8 specified in the Statement of Work under Section C of Contract NAS1-17077, Amendment/Modification No. 17. These tasks are associated directly with the engineering level DEMON3 computer program designed for the aerodynamic analysis of supersonic configurations consisting of a forward fin section and a tail fin section mounted on a body with arbitrary cross section. The initial development of the DEMON3 program was started under Contract No. 1-16469. As a result of the initial findings, certain fundamental problems related to the supersonic panel solutions were defined. Additional tasks to alleviate the problems, to add nonlinear effects of body vorticity, and to extend the range of applicability in terms of Mach number were included in the statement of work referenced above. Specifically, the Contractor performed work to accomplish the following tasks.

Task 1.   Improve the fin-on-body interference account by the incorporation of constant u-velocity panels in the interference shell; retain triplet panels to

model noncircular cross section body-volume and angle-of-attack effects. Apply the improved program to sample cases and to cases for which experimental data are available.

Task 2.   Automate the sequential use of the subprograms by the incorporation of the driver routine designed to manage the step-wise procedure and exchange of data sets including fin vortex characteristics between the subprograms; to the maximum extent possible, simplify program input.

Task 6.   Update DEMON3 as follows: Extend fin pressure calculations to include as an option the combined nonlinear/linear pressure calculation methods; make arrangements for exchanging data sets with NOSEVTX (see below); improve fin thickness routines to handle fins that are not located in radial planes. This task continues and modifies the effort described for Task 1 above.

Task 7.   Join DEMON3 and NOSEVTX to treat a complete configuration consisting of a forward-finned section and a tail-finned section mounted on a body with arbitrary cross sections. Develop an executive routine to manage the stepwise procedure and to organize the exchange of information between module DEMON3 and NOSEVTX. Make comparisons with experimental data. This task will continue and modify the efforts described in Task 2 above.

Task 8.   Validate the methodology developed under the Tasks 1, 2, 6, and 7 by comparison with experimental data. Describe the methodology and results in a final technical report.

The DEMON3 computer program is an improved, extended, and unified version of the earlier DEMON2 set of separate programs for analyzing supersonic monoplane or cruciform wing-body-tail combinations with round or elliptical bodies (Reference 1). During the initial development of program DEMON3 (Ref. 2), it was found necessary to model the finned section, comprising the lifting surfaces attached to the interference shell, with one set of constant u-velocity panels. As described in Reference 2, a convergent solution can not be obtained if the lifting surfaces in the finned section are modeled by constant u-velocity panels and if the interference shell in the same finned section is modeled by source or triplet panels. This fundamental problem appeared to be related to mathematical incompatibilities that prevent convergence in the matrix solution when the number of the two different types of panels is increased. This problem gave rise to Task 1 above.

In the above task descriptions, program NOSEVTX refers to the vortex shedding computer program described in Reference 3. An improved version of program NOSEVTX, designated NOZVTX, is described in Reference 4. The final improved version of the vortex shedding program applicable to bodies with noncircular cross section is designated SUPVTX and is documented in Reference 5. The vortex shedding model employed for the body in DEMON3 makes use of the NOZVTX methodology in Reference 4 with some updates extracted from program SUPVTX of Reference 5.

During the development of the computer DEMON3 program, various portions of its emerging technology were extracted, modified, and/or improved resulting in various engineering level computer programs assembled to accomplish special tasks for NASA, U. S. Navy, and U. S. Army Agencies. A special version was developed for supersonic finned configurations with axisymmetric bodies. The NASA Langley Center version was designated LRCDM2 (Reference 6). The axisymmetric body version was extended to generate bulk force input for NASTRAN structural analysis resulting in the NWCDM-NSTRN program described in References 7 and 8. The NWCDM-NSTRN version can also include effects of steady angular rates in the calculated missile aerodynamic loadings. In addition, the LRCDM2 program was modified and the forebody vortex model improved to treat configurations with wrap-around fins in the AMICDM program (Reference 9). The DEMON3 program, without body vortical effects, was modified and extended to include supersonic inlets for the prediction of aerodynamic characteristics of airbreathing configurations at low angle of attack. This version was designated DM3INL and documented in Reference 10. The inlet modeling scheme, based on triplet panels, was extracted from DM3INL and improved which resulted in a separate module designated INLADD for estimating additive forces and moments associated with supersonic two-dimensional and axisymmetric inlets (Reference 11). Finally, as part of a DEMON3 improvement effort, the SUBSAL program was developed for the Naval Weapons Center with NASA Langley Center as the monitoring agency. Program SUBSAL applies to subsonic configurations consisting of an axisymmetric body with up to two finned sections. This work is documented in Reference 12.

The following sections describe the general approach embodied in program DEMON3, provide some details of the methods of analysis, and provide examples of the results predicted by the program. Limitations in the methodology of the DEMON3 program are discussed. This report includes a section describing the stepwise procedure incorporated in the DEMON3 computer program followed by descriptions of the input, output, and a sample case. Recommendations for improvements are furnished in the concluding section of this report.

LIST OF SYMBOLS

$b/2$	exposed span of a lifting surface. See Figure 5
c	fin local chord
c_n	span load, normal force (lbs)/unit span divided by dynamic head times local chord
C_l	rolling moment coefficient about x_B-axis, positive right fin down, looking forward, moment/$(q_\infty S_{Ref} L_{Ref})$. See Figure 19
C_m	pitching moment coefficient about y_B-axis, nose up positive, moment/$(q_\infty S_{Ref} L_{Ref})$. See Figure 19
C_n	yawing moment coefficient about z_B-axis, nose to right positive, moment/$(q_\infty S_{Ref} L_{Ref})$. See Figure 19
C_N	normal force coefficient along z_B-axis, force/$(q_\infty S_{Ref})$. See Figure 19
C_Y	side force coefficient along y_B-axis, force/$(q_\infty S_{Ref})$. See Figure 19
C_p	pressure coefficient, $(p-p_\infty)/q_\infty$
D	diameter of circular body or equivalent diameter of noncircular body based on cross sectional area
FVN	influence function, velocity component normal to surface induced by panel with unit strength
L	length of body
L_{Ref}	reference length (normally body diameter)
M_∞	free stream Mach number
p	local static pressure
p_∞	free stream static pressure
q_∞	free stream dynamic pressure, $1/2\,(\rho\,V_\infty^2)$
S_{Ref}	reference area (normally body cross sectional area)
u,v,w	axial, lateral, upward perturbation velocity components along body fixed coordinates x_B, y_B, z_B, refer to Figures 2 and 19
V_R	magnitude of resultant velocity
V_∞	free stream velocity
x	axial distance from body nose

x_B, y_B, z_B body fixed coordinate system with origin at nose tip, refer to Figures 2 and 19

x_{CP} axial location of center of pressure

x_{mom} moment center location measured aft of body nose

x_W, y_W, z_W wing coordinate system for a fin set parallel to x_B, y_B, z_B system with origin on body longitudinal axis, x_B, at leading edge of fin set

y_F distance from root chord along span of lifting surface. See Figure 5

α angle of pitch, degrees; impressed normal velocity

α_c included angle of attack, degrees, angle between free stream velocity vector and body longitudinal axis, x_B, refer to Figure 19

ϕ angle of roll, degrees, positive right wing down, refer to Figure 19

Γ vorticity; discrete vortex strength

ρ free stream density

σ panel strength

Subscripts

∞ condition at infinity

B   body

BB   body-on-body

F   fin

FF   fin-on-fin

I   interference shell

II   interference shell-on-interference shell

IF   interference shell-on-fin

FI   fin-on-interference shell

TE   trailing edge

GENERAL APPROACH

The need exists for fast, engineering level aerodynamic prediction methods capable of analyzing nonconventional wing-body-tail configurations. Methods based on experimental data bases are usually limited to geometrically restricted configurations; for example, conventional configurations with axisymmetric bodies and cruciform fin sections. Methods based on high order flow solvers (Computational Fluid Dynamics) contain the proper physics and can handle complex geometries but require substantial computer resources. Nonconventional configurations can be analyzed by panel methods since these methods are applicable to nonaxisymmetric bodies and arbitrary lifting surface layouts. Supersonic (and subsonic) panel methods are derived from the linear potential flow equation. The quality of the solution depends on the level of mathematical sophistication (treatment of boundary condition, treatment of continuity across the panels, etc.) encompassed in the particular panel method. High order panel methods provide the best solutions. However, high order panel methods can require as much computer resources as the simpler of the CFD-based methods, and the results will still be limited to the range of validity of linear theory. In supersonic flow, the best panel solutions can not inherently account for nonlinearities associated with the presence of shocks and vortical effects.

The DEMON3 program described in this report makes use of low order supersonic panel solutions for the sake of economy. In order to increase the usefulness of the code, relatively simple models are incorporated to account for the nonlinear effects of lifting surface wakes and flow separation vortices from the the body which may be noncircular in cross section. The vortex tracking and vortex effects calculations are based on two-dimensional (slender body) concepts and are uncoupled from the three-dimensional paneling analysis. However, the vortical effects are included in the pressure calculations at points on the body and lifting surfaces.

In addition, nonlinear effects of compressibility due to close proximity of shocks to the surfaces of the configuration can be optionally included. This is accomplished by calculating the pressures from the nonlinear two-dimensional shock expansion and Newtonian or impact pressure calculation methods. One of the unique features of DEMON3 is the extension of the two-dimensional nonlinear pressure calculations to include effects of aerodynamic interference obtained from linear theory (the panel solutions).

METHODS OF ANALYSIS

In order to compute pressure distributions, component loads, and overall forces and moments on a supersonic configuration consisting of a body which may have noncircular cross section and with up to two fin sets in various layouts, program DEMON3 makes use of different supersonic panel solutions to model the body and the fin sets. Specifically, the body is modeled by triplet panels developed by Woodward (Ref. 13) as an improvement to the supersonic source panels (Ref. 14). The lifting surfaces and the portion of body next to the lifting surfaces in a fin section are modeled by Woodward's constant u-velocity panels (Ref. 15) for lift on the surfaces and for lift carry-over on the interference shell, and thickness effects are modeled by supersonic planar source panels for thickness also originated by

Woodward (Ref. 14). A modified version of the vortex cloud method including the vortex tracking scheme described in References 4 and 5 is incorporated in DEMON3 to model vortex shedding from the body and to track vorticity down the length of the body. The concentrated multiple vortex wake model for the lifting surfaces as developed for the work reported in Reference 6 (the LRCDM2 computer program) is also incorporated into DEMON3.

Program DEMON3 analyzes a given configuration from the nose to the base in a four (4) step procedure organized by an executive routine. The stepwise procedure is described in a later section describing the DEMON3 computer program. In this process, body-on-lifting surfaces and lifting surfaces-on-body interference as well as vortical interference effects are included. For example, after the body solution is accomplished the effects of all the triplet panels are included in the flow tangency condition applied at points on the lifting surfaces. For each fin section, the strengths of the constant u-velocity panels on the lifting surfaces are obtained from a unified matrix solution which includes the constant u-velocity panels in the interference shell on the body next to the lifting surfaces. In this way, lift carry-over or lifting surface-on-body interference effects are modeled. Further details of the modeling schemes are given below.

Lifting And Volume Panels For The Body

In Reference 1 describing the predecessor (DEMON2) of DEMON3, the body is modeled by a distribution of supersonic source panels on its surface. The source panel models both lift and body volume effects. The particular source panel solution was developed by Woodward and is described in Reference 14. This type of low order body surface paneling generates a multitude of two-dimensional disturbances radiating towards the interior of the body. In the application to long bodies with open bases or to complete closed bodies, the wave-like disturbances reflect back and forth and can cause numerical difficulties in the solution of the source panel strengths especially at low supersonic Mach numbers. As a result, the magnitudes of the resulting panel strengths can be erratic and very high thereby causing the perturbation velocities to be unrealistic at points on and off the body although the flow tangency boundary condition is still satisfied. The distribution of surface pressures based on the velocity components calculated at points on the body can also be erratic and unrealistic. In an effort to remedy this difficulty, Woodward developed the triplet panel which essentially eliminates the two-dimensional portion of the internal waves. The salient features of the triplet panel are summarized next. Details of the solution are given in References 13 and 16.

Triplet Panel Singularity

The triplet panel singularity is a linear combination of source and vortex singularity distributions. Since the vortex (or doublet) sheet may be considered the result of combining, in a special limiting process, two source sheets of equal and opposite strength, the combination of a vortex sheet and a source sheet has been termed a triplet. This superposition is illustrated in Figure 1(a) which shows in the two-dimensional sense that the axial and normal velocity components add in the flow field above the panel, but cancel exactly below the panel, resulting in the desired unidirectional perturbation velocity field. The triplet panel models lift and body volume effects.

As described in References 13 and 16, the extension of the above two-dimensional unidirectional concept to a body having arbitrary cross section requires a triplet panel grouping of six (6) panels in which the vortex loops are closed. A typical example is indicated in Figure 1(b). Depending on the orientation, the panels within a grouping are designated axial, circumferential, and radial triplets. The references show various pressure distributions calculated with the new triplet panel approach and by the original source panel solutions. In most cases, the erratic behavior of the original source distribution especially near the base of the bodies has been eliminated.

In the application to bodies, the triplet panel solution originally set up by Woodward made use of the simplifications associated with the assumption of a vertical plane of symmetry with regard to both geometry and the oncoming flow. In the DEMON3 program, the symmetry built into the triplet solution with regard to the oncoming flow had to be relaxed in order to handle nonzero roll angle. This was accomplished by modifying the subroutines of a later version of Woodward's USSAERO code which includes the triplet panel update. The original version of the USSAERO code for subsonic and supersonic analysis of aircraft configurations is described in Reference 17.

Flow Tangency Condition On The Body

The strengths of the triplet panels used to model the body of a complete configuration are obtained from the set of simultaneous equations that are the result of applying the flow tangency condition at the control points of the triplet panel. The control points are located at the centroids of the individual triplet panel areas. One control point is shown in Figure 1(b). At a given control point, the velocity component normal to the plane of one triplet panel induced or influenced by another triplet panel of unit strength is expressed in terms of the influence function FVN. As mentioned earlier, the solution and thus the influence per unit strength of a triplet panel involves groupings of six (6) panels. In matrix notation, the flow tangency condition can be written as

$$[FVN_{BB}] \, [\sigma_B] = [\alpha_B] \tag{1}$$

where subscript BB denotes body-on-body triplet panel influence, each row in the matrix FVN represents the sum of the influences per unit strength of all the triplet panels at the control point of one panel, vector $[\sigma_B]$ contains the strengths of the panels, and vector $[\alpha_B]$ contains the set of impressed velocities at the control points.

In program DEMON3, the impressed normal velocities depend on the free stream and the panel inclination angle.

Lifting And Thickness Panels For The Fin Section

A typical fin section made up of cruciform fins on an axisymmetric body is shown in Figure 2. As stated earlier, program DEMON3 is not limited to this conventional layout and the following discussion pertains to nonconventional layouts with nonaxisymmetric body cross sections as well.

The lifting surfaces and the interference shell indicated in Figure 2 are covered by constant u-velocity panels originally called constant pressure panels by Woodward and described in Reference 14. These panels model the lift effects and are positioned in the chordal planes of the lifting surfaces. Therefore, the constant u-velocity panel method is not a surface paneling method.

In addition, thickness effects of the lifting surfaces are modeled by a layout of supersonic planar source panels. In the DEMON3 program, the spanwise layout of the source panels is the same as for the lifting constant u-velocity panels. However, in order to resolve streamwise thickness effects, the chordwise layout is normally more dense. The strength of a source panel is directly related to the local thickness slope of the lifting surface.

Constant U-Velocity And Source Singularities

The particular singularity solution of the constant u-velocity panel is one for generating lift in supersonic flow. This means that the axial and lateral velocities immediately above and below the panels are equal and opposite in sign. The normal component induced by the panel is continuous across the plane of the panel and is made to counteract the impressed normal velocity.

The source panel singularity has continuous axial and lateral velocity components immediately above and below its plane. The normal velocity component is continuous across the plane of the source panel. The source panel strengths are directly related to the local thickness slope.

A detailed description of the two types of panel solutions and the particular solutions in the respective panel planes are listed in Appendix II of Reference 18.

Flow Tangency Condition On The Lifting Surfaces

The flow tangency condition is applied at the control points of the constant u-velocity panels on the lifting surfaces and on the interference shell. Two control points are indicated in Figure 2.

On the lifting surfaces, the impressed velocity in the flow tangency condition includes a contribution from the free stream, body-induced flow (upwash), and effects of external vortices from the upstream fin section (if applicable) and the body. The constant u-velocity panels on the lifting surfaces interact with the constant u-velocity panels on the interference shell. In this way, lift carry-over effects are included. On the interference shell around the body, the impressed velocity is due to lifting surface thickness only. All other impressed velocities are included in the triplet panel solution for the body as described in an earlier section.

The velocity component induced by one constant u-velocity panel of unit strength normal to the plane of another panel at its control point is the influence function FVN. The boundary condition can be expressed in matrix notation as follows:

$$\begin{bmatrix} FVN_{FF} & FVN_{IF} \\ FVN_{FI} & FVN_{II} \end{bmatrix} \begin{bmatrix} \sigma_F \\ \sigma_I \end{bmatrix} = \begin{bmatrix} \alpha_F \\ \alpha_I \end{bmatrix} \qquad (2)$$

In the above expression, subscript FF denotes one constant u-velocity panel on a lifting surface influencing another panel on the same or other lifting surface, subscript II refers to one panel on the interference shell influencing another panel on the interference shell, subscript FI means one panel on a lifting surface influencing a panel on the interference shell, and subscript IF relates to one panel on the interference shell influencing a panel on a lifting surface. Vector $[\sigma]$ contains the strengths of the constant u-velocity panels on the lifting surfaces and the interference shell in a fin section. Vector $[\alpha]$ represents the set of impressed velocities enumerated above. Note that $[\alpha_I]$ is zero unless the thickness effects of the lifting surfaces are included.

Body Vorticity Model

The body vorticity model incorporated in program DEMON3 is nearly identical to the engineering level vortex shedding prediction method described in Reference 4. One of the differences is the replacement of the source panels by triplet panels for the inviscid modeling of the body. In addition, information including vortex strengths and positions as well as body forces and moments are exchanged between the body vorticity routines and the fin section routines.

In short, the body is represented by the supersonic triplet panel method (as described in an earlier section), and the leeside vortex wake is modeled by discrete vortices in cross flow planes. The three-dimensional steady flow problem is reduced to a two-dimensional, unsteady, separated flow problem for solution which makes use of conformal mapping schemes to transform noncircular body cross sections to a circular contour. The predicted pressure distribution on the body under the influence of free stream and the body separation wake is used to calculate the body loads. The effects of the body separation wake are included in the analysis of the fin section. A typical example of the vortex patterns on a 3:1 elliptic body is shown in Figure 3, taken from Reference 4, for zero and 45 deg roll angles, respectively.

Bernoulli Pressures, Forces And Moments

The calculations of pressure at points on the body and at points on the fin sets are based on the compressible Bernoulli pressure/velocity relationship. Due to the presence of vortices on the body when the angle of attack is sufficiently high, the formulation of the pressure equation for the body is somewhat different than that employed on the fin set. Details of either pressure calculation are available in Reference 4 and in Reference 6 for the body and for the fin sets, respectively. For the sake of completeness, the pressure calculation methods are summarized below.

Pressures On The Body

The following pertains to the section(s) of the body which are not part of the fin sets of a complete wing-body-tail configuration. Circumferential pressure distributions are required at many axial stations along the body in order to calculate the contributions to the overall aerodynamic forces and moment acting on the complete configuration. The pressure distributions on the body sections also determine the flow separation points in the cross flow planes. At each axial station, the pressures are calculated at 73 points placed at equal angular intervals on the body contour. The Bernoulli equation is written in the following pressure coefficient form where $\gamma = 1.4$ for air.

$$C_P = \frac{p - p_\infty}{\frac{1}{2}\,\rho V_\infty^2} = \frac{2}{\gamma M_\infty^2}\left\{\left[1 + \frac{\gamma-1}{2}\,M_\infty^2(C_{P_I}]^{\frac{\gamma}{\gamma-1}} - 1\right\}\right. \tag{3}$$

The incompressible contribution C_{P_I} is given by the following expression.

$$C_{P_I} = 1 - \left[\frac{U}{V_\infty}\right]^2 - \frac{2\cos\alpha_c}{V_\infty}\frac{d\phi}{dx} \tag{4}$$

In the above, U is the total velocity including free stream at a point on the body. In the calculation of this total velocity, the axial and lateral perturbation velocity contributions from the triplet panels (modeling body lift and volume effects) are included. The lateral velocity contributions from the external vortices, composed of the wake vortices from the upstream fin set and the body shed vortices, are added to the body-induced velocities. The last term in Equation 4 represents the axial velocity component induced by the external vortices by virtue of their inclination relative to the body centerline. The details of this contribution to the axial flow component are given in Reference 4 which shows that this component is related to the coordinates of the vortices in successive cross flow planes. Since the pressure coefficient as expressed in the above formulations depends on velocity components obtained from linear theory, it is possible that local pressures lower than free stream static pressure are calculated. Therefore, the calculated pressure coefficients are limited to the free stream value as follows ($\gamma = 1.4$ for air).

$$C_P\bigg|_{min} = \frac{p - p_\infty}{\frac{1}{2}\,\rho V_\infty^2} = -\frac{2}{\gamma M_\infty^2} \tag{5}$$

It is worth noting here that the vortex tracking and vortex-induced effects calculations are based on slender body theory (for example, two-dimensional doublets). This means that apart from the separation point determination procedure, the three-dimensional body flow model (the triplet panel solution for the body at angle of attack) and the fin set flow model (the constant u-velocity panel and thickness panel solutions) do not take part in the vortex tracking calculation. The exception is the axial velocity component from the body volume effects (zero angle of attack triplet solution) which is included in the vortex tracking procedure. In that procedure, the vortices are made to follow the streamlines associated

with the flow which includes all upstream effects. In this way, the vortex model is essentially uncoupled from the panel method modeling scheme for the body. On the fin set, the effects of the vortices are included in the flow tangency boundary condition as described below.

The individual aerodynamic force coefficients are obtained by multiplying the pressures calculated by the method above times the appropriate areas on the body surface. The individual moment coefficients are calculated by multiplying the individual force coefficients by the appropriate moment arms. The total body contributions to the overall force and moment coefficients are then obtained from the sums of the individual force and moment coefficients.

Pressures On the Fin Set

The pressures are calculated immediately above and below the plane of the constant u-velocity panels at the individual panel area centroids. These panels are distributed on the lifting surfaces and on the interference shell in the fin set. On the interference shell, the pressures are calculated on the exterior of the panels only.

The Bernoulli pressure/velocity relationship used in the fin set is given by the following expression in terms of the resultant velocity V_R ($\gamma = 1.4$ for air).

$$C_p = \frac{p - p_\infty}{\frac{1}{2} \rho V_\infty^2} = \frac{2}{\gamma M_\infty^2} \left\{ \left[1 + \frac{\gamma - 1}{2} M_\infty^2 \left[1 - \frac{V_R^2}{V_\infty^2} \right] \right]^{\frac{\gamma}{\gamma-1}} - 1 \right\} \quad (6)$$

The resultant velocity ratio is given by

$$\frac{V_R^2}{V_\infty^2} = 1 + \frac{2u}{V_\infty} \cos\alpha_c - \frac{2v}{V_\infty} \sin\alpha_c \sin\phi + \frac{2w}{V_\infty} \sin\alpha_c \cos\phi + \frac{u^2 + v^2 + w^2}{V_\infty^2} \quad (7)$$

where α_c is the included angle of attack and ϕ is the angle of roll related to the the pitch-roll definition for angle of pitch and side slip (refer to Ref. 6, Equation (3)). The perturbation velocities u, v, w induced by the body, lifting surface, and interference panel methods can be unduly large in magnitude and cause the term in the square brackets in Equation (6) to become negative. In such cases, the pressure coefficient is limited to the value given by Equation 5 shown above. In program DEMON3, therefore, the pressures calculated from the panel solutions with the Bernoulli expressions are nonlinear in terms of angle of attack by virtue of its formulation and the imposed limiting value.

The perturbation velocities u, v, and w included in the pressure calculation at points in the fin set (Eqs. 6 and 7) are made up of contributions from the body triplet panels, the constant u-velocity panels and thickness panels on the lifting surfaces, the interference shell of the fin set, and from the vortices generated by the upstream body section and fin set if applicable. In this procedure, the vortices are "frozen" at the leading edge of the fin set

(actually the axial station corresponding to the leading edge of the fin rootchords). This means that at the leading edge position, the vortices are considered as two-dimensional point vortices with known strengths and positions calculated by the tracking scheme. This is equivalent to assuming the vortex paths to be parallel to the body centerline through the fin set section. This is in contrast to the vortex tracking scheme in the DEMON2 program of Reference 1 in which the vortices are tracked through the fin set section. It was found in later developments that the DEMON2 tracking approach adds complications without necessarily increasing accuracy.

Special care has to be taken in the calculation of the lifting surface panel contributions to the perturbation velocities used in the pressure calculations immediately above and below the surfaces of the lifting surfaces. Because of the planar (non-surface panel) nature of both the constant u-velocity and the thickness (or source panel solutions), the DEMON3 program has to determine the proper values of the panel-induced velocities immediately above and below the panel planes.

In the fin set pressure calculations, the external vortices (assumed to run parallel to the body centerline through the fin set section) only induce lateral (v, w) velocity components. It should be noted, however, that the lateral velocities induced by the vortices are included in the flow tangency condition applied at the control points of the constant u-velocity panels distributed on the lifting surfaces as described in an earlier section. Therefore, the constant u-velocity panels under the influence of the vortices will induce u, v, w velocity components which reflect the presence of vortices to first approximation. This approximate approach is successfully employed in the various derivations of the DEMON3 program (Refs. 6-9, 12) as well as in other aerodynamic interference prediction methods based on the equivalent angle of attack approach.

The force and moment calculations are performed in essentially the same manner as used on the body with the exception that the areas over which the pressures act are the actual constant u-panel areas.

Shock Expansion And Newtonian Pressure Calculations

As an option, program DEMON3 can calculate pressures on both the body and the lifting surfaces based on two-dimensional shock expansion and Newtonian theories. The designation two-dimensional means that these nonlinear pressure calculations are performed along meridians of the body and along chordwise strips on the lifting surfaces. The optional pressure calculation methods are applicable to configurations at high Mach numbers (in excess of approximately Mach 2.5 up to Mach 6). The Newtonian method is implemented in DEMON3 in its simplest form and assumes zero pressure for any "shaded" portion of the configuration. It should only be applied to configurations for which the Mach number is in excess of 5.

The shock expansion calculations are based on the assumption of attached shocks, and the strip theory approach used in DEMON3 is general as opposed to second order. In the general shock expansion theory, the pressure is constant along a segment of a strip. In second order theory, the pressure varies along the segments of the strip. The validity of general shock expansion versus second order depends on the hypersonic similarity

parameter. This parameter is the ratio of free stream Mach number over fineness ratio. If this ratio is much larger than one (high Mach number), general shock expansion theory is valid. If the ratio is about one, second order theory should be used.

In programs such as DEMON3 and its derivatives based on either low order panel or line singularities to model the body, linear theory requires that the Mach cone attached to the body nose lie outside the body meridional contour as modeled by the respective programs. This requirement can be violated in any case when the body nose is blunt and/or when the free stream Mach number is high for all but the sharpest body noses. This problem can be circumvented by reducing the body slopes near the nose. When this user arranged procedure is used, the pressures (Bernoulli, as well as the shock expansion and Newtonian) near the nose will be underpredicted, however.

The unique feature of the shock expansion and Newtonian pressure calculation methods in DEMON3 is the inclusion of an approximate scheme to correct the nonlinear pressures for strip-on-strip, fin-on-fin, mutual body-fin, and vortical aerodynamic interference effects. In fact, the interference on the flow deflection angles is obtained from the panel solutions (linear theory) and the vortical induced effects. The modified flow deflection angles are used in the nonlinear shock expansion and Newtonian pressure coefficient calculations. This engineering level procedure was originated by Carlson (Ref. 18) and first implemented in the LRCDM2 program (Ref. 6). The actual formulations of the nonlinear pressure calculation methods and the corrections to the flow deflection angles are described in detail in the main body and in Appendix D of Reference 6. A summarized account is provided in Reference 19. In the LRCDM2 program, the methodology is really applicable to the lifting surfaces only because analytical tangent wedge (oblique shock) solutions are incorporated for the pressures and local Mach number immediately behind the shock on the leading edge. The LRCDM2 program can also calculate shock expansion and Newtonian pressure as an option on the axisymmetric forebody. However, the analytical tangent wedge (oblique shock) expressions are used to compute pressure at the nose tip as a first approximation instead of using the proper tangent cone values which are not available in exact analytical form. This limitation has been relaxed somewhat in the DEMON3 program by the inclusion of approximate tangent cone relationships. The procedure and specific shock cone relationships used in program DEMON3 are enumerated below.

Tangent Cone Relationships Used In DEMON3

In program DEMON3, the optional shock expansion and Newtonian pressure calculation method including the flow deflection angle corrections are applicable to the forebody which may be noncircular in cross section. The geometric layout scheme in DEMON3 establishes the meridional strips and the axial stations from the body nose to the forward fin set at which the optional pressure calculations will be performed. At the beginning or leading edge of each strip (at the body nose), the analysis assumes the strip under consideration to be part of an axisymmetric cone and independent from the other strips around the body. For each strip at the body nose, the shock expansion analysis requires values of shock detachment angle (in order to determine if the analysis can proceed), Mach number normal to the shock, cone surface Mach number, cone surface pressure, and ratio of stagnation pressure across the shock. These parameters are not available in exact analytical form as is the case for the tangent wedge case. One possibility is

to incorporate data bases or to employ approximate relationships. The present version of DEMON3 uses various expressions that approximate the tangent cone shock parameters.

The shock detachment angle and the cone surface Mach number immediately behind the shock are determined using the approximate solutions developed by Hammitt and Murthy and described in Reference 20. These approximate solutions are based on Taylor series expansions for the velocities between the cone shock and body and involve the body cone half angle, free stream Mach number, and shock angle. The value of the Mach number normal to the shock and the cone surface pressure are obtained from the tangent cone approximations modified by Edwards and specified in the appendix of Reference 21. These approximations are based on previously developed empirical representations and involve the flow deflection angle and free stream Mach number. In program DEMON3, the approximate tangent cone relationships are programmed in subroutine SHKXB.

Lifting Surface Wake Vortex Model

In the DEMON3 program, the wake at the trailing edges of the lifting surfaces or fins in a fin set is represented by a set of discrete vortices. In addition to the trailing edge vorticity related to attached flow, the wake model includes leading and side edge vortices which develop and dominate the fin wakes as the angle of attack is increased. For lifting surfaces with long side edges, vorticity can be generated along the edge for angles of attack as low as 5 deg. A typical fin wake model as generated by the program is depicted in Figure 4 which shows the trailing edge vortex (more than one can exist) and the combined leading and side edge vortex which is elevated from the fin plane. These vortices are included in the tracking scheme that is part of the body vortex shedding model described in an earlier section. Therefore, the fin wake vortices influence the body vortex shedding process along the afterbody as well as the loads acting on the tail fin set.

The actual wake model used in DEMON3 is nearly identical to that of the LRCDM2 program (Ref. 6), and a summarized description is also available in Reference 19. The only difference in the wake model is related to the attached flow vortices as described below.

Updated Trailing Vortex Model For Attached Flow

As described in References 6 and 19, the trailing edge vorticity Γ_{TE} associated with attached flow on the lifting surface can be related to the span loading c_n as follows (c is local chord).

$$\frac{1}{V_\infty} \frac{\partial \Gamma_{TE}}{\partial y_F} = -\frac{1}{2} \frac{\partial}{\partial y_F} (cc_n) \qquad (8)$$

The cited references contain the analytical expressions derived from the above differential equation on the basis of only one extremum in the span load distribution. An example is shown in Figure 5 for a delta fin on a body and under the influence of an external vortex. In actuality, the span loading may exhibit multiple extrema depending on the oncoming flow and possibly the particular fin-on-body attachment when the body is noncircular. Therefore, the integration of Equation (8) was extended to account for multiple extrema.

The strengths and positions of the wake vortices are calculated in subroutine SPNLD of program DEMON3.

RESULTS

This section presents results calculated with the DEMON3 aerodynamic prediction program. Results have been obtained for a variety of configurations. Comparisons are made between DEMON3 results, experimental results, and results from other prediction programs and theory for the purpose of validation and verification. The first comparison is for a conventional missile configuration with a round body and cruciform canard and tail fin sections (Ref. 22). The second and third configurations are monoplane wing and tail configurations with noncircular bodies (Refs. 23 and 24). Finally, the shock expansion option in the code is exercised and compared with data for a rectangular wing (Ref. 25) and for an ogive cylinder body (Ref. 26).

Cruciform Canard Control, Cruciform Tail Configuration

Comparisons of measured and predicted characteristics of a canard-body-tail model are described in this section. The configuration is the canard-controlled wind tunnel model described in Reference 22 and depicted at the top of Figure 6. The body is a 2.25-caliber ogive nose followed by a 21.9-diameter cylindrical body. The canard fins have an aspect ratio of 2.00, a taper ratio of 0.30, and a body radius to fin semispan ratio of 0.226. The canard leading edge is located 3.73 diameters aft of the nose tip. The tail fins under consideration have an aspect ratio of 1.06, a taper ratio of 0.58, and a body radius to fin semispan ratio of 0.19. The tail fins are located 12.7 diameters aft of the canard trailing edge. Overall loads on the model at several supersonic Mach numbers are available, but only results for $M_\infty = 2.5$ are presented here.

Measured and predicted longitudinal aerodynamic characteristics are indicated in Figure 6 for the canard-body-tail model shown at the top of the figure at zero roll angle. Figure 7 shows the measured and predicted lateral directional aerodynamic characteristics. The Mach number is 2.5. The right and left horizontal canard fins are deflected +5 deg and -5 deg, respectively, for right wing up (negative) roll control. In addition to the DEMON3 predictions, results are included from the SUPDL program (designated NWCDM-NSTRN in Ref. 8). Program DEMON3 models the body of the configuration with supersonic triplet panels, whereas program SUPDL makes use of linearly varying supersonic line sources/sinks and doublets. Both programs employ the same fin set modeling method, and both include models to account for the nonlinear effects of body vorticity and fin wakes as described in earlier sections. In Figures 6 and 7, SUPDL results are shown with (w/BDYSHD) and without vortex shedding from the length of body between the canard and tail fins. All DEMON3 results include body vortex shedding.

The normal force and pitching moment coefficients shown in Figure 6 exhibit some nonlinearity with angle of attack. All three predictions shown in Figure 6 show the same nonlinear trend due to the inclusion of the fin wake effects. Body vortex shedding has negligible influence in the longitudinal charateristics. In general, the DEMON3 results agree best with the experimental data.

The yawing moment, side force, and rolling moment coefficients shown in Figure 7 are small compared with the longitudinal characteristics. The rolling moment behavior is of major interest, however. Experimental data for the rolling moment acting on the configuration with the tail section removed are also shown in the bottom portion of the figure. For the complete configuration at low angles of attack, the canard rolling moment (tail off) is counteracted by the rolling moment induced by the canard wake on the tail fins resulting in near zero overall rolling moment. As the angle of attack is increased, this adverse effect disappears. Above about 10 deg angle of attack, the magnitude of the overall rolling moment is higher than the canard fin alone (or tail off) value. At angles of attack in excess of 15 deg, the overall rolling moment returns to the canard alone value up to canard fin stall condition resulting in zero rolling moment. The DEMON3 and SUPDL predictions match the tail off value. The nonlinear trends of the overall rolling moment are predicted fairly well by the DEMON3 and SUPDL codes provided body shedding is included in the latter. The lines associated with the predictions connect points calculated at 5 deg intervals in angle of attack.

Mid Monoplane Wing and Tail Configuration

This section presents comparisons for the monoplane wing and tail model of Reference 23 depicted in Figure 8. The body of the configuration is nearly circular over the ogive nose and transitions to an elongated (vertical) circular section on the forebody. Before the wing leading edge, the cross section transitions to a circular bottom and square top. Over the wing root chord, the cross section transitions back to an elongated (vertical) circle and maintains this shape to the base. Tails are located at the rear of the configuration.

Comparison between measured and predicted results for $M_\infty = 1.6$ is shown in Figure 9. Results are also included from preliminary analysis and design programs MISL3 (Ref. 27) and Missile DATCOM (Ref. 28). For MISL3 and Missile DATCOM, a circular body has been used. The normal force coefficient is predicted well by all the programs, Figure 9(a). Program DEMON3 predicts the pitching moment well for angles of attack up to ten degrees, Figure 9(b). Above ten degrees the pitching moment may be in error because of wing and/or tail fin stall. DEMON3 does not currently include a stall model. The MISL3 and Missile DATCOM programs do not predict the pitching moment indicated by the experimental data. Note that for this configuration, the pitching moment from the nose and tail fins counteract one another; therefore, the pitching moment is sensitive to the wing center of pressure. The wing is large but located near the moment center; therefore, an error in the wing center of pressure can have a large effect on the pitching moment.

There are several possible reasons why MISL3 and Missile DATCOM do not predict the correct pitching moment: the wing center of pressure is not predicted correctly and/or the effect of the noncircular body affects the pitching moment (not modeled by MISL3 and Missile DATCOM). The body cross section grows from an elongated (vertical) circle to a circular bottom with a square top cross section before the wing leading edge. Over the wing root chord section it transitions back. This transition back to the elongated (vertical) circle accelerates the flow over the top portion of the body and wing. This accelerated flow affects the wing load, load distibution, and hence pitching moment. MISL3 and Missile DATCOM

do not include this effect. The triplet panel body model in DEMON3 models the effects of the actual body shape.

The measured and predicted locations of the configuration center of pressure (measured from the moment center and referenced to the mean aerodynamic chord of the wing) are shown in Figure 9(c). DEMON3 predicts the center of pressure location well for this configuration.

Comparison between measured and predicted results for $M_\infty = 2.0$ is shown in Figure 10. The DEMON3 results overpredict the normal force and pitching moment at the higher angles of attack for this Mach number. This may be due to wing and/or tail fin stall which is currently not modeled by the program. Less wing and/or tail fin normal force would reduce both the overall normal force and pitching moment.

High Monoplane Wing Tri-tail Configuration

Comparisons of DEMON3 with predicted results from a modified version of the MISL3 program for the Pegasus[TM] launch vehicle (Ref. 24) are described in this section. The configuration consists of a circular cross section forebody which transitions to noncircular cross section ahead of the high wing. The noncircular body shape extends aft of the wing trailing edge. The body transitions back to circular before the tri-tail configuration. There are two horizontal tail fins and one vertical fin. This configuration is depicted in Figure 11.

Overall pitch plane loads on the model at $M_\infty = 2.0$ are shown in Figure 12 with and without 10 deg of horizontal tail deflection. The DEMON3 predicted normal force and pitching moment coefficients agree well with those obtained with a modified version of the MISL3 program. The effect of deflection also agrees well. One of the advantages of the DEMON3 program is its capability of providing aerodynamic force distributions which can be incorporated in a structural analysis.

Shock Expansion and Newtonian Theory Applications

In this section, two examples are discussed of shock expansion and Newtonian pressure calculations including interference corrections. The first example involves a rectangular wing alone, the second example is concerned with an ogive cylinder body.

Rectangular Wing

Pressure distributions are available (Ref. 25) for the beveled, aspect ratio 2, rectangular wing shown in Figure 13. The figure shows the pressure tap locations and the panel layout on one-half of the wing for the calculations referred to below. The chordwise pressures measured on the upper and lower surfaces at the one-half semispan location of the wing are shown in Figure 14. The angle of attack is 10.3 deg and the Mach number is 2.86. The figure shows the strong effects of the beveled portions of the wing as indicated by the experimental data.

Comparisons between results calculated by the LRCDM2 program and the experimental data are shown in References 6 and 19. The purpose of the comparisons

shown in Figure 14 between the DEMON3 results and the experimental data is to ascertain that the optional nonlinear pressure calculation methods perform properly in the DEMON3 program. The methods for the wing pressures in DEMON3 are essentially the same as in LRCDM2 with the exception of an improvement in the determination of the panel-induced velocities immediately above and below the plane of the panels. It is worth noting that the LRCDM2 program can handle a wing alone. The present version of the DEMON3 program requires the presence of a small body in "wing alone" calculations.

The linear theory results generated by the DEMON3 program are based on a 10 chordwise by 10 spanwise layout of constant u-velocity panels to model lift, and the same layout of source panels used to model the thickness envelope. The shock expansion and Newtonian analyses make use of 10 chordwise strips with 10 segments in each. A length of body with radius equal to the wing thickness is placed on the root chord. The results labeled "linear" are based on the panel solutions (linear theory) and the compressible Bernoulli pressure expression (Eq. 6). The results labeled "shock expansion, corrected" are based on the shock expansion theory with flow deflection angles corrected for strip-on-strip interference by the panel solutions as summarized in an earlier section. The results labeled "Newtonian, corrected" are based on the simple impact theory method ($C_P = 2 \sin^2 \delta$, $C_P = 0.0$ for shaded areas) with the flow deflection angle δ corrected by the panel solutions.

Because of the presence of the strong oblique shock attached to the leading edge, the linear result underestimates the pressure coefficients on the upper and lower surfaces of the wing. The corrected shock expansion results are in good agreement in the region near the leading edge. This case is representative of nonlinear compressibility influencing the pressures due to the close proximity of the leading edge shock to the wing surfaces. Over the flat portion, the linear and shock expansion methods agree well with the experimental data. On the beveled trailing edge, the linear and corrected shock expansion method predict lower than measured pressure on the upper (suction) surface. As mentioned in References 6 and 19, this is most likely due to boundary layer separation effects. On the lower (windward) side, the corrected shock expansion method matches the experimental data better. The corrected Newtonian result severely underestimates the pressures on the lower surface, and the pressures are zero on the upper surface. The Mach number in this case is too low for application of the Newtonian pressure method.

In this example, the correction to the flow deflection angles is minimal due to the two-dimensional flow character in the midspan region of the rectangular wing. The basic strip theory is adequate already. The DEMON3 results shown in Figure 14 closely match the results generated by LRCDM2 published in References 6 and 19.

Ogive Cylinder

In order to assess the capability of the pressure calculation methods implemented in the DEMON3 program in the application to bodies, comparisons with experimental data for an ogive cylinder body are shown in Figure 15. The geometric details of the body are shown in the lower portion of the figure. The angle of attack is zero and the Mach number is 2.96.

On Figure 15, experimental pressure coefficients are shown by the open symbols for the upper and lower meridians of the pointed ogive-cylinder. The two measurements should

be identical for the zero angle of attack case. The pressures overshoot the zero level in the region of the tangency point.

In the application to a body alone, program DEMON3 does not need to model a dummy wing unlike the LRCDM2 program (Ref. 6, Section 3.5). The DEMON3 predictions are based on a distribution of triplet panels on the body consisting of 15 rings along the body with 8 panels each around the circumference. The rings are clustered near the body nose for the sake of resolving details of the nose shape. For the shock expansion and Newtonian pressure calculation methods, program DEMON3 automatically lays out 73 strips around the body, and the program input was arranged to specify 13 axial stations at which circumferential pressure distributions are calculated.

In Figure 15, the Bernoulli pressures calculated by Equation (3) with velocities induced by the triplet panels underpredict the experimental pressures from the nose tip up to about half the length of the ogive nose. Aft of this station, the Bernoulli pressures agree fairly well with the experimental data including the overshoot. The uncorrected shock expansion pressures match the experimental data considerably better on the nose although the pressures are somewhat underpredicted in this region. The corrected shock expansion pressures are a little lower still. Aft of the tangency point, the shock expansion pressures systematically underpredict. This deficiency is thought to be related to the use of general shock expansion rather than second order shock expansion. In general, on the nose these results are a definite improvement over the results obtained by the LRCDM2 code as published in Reference 6. The main reason for the improvement is the incorporation of the approximate tangent cone relationships in lieu of the tangent wedge expressions for conditions immediately behind the shock. The Newtonian prediction underestimates the pressures over the entire nose. In this case, the Newtonian-based pressures are not applicable due to the low Mach number. Additional comparisons with experimental data for noncircular bodies at angle of attack need to be performed.

LIMITATIONS IN THE METHODOLOGY

The DEMON3 computer program is subject to certain limitations and deficiencies due in part to the low order supersonic panel modeling employed and the associated limitations in the geometric details that can be modeled. Additionally, there is a shortcoming due to the general shock expansion theory employed in the optional nonlinear pressure calculations on the body. Five limitations and deficiencies are listed below.

Supersonic Paneling Deficiencies

The following deficiencies are related to the triplet panel and constant u-velocity panels used to model the body and the lifting surfaces, respectively.

Body Triplet Panels

As stated in the technical approach, the DEMON3 program makes use of Woodward's triplet panels (Ref. 13) to model the body which may be noncircular in cross section. There are at least three problems associated with the triplet panel in its present form.

(1) The triplet panel geometrical layout and theoretical solution are based on the panel being flat so that the four panel corners lie in the same plane. In cases for which the body cross sectional contours are similar from the nose to the base, all of the triplet panels will be planar and the solution will be valid within the constraints of linear supersonic panel theory and the specific characteristics of the low order triplet panel. If the body contours are dissimilar, the triplet panels may be nonplanar or twisted if they are defined with four corners. The triplet routines in DEMON3 (taken from a later version of the USSAERO program described in Reference 17 and modified for DEMON3 to handle asymmetric flow conditions) will still generate solutions. It is clear that the solutions in cases with twisted panels may not be valid. However, a twisted panel can be divided into two triangular planar panels. Unfortunately, the present triplet panel layout routines do not divide four cornered twisted panels into three cornered panels automatically. However, the input of DEMON3 allows the user to arrange for two corners to coincide resulting in a triangular panel. Therefore, to the extent possible the user should avoid generating layouts resulting in twisted or nonplanar panels This can be done by rearranging and/or dividing a nonplanar panel into two triangular panels by judicious selection of panel layout coordinates in the input.

(2) Notwithstanding the improvements embodied in the triplet panel relative to the source panel solution to avoid internal reflections (Refs. 13 and 16), it is possible to encounter cases where the panel solution results in erratic and very high panel strengths towards the base of the body. The flow tangency boundary condition is still satisfied but the panel strengths have large magnitudes which may oscillate down the body. As a result, the velocity components assume large values which affect the pressures calculated on the body. This problem can happen when the body is slender (or long) and the Mach number relatively low. In such cases, the residual or uncancelled portion of the influences radiating aft inside the body from the corners of the triplet panels along Mach waves or cones are amplified as they reflect back and forth. Other than updating to a higher order paneling method which mathematically assures that there are no internal influences, there is no easy remedy for the residual internal reflection problem related to the triplet panel.

(3) The triplet singularity solution is based on the requirement that the triplet panel must lie inside the Mach wedge and Mach cones attached to the leading edge and its corner points. The wedge and cone angles depend on the free stream Mach number. At and/or near the nose, the panel inclination angles may be too large depending on the body nose geometry resulting in superinclined panels. In such cases, the DEMON3 program will

- 21 -

stop with a message described in a later section concerned with the computer program description. The user should reduce the panel inclination angles by lengthening the first sets of circumferential panels until the planes of the panels lie inside the Mach cone attached to the nose.

Constant U-velocity Panels on the Lifting Surfaces

(4) The wing or fin layout routines in the present version of program DEMON3 can not account for actual gaps between the fin root chords and the body. These gaps may be streamwise for undeflected control fins and/or they may be due to the fin root chord separated from the surface of the body for a deflected fin. Furthermore, the fin deflection angle is only included in the flow tangency condition applied at points in the geometrically undeflected fin plane. This simplification may cause errors at high fin deflection angles. The latest version of the NWCDM-NSTRN program (derived from the code described in Reference 8 and extended in connection with on-going work in fin tailoring to control the axial location of center of pressure (Reference 29) contains subroutines to rotate the control fin in accordance with its deflection angle. As such, the influence of fin gap is included in the fin loadings as far as inviscid effects are concerned within the limitations of supersonic linear theory. Unpublished preliminary results show the same trends with gap size and deflection angle as shown by available experimental data. The fin tailor version of NWCDM-NSTRN can not account for the effects of shocks and shock-boundary layer interactions present in the gap. This area of research needs to be studied in detail (with Navier-Stokes solvers and suitable grids) since control fin effectiveness and, thus, sizing can depend greatly on fin gaps.

Shock Expansion Method

(5) As described in an earlier section, program DEMON3 can optionally engage shock expansion and Newtonian methods for calculating the pressures acting at points on the body meridians and at points along strips on the lifting surfaces. The pressures calculated by the method incorporated in DEMON3 include effects of aerodynamic interference by modifying the flow deflection angles used in the nonlinear pressure calculation methods. In the shock expansion procedure, the strip calculations, prior to modifying the flow angles, are based on general shock expansion theory. On the lifting surfaces, the general approach appears to be adequate. On the body, the general method should be upgraded to second-order shock expansion.

COMPUTER PROGRAM DEMON3

General Description

The DEMON3 computer program, presented in this section, has application as an engineering level prediction method to wing-body-tail configurations at angles of attack up to 25 deg and for supersonic Mach numbers up to 2.5 if the standard panel method/Bernoulli pressure method is used. If the nonlinear (shock expansion/Newtonian with interference effects obtained from the panel solutions) pressure calculation method is engaged, the upper bound on the Mach number is approximately 6 but the body nose and fin leading edge shocks must be attached. On the lifting surfaces, the nonlinear pressure calculations compare well with experimental data; however, on the forebody the nonlinear pressure calculation on the forebody as implemented in the present version of DEMON3 needs to be updated to second order.

The DEMON3 program consists of an executive routine, also designated DEMON3, and 79 subroutines. An alphabetical listing of all the routines is provided in Table I. The subroutine calling sequence is indicated in Table II. Program DEMON3 is written in standard FORTRAN language. Operation requires two (2) auxiliary files in addition to the standard input and output units. Core storage for execution is approximately 170 kilobytes. On a SunSPARC work station, execution time can vary from one minute to one hour depending on the configuration, the number of panels selected to model the body and fin sections, and the length of body along which body vortices are shed and tracked.

Program stops are listed in Table III. Some of the stops print the reason(s) for the program stop. All stops specify the subroutine from which they are printed.

Stepwise Procedure

A complete configuration consisting of a body with a forward fin set and a tail fin set is handled by DEMON3 in four (4) steps. The stepwise procedure is shown in Figure 16. The calculations performed for each step are itemized below.

Step 1.   Obtain triplet panel solution for complete body; perform body vortex shedding (when applicable) and pressure calculations on the forbody; save forebody force and moment data and forebody vortex strength and position data for transfer to routines for Step 2.

Step 2.   Obtain constant u-velocity panel solution for the forward fin section under the influence of forebody vortices (when present); calculate pressures and forces and moments acting on the lifting surfaces and interference shell; determine discrete vortex model of the wake for each lifting surface at the trailing edge of the forward fin section; transfer wake vortex strengths and positions to the routines for Step 3.

Step 3.   Continue the body shedding calculations along the portion of body (afterbody) between the forward fin set and the tail fin set under the influence of the vorticity associated with the forward fin set and forebody vorticity (when applicable); calculate pressures and forces and moments on the afterbody; save vortex strengths and positions and forces and moments for inclusion in the final Step4.

Step 4.   Obtain solution for the constant u-velocity panels on the lifting surfaces and the interference shell in the tail fin set under the influence of upstream vorticity associated with the forebody, forward fin set, and afterbody.

Input Description

The following is a description of the input variables required by the present version of program DEMON3. The description is given in the sequence of the stepwise procedure described above.

INPUT VARIABLES FOR PROGRAM DEMON3

Program Variable	Format	Comments

Input Variables Required for All Runs

Normally these items are input to Step 1. However, if restarting the calculation on the afterbody section with NSTART = 3 in Item 1 below, these items are required as input to Step 3.

Item 1	(215)	Beginning and ending steps in calculation.
NSTART		Step at which calculations are started or restarted. NSTART = 1 or 3.
NSTOP		Step after which calculations are stopped, $1 \le NSTOP \le 4$.
Item 2	(16I5)	
NCIR		Cross Section shape index.

=0,   circular cross section, do not use; use NCIR = 1 instead

=1,   elliptic cross section

=2,   arbitrary cross section

Program Variable	Format	Comments
NCF		Numerical transformation index.

=0, mapping coefficients are calculated based on body shape input and are saved on Unit 8

=1, mapping coefficients from previous run are read in from Unit 8

ISYM   Symmetry index.

=0, right-left flow symmetry

=1, no symmetry (required if $\phi \neq 0°$)

NBLSEP   Body vortex separation index.

=0, no separation (required if $\alpha_c = 0°$ and preferred if $\alpha_c \geq 10$ in Item 6)

=1, laminar separation

=2, turbulent separation

NSEPR   Reverse flow separation index.

=0, no separation, recommended

=1, laminar separation in reverse flow region

NSMOTH   Vortex-induced velocity smoothing index.

=0, no smoothing

=1, smoothing of vortex-induced velocities used in pressure calculation

=2, smoothing of vortex-induced velocities used in pressure calculation and smoothing of $\partial \phi / \partial x$ calculation

NDFUS   Vortex core model index.

=0, potential vortex

=1, diffusion core model; preferred (see RCORE in Item 6)

NDPHI   Unsteady pressure term index.

Program Variable	Format	Comments

		=0, omit $\partial\phi/\partial x$ from C_p calculation
		=1, include $\partial\phi/\partial x$ term; preferred
INP		Nose force index.
		=0, region between nose tip and XI divided into 10 evenly spaced sections, and pressure integration is performed over this region. Pressures at each section are obtained by interpolating between XI and the nose tip, which for Bernoulli pressures, is assumed to be a stagnation point. Pressures are constant over the region and equal to the pressure at XI when calculating 2-D nonlinear pressures. Preferred.
		=1, no forces calculated ahead of XI. Forces at XI are input in Item 18. Required value for restart option.
NXFV		Number of x-stations at which flowfield is calculated or special output generated. See Item 15. $0 \le NXFV \le 8$
NFV		Number of field points for flowfield calculation. See Item 16. $0 \le NFV \le 100$
NVP		Number of $+\Gamma$ vortices on $+y$ side of body to be input for restart calculation. See Item 18. $0 \le NVP \le 70$
NVR		Number of $-\Gamma$ reverse flow vortices on $+y$ side of body to be input for restart calculation. See Item 20. $0 \le NVR \le 30$
NVM		Number of $-\Gamma$ vortices on $-y$ side of body to be input for restart calculation. See Item 21. NVM = 0 if ISYM = 0. $0 \le NVM \le 70$
NVA		Number of $+\Gamma$ reverse flow vortices on $-y$ side of body to be input for restart calculation. See Item 22. NVA = 0 is ISYM = 0. $0 \le NVA \le 30$
NASYM		Asymmetric vortex shedding index. See Item 8.
		=0, no forced asymmetry; preferred
		=1, forced asymmetry
Item 3	(12I5)	

Program Variable	Format	Comments
NHEAD		Number of title cards in Item 3. NHEAD ≥ 1
NPRNTP		Pressure distribution print index.
		=0, no pressure output except at special x-stations specified by Item 15
		=1, pressure distribution output at each x-station
NPRNTS		Vortex separation print index.
		=0, no output
		=1, output at each x-station; preferred
		=2, detailed separation calculation output; for debugging purposes only
NPRNTV		Vortex cloud summary output index.
		=0, no vortex cloud output
		=1, vortex cloud output; preferred
NPLOTV		Vortex cloud printer-plot option.
		=0, no plot
		=1, plot full cross-section on a constant scale
		=2, plot upper half cross-section on a constant scale.
		=3, plot full cross-section on a variable scale; preferred.
NPLOTA		Plot frequency index.
		=0, no plots
		=1, plot vortex cloud at x-stations specified by Item 15
		=2, plot vortex cloud at each x-station
NPRTVL		Velocity calculation auxiliary output for debugging purposes only (Sub. VLOCTY).
		=0, no output; preferred
		=1, print velocity components at field points; see Items 15 and 16

Program Variable	Format	Comments
		=2, print velocity components at body control points during pressure calculations. This option can produce massive quantities of output (not recommended).
NCNTR		Center vortex control index.
		=0, no center vortex
		=1, center vortex calculated
NCORE		Vortex core size index.
		=0, ratio of the local vortex core radius to the local body diameter = 0.025, default value
		=1, vortex core, RCORE, input in Item 6.
NVTRNS		Vortex cloud representation index.
		=0, forebody vortices represented by centroids.
		=1, entire set of forebody-shed vortices transferred to fin subroutine SPNLD, and thus present during afterbody and tail fin calculations.
NRSTRT		Restart control index.
		=0, calculation is not a restart
		=1, calculation is a restart. Additional input required, Items 16 and 18.
N2DPRB		Index which controls type of loading calculation performed on the body surface.
		=0, Bernoulli pressure coefficients
		=1, shock expansion and Newtonian pressure coefficients
		=2, shock expansion and Newtonian pressure coefficients corrected with linear theory
Item 4	(20A4)	Hollerith information identifying the run
TITLE		NHEAD lines of identification. Information to be printed at top of output sheets.

Program Variable	Format	Comments
Item 5	(8F10.0)	Reference information used in forming aerodynamics coefficients.
REFS		Reference area. REFS > 0
REFL		Reference length. REFL > 0
XM		x_B-coordinate of moment center.
ZM		z_B-coordinate of moment center.
SL		Body length (L).
SD		Body maximum diameter, or equivalent noncircular body diameter (D). Used in definition of RE.
Item 6	(8F10.0)	
ALPHAC		Angle of incidence, degrees. $0° < a_c < 90°$ if $\alpha_c = 0°$, NBLSEP = 0 in Item 2.
PHI		Angle of roll, degrees (ϕ).
RE		Reynolds number ($V_\infty D / \nu$).
RCORE		Ratio of the local vortex core radius to the local body diameter. Default value is .025, and maximum allowable value permitted in the code is $.05^* SD/r_o$.
XMACH		Mach number, M_∞.
Item 7	(8F10.0)	
XI		Initial x-station. XI > 0.
XF		Final x-station. XF > XI.
DX		Increment in x for vortex shedding calculation. Typical value, DX ≈ D/2 when FDX = 0.0. For variable DX, set DX = 0.0 and FDX > 0.0. When N2DPRB < 0 (Item 3), DX < XI.
EMKF		Minimum distance of shed vortex starting position from body surface.
		=1.0, vortices positioned such that separation point is a stagnation point in the crossflow plane

Program Variable	Format	Comments
		>1.0, minimum radii away from body surface for shed vortices. Typical value, EMKF = 1.05.
RGAM		Vortex combination factor.
		=0.0, vortices not combined; preferred (set RGAM = 0)
		>0.0 radial distance within which vortices are combined. Typical value, RGAM = 0.05 D
VRF		Vortex reduction factor to account for observed decrease in vortex strength.
		=0.6, for subsonic flow
		=1.0, for closed bodies, or supersonic flow; preferred
FDX		Factor for variable x-increments. When FDX > 0.0 DX = FDX * (local body radius). DX should be input as zero when this option is used.
Item 8	(8F10.0)	This item contains only one variable that is of general use in program DEMON3 and that is the integration error tolerance, E5. The variable XTABL is for diagnostic purposes only. The next three variables concern the use of forced asymmetry for bodies at very high angles of attack. The variables are defined as follows:
E5		Error tolerance for vortex trajectory calculation. (Relative error in vortex position.) Typical range, E5 = 0.01 to 0.05. Set E5 = 0.0.
XTABL		x-location after which a table of corresponding points between the real body and the transformed circle is not printed. For diagnostic purposes on noncircular shapes. Typical value, XTABL = 0.0.
XASYMI		Initial x-location at which forced asymmetry of separation points is used. Typical value, XASYMI = 0.0.
XASYMF		Final x-location at which forced asymmetry of separation points is used. Typical value, XASYMF = 0.0.
DBETA		Amount of forced asymmetry for separation points on body, degrees. Typical value, DBETA = 0.0.

Items 9, 10 provide a table of geometry characteristics that must be input for all bodies, circular or noncircular in cross-section.

Program Variable	Format	Comments
Item 9	(I5)	
NXR		Number of entries in body geometry table ($1 <$ NXR < 50).
Item 10	(5F10.0)	NXR lines of input
XR		x-stations for geometry table (NXR values, 8 per record).
R		r_0, circular body radius at x-stations, or radius of transformed circle (NXR values, 8 per record). For an ellipse, $r_0 = (a + b)/2$.
DR		dr_0/dx, body slope of transformed shape at x-stations (NXR values, 8 per record)
AE		a, horizontal half-axis of elliptic cross-section (NXR values, 8 per record).
BE		b, vertical half-axis of elliptic cross-section (NXR values, 8 per record).

Items 11 through 14 are included only if NCIR = 2; that is, for a body with arbitrary cross-section that must be handled with the numerical transformation and conformal mapping procedures.

Item 11	(2I5)	
MNFC		Number of coefficients describing transformation of arbitrary body to a circle ($1 <$ MNFC < 25).
MXFC		Number of x-stations at which transformation coefficients are defined ($1 <$ MXFC < 10). For a similar shape body at all cross-sections, MXFC = 1.
Item 12	(8F10.0)	
XFC		x-stations at which transformation coefficients are defined. For a similar cross-section body, MXFC = 1, XFC(1) $<$ XI (MXFC values, 8 per record).

Items 13 and 14 are included when NCF = 0. This block of records is repeated MXFC times, once for each x-station input in Item 12.

Program Variable	Format	Comments
Item 13	(I5)	
NR		Number of coordinate pairs defining the body cross-section at the axial station defined by XFC(J). (2 < NR < 30).
Item 14	(2F10.0)	
XRC(I,J), YRC(I,J)		Coordinates of right-hand side of body. The convention for ordering the coordinates from bottom to top in a counter-clockwise fashion, as shown in Figure 17, is observed. Right/left body symmetry is required in the numerical mapping. (NR records with one set of coordinates per record).

Items 15 and 16 are included only if NXFV > 0. Item 15 specifies the axial stations at which additional output or plots are requested. Item 16 is included only if NFV > 0. Each record of this item contains the nondimensionalized y,z-coordinates of a field point at which the velocity field is calculated, at each axial station specified in Item 15.

Item 15	(8F10.0)	
XFV		x-station at which field point velocities are calculated or at which additional output is printed (NXFV values).
Item 16	(2F10.0)	Omit if NFV = 0 in Item 2.
YFV, ZFV		y/r_o, z/r_o-coordinates of field points at which velocity field is calculated, expressed as a fraction of the local body radius (NFV records with one set of coordinates per record). It is important that the field points lie outside the body surface.

Items 17 and 18 are included for a restart calculation only.

Item 17	(8F10.0)	Omit if NRSTRT = 0 in Item 3.
CPBO(I)		Bernoulli pressures at x = XI (input Item 7), for 73 meridional points from $\beta = 0$ to $\beta = 360°$; 73 values, 8 values per record. These pressures should be obtained from a previous run containing this x-station. If restarting at the beginning of the afterbody section, pressures should be taken from values at control points on body interference shell constant u-velocity panels.
Item 18	(6F10.0)	Omit if NRSTRT = 0 in Item 3. Item 18 is a single record containing the force and moment coefficients at the restart point, x = XI.

Program Variable	Format	Comments
CA		Axial force coefficient.
CN		Normal force coefficient.
CY		Side force coefficient.
CM		Pitching moment coefficient.
CR		Yawing moment coefficient.
CSL		Rolling moment coefficient.

The above six coefficients refer to the body fixed coordinate system (x_B, y_B, z_B) (Refer to Figure 19).

Program Variable	Format	Comments
Item 19	(4F10.0)	Omit if NVP = 0 in Item 2. This Item is a set of NVP records.
GAMP		Γ/V_∞, positive separation vorticity on right side of body.
YP, ZP		coordinates of discrete vortices on right side of body at starting point (XI).
XSHEDP		x-location at which individual vortex was shed (may be 0.0). This variable is used only to identify individual vortices and permit the user to follow these vortices during the calculation.
Item 20	(4F10.0)	Omit if NVR = 0 in Item 2. This item is a set of NVR records. It is a convenient way to add an arbitrary cloud of vorticity which is to be maintained separately from the other body vorticity in the field.
GAMR		Γ/V_∞, reverse flow or additional vorticity on right side of body.
XR, ZR		coordinates of discrete vortices on right side of body at starting point (XI).
XSHEDR		x-location at which individual vortex was shed (may be 0.0).
Item 21	(4F10.0)	Omit if NVM = 0 or if ISYM = 0

This item consists of NVM records. In the case of a symmetric flowfield (ISYM = 0), this block of vorticity is automatically defined as the mirror image of the positive vorticity input in Item 19. |
| GAMM | | Γ/V_∞, negative separation vorticity on left side of body. |

Program Variable	Format	Comments
YM, ZM		Coordinates of discrete vortices on left side of body at starting point (XI).
XSHEDM		x-location at which individual vortex was shed (may be 0.0).
Item 22	(4F10.0)	Omit if NVA = 0 or ISYM = 0
		This item consists of NVA records and is analogous to Item 20. This block of vorticity is automatically defined as the mirror image of the negative vorticity input in Item 20 if symmetry is required by ISYM = 0.
GAMA		Γ/V_∞, reverse flow or additional vorticity on left side of body.
YA, ZA		Coordinates of discrete vortices on left side of body at starting point (XI).
XSHEDA		x-location at which individual vortex was shed (may be 0.0).

The above 22 items make up the body vortex shedding portion of the input. Items 23 through 37 are associated with the body triplet panel layout.

Item 23	(20A4)	
TITLE		One card of identification information to be printed ahead of the paneling output.
Item 24	(2I5)	
IXZSYM		Panel symmetry option.

=0, panel symmetric half of body for symmetric flow ($\phi = 0$)

=1, panel complete symmetric body using +y side geometry for a symmetric body in asymmetric flow ($\phi = 0$)

=-1, panel complete configuration using geometry of both sides

The purpose of IXZSYM is to define the manner in which the body paneling is carried out for different flow conditions. A symmetric body in a symmetric flow ($\phi = 0°$) can benefit from the IXZSYM = 0 option, which panels only one half of the body and then utilizes the symmetry characteristics to reduce computation time. The same symmetric body in an asymmetric flow condition ($\phi \neq 0°$) must be paneled in total, IXZSYM = 1, to

Program Variable	Format	Comments

pick up the nonsymmetry in the loading around the body. The body symmetry is used to reduce the input required as described later.

ITBSYM

=0, configuration has top/bottom symmetry

=1, no top/bottom symmetry (e.g., see Fig. 10)

Item 25   (4I3)

J2

Body geometry specification option.

=1, geometry for arbitrary shaped body

=-1, circular body defined by cross-section area at XFUS stations (not recommended)

=-2, circular body defined by radius at XFUS stations

=-3, elliptic body defined by both semi-axes at XFUS stations

J6

=0, cambered body - not available

=1, body symmetrical with respect to XY-plane (uncambered body)

=-1, circular or elliptic body (preferred value)

NRADX

Number of points used to represent the body segment about the circumference. If the configuration is symmetric (IXYZSYM = 0, 1), NRADX is input for the half section only. If the entire configuration is input (IXZSYM = -1), NRADX is input for the full section. The half section or full section is divided into NRADX - 1 equal angles, and the y- and z- coordinates of the panel corner points are defined by the intersections of these meridian angles with the entire body surface (3 < NRADX < 20).

NFORX

Number of axial body stations used to define geometry (2 < NFORX < 30).

The next block of input specifies the geometry of the body for purposes of laying out the panels. This input is somewhat redundant with the input in Items 9 through 14; however, it is important that the paneling geometry be separate from the previous geometry but consistent with it. In many cases, the paneling geometry may be specified in a more coarse grid than that required by the separation portion of the program.

Program Variable	Format	Comments
Item 26	(8F10.0)	
XFUS		x-stations at which body paneling geometry is input (NFORX values, 10 values per record).
Item 27	(8F10.0)	Included only if J2 = -1 (Item 25). The circular body cross-sectional areas are specified at the XFUS stations defined in Item 26.
FUSARD		Circular body cross-sectional areas at XFUS stations (NFORX values, 10 values per record).
Item 28	(8F10.0)	Included only if J2 = -2 (Item 25). The circular body radii are specified at the XFUS stations defined in Item 26.
FUSRAD		R, circular body radii at XFUS stations (NFORX values, 10 values per record).

Items 29 and 30 are included only if J2 = -3 (Item 25). The elliptic body horizontal and vertical semi-axes are specified at the XFUS stations defined in Item 21.

Program Variable	Format	Comments
Item 29	(8F10.0)	
FUSBY		Elliptic body horizontal semi-axes at XFUS stations (NFORX values).
Item 30	(8F10.0)	
FUSAZ		Elliptic body vertical semi-axes at XFUS stations (NFORX values).
Item 31	(2F10.0)	Included only if J2 = 1 (Item 25). The y,z-coordinates of points on an arbitrary cross-section body are specified in Item 31, and there is one set of Item 31 for each of the axial stations defined by XFUS in Item 26. The convention for ordering the coordinates from bottom to top is observed (e.g., Fig. 10). If the full cross-section is to be specified (IXZSYM = -1, Item 24) the ordering continues counter-clockwise from the top of the body back to and including the bottom point to close the cross section.
YJ, ZJ		y,z-coordinates or arbitrary body at XFUS stations (NRADX records, 2 coordinates per record).

Item 31 is repeated NFORX times, once for each XFUS station.

Program Variable	Format	Comments

The purpose of the following input is to provide a simple means to adjust the actual panel layout keeping the geometry specified above unchanged.

Item 32   (20A4)

TITLE2   One card of identification information for paneling geometry.

Item 33   (5I5)   Print control options used to debug specific subroutines. Large amounts of output may be generated.

IPRINT   Panel output option.

=0, minimum output

=1, output panel corner coordinates, final source strengths, and velocities at panel control point (recommended)

=2, same as IPRINT = 1 and source strengths from previous iteration (not recommended)

=3, print source strength for each iteration (not recommended)

=4, same as IPRINT = 3 and complete aerodynamic influence matrix (not recommended)

IPRT(1)   =0, no supplementary print

>0, further triplet panel geometry information from subroutines BODPAN, CONFIG, and NEWRAD.

IPRT(2)   not used.

IPRT(3) .   =0, no supplementary print

=1, print normal influence coefficients from subroutines BICOEF and WCOEF.

=2, print above plus unit velocities, u,v,w, from subroutine BICOEF and WCOEF.

IPRT(4)   =0, no supplementary print

>0, print control indices, field point coordinates, and triplet panel-induced velocities from subroutine BODVEL.

Program Variable	Format	Comments

		>1, print above plus influencing triplet panel strengths in subroutine BODVEL.
		>2, print above plus AN arrays from subroutine BODVEL.
		>3, print above plus UB, VB, WB arrays from subroutine BODVEL.

If IPRINT < 0, the panel geometry is included with the output specified by |IPRINT|. This option provides a useful means to check the paneling arrangement.

| Item 34 | (2I5) | These indices provide a means to change the panel layout without changing the geometry input. |
| KRADX | | Number of meridian lines used to define panel edges on the body segment. |

=0, meridian lines are defined by NRADX in Item 29.

>0, meridian lines are calculated at KRADX equally spaced points (3 < KRADX < 20).

<0, meridian lines are calculated at specified values of PHIK in Item 36 (3 < |KRADX| <20).

For symmetric configurations (IXZSYM = 0,1), KRADX is the number of meridians on the half section. For full configurations (IXZSYM = -1), KRADX is the number of meridians on the full section including meridians at $0°$ and $360°$.

| KFORX | | Number of axial stations used to define leading and trailing edges of panels on the body. |

=0, the panel edges are defined by NFORX and XFUS in Items 29 and 30, respectively.

>0, the panel edges are defined by KFUSK in Item 36 (2 < KFORX < 30).

Item 35	(8F10.0)	Include only if KRADX < -3 in Item 35.
PHIK		Body meridian angles (degrees) with PHIK = $0°$ at the bottom of the body and PHIK = $180°$ at the top (|KRADX| values).
Item 36	(8F10.0)	Omit if KFORX = 0 in Item 35.

Program Variable	Format	Comments
KFUSK		Axial stations of leading and trailing edges of body panels (KFORX values). XFUSK defines the axial positions of the panel edges. If this item is not included, the panels are specified by XFUS in Item 26. The purpose of this item is to simplify the changing of the panel layout without changing the panel geometry.

Program Variable	Format	Comments

Input Variables Required for Step 2

See notes at end of Namelist $INPUT for variables marked with *.

Item 1   (namelist)   Namelist $INPUT.

B2   Exposed fin semispan of horizontal or upper right or lower left fins, dimensional.

B2V   Exposed fin semispan of vertical or upper left or lower right fins, dimensional, default is 0.0.

CRP   Rootchord or horizontal or lower left or upper right fins, dimensional.

CRPV   Rootchord of vertical or upper left or lower right fins, dimensional, default is 0.0.

DELD*   Deflection angle of vertical lower or upper left fin.

DELL*   Deflection angle of horizontal left or lower left fin. Positive: trailing edge down, degrees, default is 0.0.

DELR*   Deflection angle of horizontal right or upper right fin. Positive: trailing edge down, degrees, default is 0.0.

DELU*   Deflection angle of vertical upper or lower right fin. Positive: trailing edge to right or down, degrees, default is 0.0.

FAC   FAC = 0.95. Fraction of the constant u-velocity panel chord (which contains the centroid) where the control point is located.

FKLE   Fraction of leading-edge suction converted to normal force, default is 0.5.

FKSE   Fraction of side-edge suction converted to normal force, default is 1.0.

LVSWP   LVSWP = 0 No breaks in fin leading or trailing edges, or equal spanwise spacings of panel side edges, default value.

               LVSWP ≠ 0 Up to 19 breaks in fin leading or trailing edges or up to 19 unequal spanwise spacings.

Program Variable	Format	Comments
MSWD*		Number of spanwise constant u-velocity panels on the vertical lower or upper left fin; 1 < MSWD < 19, default is 0.
MSWL*		Number of spanwise constant u-velocity panels on the horizontal left or lower left fin; 1 < MSWL < 19, default is 0.
MSWR*		Number of spanwise constant u-velocity panels on horizontal right or upper right fin; 1 < MSWR < 19, no default.
MSWU*		Number of spanwise constant u-velocity panels on vertical upper or lower right fin; 1 < MSWU < 19, default is 0.
NCW*		Number of chordwise constant u-velocity panels on the fins.
NCWT		Number of fin thickness (source) panels in a chordwise row, default is 0. Usually NCWT > NCW to capture streamwise thickness details on a fin.
NOUT(I)		Array of 5 debug print control. Default is NOUT(I) = 0; 1 < I < 5. These variables produce print in the following routines when set equal to 1.

NOUT(1) Debug print in FINSEC
NOUT(2) Debug print in RHSFIN
NOUT(3) Print fin-load results for linear pressures
NOUT(4) Debug print in BDYSHL
NOUT(5) Debug print in FINVEL, SPECPR, SPECLD, and SPNLD

Program Variable	Format	Comments
NPR		Print control option. Large amounts of output may be generated if NOUT > 0. Default is 0.
NTDAT		NTDAT = 0 No thickness input data, default value. NTDAT = 1 Fin thickness information to be supplied (Item 6) for one or more fins of a finned section.
NTPR		NTPR = 1 Print debug output from subroutine THKVEL, default is 0.
N2DPRF		Index governing type of loading calculation performed on fin surfaces. Note: N2DPRF = 1 or 2 not applicable to cases including nonzero angular rates.

Program Variable	Format	Comments
		N2DPRF = 0 Linear and Bernoulli pressure coefficients, default value.
		N2DPRF = 1 Shock expansion and impact (Newtonian) pressure coefficient.
		N2DPRF = 2 Shock expansion and impact (Newtonian) pressure coefficients corrected with linear theory.
		For N2DPRF > 0, further input required (Item 7).
PHIDIH		PHIDIH = 0.0
PHIFR		Dihedral angle of right upper fin, in degrees. Default is 0.0 for cruciform or planar fins. See sketch below.
PHIFL		Dihedral angle of left lower fin, in degrees, default is 0.0 for cruciform or planar fins.
PHIFU		Dihedral angle of right lower fin, in degrees. Default is 90.0 for cruciform fins.
PHIFD		Dihedral angle of left upper fin, in degrees. Default is 90.0 for cruciform fins.

<u>Arbitrary Fin Layout</u>   <u>Cruciform Fin Layout</u>

<u>Looking Forward</u>
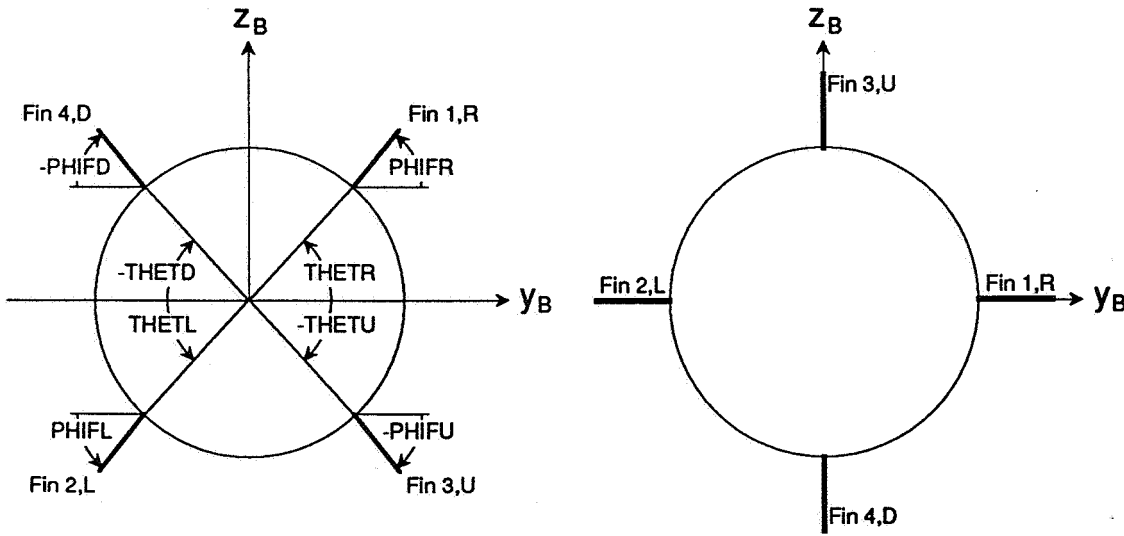
Program Variable	Format	Comments
SWLEP[*]		Vertical or upper left or lower right fin leading-edge sweep angle measured in fin planform, positive for sweep back, degrees, default is 0.0.
SWTEP[*]		Horizontal or lower left or upper right fin trailing-edge sweep angle measured in fin planform, positive for sweep back, degrees, default is 0.0.
SWTEV[*]		Vertical or upper left or lower right fin trailing-edge sweep angle measured in fin planform, positive for sweep back, degrees, default is 0.0.
THETIT		Polar angle associated with interdigitated or low profile four fin layouts, default is 0.0 for cruciform or triform fin layouts, $0 < \theta < 90°$.
THETR[**]		Polar angles of upper right fin, degrees, default is 0.0 for cruciform or planar fins.
THETL[**]		Polar angle of lower left fin, degrees, default is 0.0 for cruciform or planar fins.
THETU[**]		Polar angle of lower right fin, degrees, default is 90.0 for cruciform fins.
THETD[**]		Polar angle of upper left fin, degrees, default is 90.0 for cruciform fins.
TOLFAC		Multiplication factor used in the evaluation of the tolerance, TLRNC, used throughout the program. Default value is 1.0, on VAX 11/750 use 10,000.
XLEBIP		Axial location of fin root chord leading edge measured from body nose, dimensional, default is 0.0.
		z_B-coordinate of moment center in body coordinate system, feet, default is 0.0.
YBOD(J)[*]		y_B-coordinate of rootchord leading-edge, $1 < J < 4$. User must specify a value for each wing or fin present in input description.
ZBOD(J)[*]		z_B-coordinate or rootchord leading edge, $1 < J < 4$. User must specify a value for each fin present in input description.

[*] For fins with breaks in leading and/or trailing-edge sweep, use default values.
[**] These angles specified only for arbitrary fin layouts, refer to preceding sketch.

*The following relations must hold:

1. NWBP = NPANLS + NCWB*NBDCR < 300.
    NPANLS = NCW * (MSWR + MSWL + MWSU + MSWD) < 150.
    NBIP < 150 (NBIP = number of panels in interference shell.)***

2. Also, MSWR, MSWL, MSWU, and MSWD should be at least five for valid fin training-edge vorticity characteristics.

3. When running symmetric case, set PHI = 0.0 in Item 6, IXZSYM = 0 in Item 33 for all runs (preceding Step 2 input). If fins are deflected symmetrically, set MSWL, MSWU, MSWD, and DELL, DELU, DELD as follows:

    (1) for cruciform fins, MSWR ≠ 0, DELR ≠ 0.0.,

    > set MSWL = 0   DELL = DELR
    >   MSWU = 0   DELU = 0
    >   MSWD = 0   DELD = 0

    (2) for arbitrary but symmetric fin layout, MSWR ≠ 0, MSWU ≠ 0, 2 cases:

    <u>a</u> no fin deflection
    > set MSWL = 0
    >   MSWD = 0

    <u>b</u> with fin deflection, set DELR ≠ 0.0, DELU ≠ 0.0,
    > set MSWL = MSWU   DELD = DELR
    >   MSWD = MSWR   DELL = DELU

    The following four variables are used below in the description of the input variables. The terms "right" and "left" refer to an observer looking forward.

    MSWRP: Number of chordwise rows on horizontal right or upper right fin + 1; upper right, lower left fin, etc., terminology is used for arbitrary fin layouts shown in preceding sketch.
    MSWRP = MSWR + 1

    MSWLP: Number of chordwise rows on horizontal left or lower left fin + 1;
    MSWLP = MSWR + 1

    MSWUP: Number of chordwise rows on vertical upper or lower right fin + 1;
    MSWUP = MSWU + 1

    MSWDP: Number of chordwise rows on vertical lower or upper left fin + 1;
    MSWDP = MSWD + 1

*** NBIP is set by user. It is determined by selection of triplet panel layout on the body over the length of the fin rootchord.

Program Variable	Format	Comments
Item 2	(3F10.0)	Optional input for fin-body combination (if LVSWP = 0).
YRT(KJ)		Distance from fin rootchord to the constant u-velocity panel outboard side edge on right horizontal or upper right fin, dimensional $1 \le KJ \le MSWRP$, (MSWRP $\le$ 20), YRT(1) = 0.0, YRT(MSWRP) = B2.
VSWLER(KJ)		Leading-edge sweep of fin between YRT(KJ - 1) and YRT(KJ), positive for sweep back, degrees, $1 \le KJ \le MSWRP$, (MSWRP $\le$ 20), VSWLER(1) = 0.0. Sweep angle is measured in fin planform plane.
VSWTER(KJ)		Trailing-edge sweep of fin between YRT(KJ - 1) and YRT(KJ), positive for sweep back, degrees, $1 \le KJ \le MSWRP$, (MSWRP $\le$ 20), NSWTER(1) = 0.0. Sweep angle is measured in fin planform plane.
Item 3	(3F10.0)	Optional input for fin-body combination (if LVSWP $\ne$ 0). Omit if MSWL = 0.
YLT(KJ)		distance (negative) from fin rootchord to the constant u-velocity panel outboard side edge on left horizontal or lower left fin, dimensional, $1 \le KJ \le MSWLP$, (MSWLP $\le$ 20), YLT(1) = 0.0, YLT(MSWLP) = -B2.
VSWLEL(KJ)		Leading-edge sweep of fin between YLT(KJ - 1) and YLT(KJ), negative for sweep back, degrees, $1 \le KJ \le MSWLP$, (MSWLP $\le$ 20), VWSTEL(1) = 0.0. Sweep angle is measured in fin planform plane.
Item 4	(3F10.0)	Optional input for cruciform fin-body combination (if LVSWP $\ne$ 0). Omit if MSWU = 0.
ZUT(KJ)		Distance from fin rootchord to the constant u-velocity panel outboard side edge on upper vertical or lower right fin, dimensional, $1 \le KJ \le MSWUP$, (MSWUP $\le$ 20), ZUT(1) = 0.0, ZUT(MSWUP) = B2V.
VSWLEU(KJ)		Leading-edge sweep of fin between ZUT(KJ - 1) and ZUT(KJ), positive for sweep back, degrees, $1 \le KJ \le MSWUP$, (MSWUP $\le$ 20), NSWLEU(1) = 0.0. Sweep angle if measured in fin planform plane.
VSWTEU(KJ)		Trailing-edge sweep of fin between ZUT(KJ - 1) and ZUT(KJ), positive for sweep back, degrees, $1 \le KJ \le MSWUP$, (MSWUP $\le$ 20) VSWTEU(1) = 0.0. Sweep angle is measured in fin planform plane.

Program Variable	Format	Comments
Item 5	(3F10.0)	Optional input for cruciform wing-body combination (if LVSWP ≠ 0). Omit if MSWD = 0.
ZDT(KJ)		Distance (negative) from fin rootchord to the constant u-velocity panel outboard side edge on lower or upper left fin, dimensional, $1 \le KJ \le MSWDP$, (MSWDP ≤ 20), ZDT(1) = 0.0, ZDT(MSWDP) = -B2V.
VSWLED(KJ)		Leading-edge sweep of fin between ZDT(KJ - 1) and ZDT(KJ), negative for sweep back, degrees, $1 \le KJ \le MSWDPL$ (MSWDP ≤ 20), VSWLED(1) = 0.0. Sweep angle is measured in fin planform plane.
VSWTED(KJ)		Trailing-edge sweep of fin between ZDT(KJ - 1) and ZDT(KJ), negative for sweep back, degrees, $1 \le KJ \le MSWDP$, (MSWDP ≤ 20), VSWTED(1) = 0.0. Sweep angle is measured in fin planform plane.
Item 6		Optional thickness input data when NTDAT ≠ 0 in namelist $INPUT. The maximum number of source panels for one finned section cannot exceed 400; therefore, $$\sum_{1}^{\text{fins}} (MSWT * NCWT) \le 400;$$ NCWT is specified in namelist $INPUT.
Item 6(a)	(10I5)	Information in Items 6(a), 6(b), and 6(c) is read in by subroutine THKIN for the right horizontal fin.
MSWT		Number of source panels in the spanwise direction, $1 \le MSWT \le 19$.
LVSWT		LVSWT = 0 No breaks in fin leading or trailing edges, or equal spanwise spacings of source panel sides, default is 0.
		LVSWT = 1 Up to 29 breaks in fin leading or trailing edges or up to 19 unequal spanwise spacings.
NUNIS		NUNIS = 0 Chordwise thickness distribution varies over the span.
		NUNIS = 1 Chordwise thickness distribution constant over the span.
Item 6(b)	(3F10.0)	Optional input for LVSWT = 1.

Program Variable	Format	Comments
YTH(1,J)		Distance from fin chord to the source panel outboard side edge, $1 \leq J \leq MSWT + 1$.
SWLET(1,J)		Leading-edge sweep of fin between YTH (1,J-1) and YTH(1,J), positive for sweep back, degrees, $1 \leq J \leq MSWT + 1$.
SWTET(1,J)		Trailing-edge sweep of fin between YTH(1,J-1) and YTH(1,J) positive for sweep back, degrees, $1 \leq J \leq MSWT + 1$.
Item 6(c)	(8F10.0)	Optional input specifying streamwise thickness slopes read in by subroutine THETIN in groups of NCWT values.
THET(K)		NUNIS = 1 K = 1, NCWT. Input one set of NCWT values. NUNIS = 0 K = 1, (NCWT*MSWT). Input MSWT sets, each set containing NCWT values. $1 \leq K \leq 400$.
Item 6(d)	(8F10.0)	Optional thickness input for left fin for cases with nonzero roll or asymmetric fin deflection (MSWL > 0). All input same as for right fin above, Items 6(a), 6(b), and 6(c). Refer to Item 3 above for positive directions.
Item 6(e)	(8F10.0)	Optional thickness input for upper fin when MSWU > 0 in namelist $INPUT. Same input as for right fin, Items 6(a), 6(b), and 6(c). Refer to Item 4 above for positive directions.
Item 6(f)	(8F10.0)	Optional thickness input for lower fin when MSWD > 0 in namelist $INPUT. All inputs same as for right fin, Items 6(a), 6(b), and 6(c). Refer to Item 5 above for positive directions.
Item 7		Optional input for calculation of 2-D nonlinear pressures on fins. Read when N2DPRF > 0.
Item 7(a)	(F10.0)	
CONSTK		Constant used in Newtonian pressure coefficient, normally CONSTK = 2.

Program Variable	Format	Comments
Item 7(b)	(I5)	
NSEG		Number of 2-D segments used to describe fin profile, $2 \le NSEG \le 100$.
Item 7(c)	(8F10.0)	
THETA(J)		Slope angles of 2-D segments on upper surface of fin measured relative to fin chordal plane, degrees, $1 \le J \le NSEG$.
Item 7(c)	(8F10.0)	
THETB(J)		Slope angles of 2-D segments on lower surface of fin measured relative to fin chordal plane, degrees. Note: Items 7(b) through 7(d) are repeated for each chordwise row of control points on each fin. That is, there are MSWR + MSWL + MSWD + MSWU repetitions of Items 7(b) through 7(d).

Input Variables Required for Step 3

Optional input if NSTART = 1 and NSTOP > 2 in Item 1 for all runs. The following items from the input required for all runs are repeated here as input to Step 3 for the afterbody calculation.

<u>Item 1</u>   Defined as Item 2 in Step 1 input section.

<u>Item 2</u>   Defined as Item 3 in Step 1 input section.

<u>Item 3</u>   Defined as Item 4 in Step 1 input section.

<u>Item 4</u>   Defined as Item 7 in Step 1 input section.

Input Variables Required for Step 4

Optional input if NSTOP = 4 in Item 1 for all runs. Same as for Step 2, applied to the tail section.

Sample Cases, Input Description

This section describes a sample case input file corresponding to the model of Reference 23 and shown in Figure 8. The configuration has a monoplane wing and tail fin sections and a noncircular body. The body of the configuration is nearly circular over the ogive nose then transitions to an elongated (vertical) circular section on the forebody. Before the wing leading edge, the cross section transitions to have a circular bottom and a rectangular top. Over the wing root chord, the cross section transitions back to an elongated (vertical) circle and maintains this shape to the base. Tail fins are located at the rear of the configuration.

The input file for sample case 1 is shown in Figure 18. Input for calculation step 1 is shown on pages 1 through 10, Figure 18(a) through 18(j). Input for calculation steps 2 through 4 follow on pages 11 through 13, respectively. The input will now be described in detail.

NSTART = 1 and NSTOP = 4 in input item 1 indicate that the calculation procedure will start at step 1 (forebody) and stop after step 4 (second fin section).

Input item 2 consists of many control variables for the body calculation procedure. In input item 2, NCIR = 3 indicates that the body cross section is noncircular and changes shape (contour) along the length of body. NCF = 1 indicates that the conformal mapping coefficient for the noncircular body cross sections have been calculated previously and are read from a data file. ISYM = 0 indicates that the geometry and flow conditions have right-left symmetry (symmetric geometry and $\phi = 0\,°$). NBLSEP = 1 indicates that the Stratford laminar separation criteria is used to determine if body separation occurs. No reverse flow separation is considered, NSEPR = 0, and vortex induced velocity smoothing is not done, NSMOTH = 0. NDFUS = 1 and NDPHI = 1 indicate that a vortex core model is used and

that the $\partial\phi/\partial x$ term is included in the pressure calculation. INP = 0 indicates that nose forces are estimated ahead of the first axial station XI. The remaining variables in input item 2 are zero. These variables govern special output stations, field point velocity calculations, and input vortices for a restart calculation. These options are not invoked for this sample case.

Input item 3 consists of additional control variables for the body calculation procedure. NHEAD = 1 indicates that one title line for the run is to be read in item 4. NPRNTP, NPRNTS, and NPRNTV are all set to 1 indicating that the pressure distribution, separation summary, and vortex summary output pages will be printed at each axial station along the body. NPLOTV = 3 indicates that the vortex cloud plots will be plotted on a variable scale from one axial station to the next. NPLOTA = 2 indicates that a vortex cloud plot will be made at each axial station at which vortices are present. NPRTVL = 0 indicates that no debug output is requested from the velocity calculation subroutine VLOCTY. NCNTR = 0 indicates that the center vortex is not included in the calculation. NCORE = 0 indicates that the default vortex core size of 0.025 of the local body diameter is used. NVTRNS = 1 indicates that the entire vortex field is transferred to the fin section calculation procedure of step 2. NRSTRT = 0 indicates that the calculation is not a restart. N2DPRB = 0 indicates that Bernoulli pressure coefficients are calculated.

Input item 4 is a single line (NHEAD) describing the run.

Input item 5 specifies the reference area, REFS = 159.9984, the reference length, REFL = 9.176, the axial coordinate of the moment center, XM = 25.15, the vertical location of the moment center, ZM = 0.0, the body length = 38.462, and the maximum body diameter, SD = 3.0.

Input item 6 contains the flow conditions for the run. The angle of attack is 10.0°, ALPHAC, the body roll angle is 0.0°, PHI, the Reynolds number based on diameter is 1.26×10^8, RE, the vortex core size is 0.025, RCORE, and the freestream Mach number is 1.6, XMACH.

Input item 7 contains variables associated with the calculation procedure along the forebody. The first axial station, XI, is 1.0, the final station, XF, is 18.784, and the axial marching step size, DX, is 1.0. The final axial station corresponds to the wing root chord leading edge location. EMKF = 1.05 indicates that vortices are placed a minimum of 1.05 times the local radius away from the body. RGAM = 0 indicates that vortices are not combined. The vortex reduction factor, VRF, is set to 1.0. FDX = 0.0 indicates that a variable axial step size is not used.

In input item 8 the tolerance for the vortex tracking integration subroutine is set to 0.05.

NXR = 14 in input item 9 indicates that 14 points make up the body radius table input in item 10. Item 10 is a set of NXR input lines specifying the body radius distribution table. For noncircular bodies, the radius corresponds to transformed radius from the conformal mapping procedure. The axial station, XR, the transformed radius, R, and the "body slope" d(R)/dx are input.

MNFC = 25 and MXFC = 6 in input item 11 indicate that 25 mapping coefficients are used to model the noncircular cross sections at 6 axial stations. The program interpolates at axial stations between the 6 input stations. Item 12 specifies the 6 axial stations where the body cross section is input. Items 13 and 14 specify the cross section shape and are included for each of the 6 stations specified in item 12. Item 13 specifies the number of coordinate points specifying the cross section, NR. Item 14 specifies the coordinates, XRC(I) and YRC(I), of the right half of the cross section. Right/left symmetry is required.

Input items 15 through 22 are not required by this sample case. Most of these items pertain to a restart calculation. Items 23 through 36 pertain to the body paneling.

Input item 23 is a single title line for the paneling part of the input. IXZSYM = 0 in item 24 indicates that the body and flow are symmetric and that only half the body will be paneled. ITBSYM = 1 indicates that the body does not have top/bottom symmetry. In item 25, J2 = 1 indicates the body cross sections are noncircular and nonelliptic, and J6 = -1, NRADX = 15, and NFORX = 24 indicate that 14 panels around the half circumference by 23 panels along the body length are used to model the body. This results in a total of 322 panels on the half body. Only half of the body is modeled because of symmetry.

Item 26 specifies the 24 (NFORX) axial stations specifying the panel edge points, XFUS. The first point is at 0.0 and the last point is at the end of the body 38.462. Items 27 through 30 are not included because the model is not circular or elliptic. Item 31 contains the coordinates of the panel edge point around the circumference of the body cross sections. Item 31 is repeated for each of the 24 XFUS axial stations. Item 31 contains the 15 (NRADX) coordinates YJ and ZJ for each axial station XFUS.

Input item 32 is a single input title line for the additional paneling options in the program. In item 33, IPRINT = 1 indicates that panel corner points, final source strengths, and velocities at panel control points are printed. The following variable in item 33, IPRT(1) through IPRT(4), are set to 0 indicating that no additional supplementary (or debug) output is requested. KRADX = 0 and KFORX = 0 in item 24 indicates that the paneling geometry defined in items 23 through 31 are to be used to panel the body. Items 35 and 36 are not required for this sample case.

This completes the input description for the required variables for step 1 of the calculation procedure. The variables for step 2 through 4 are described next.

The variables for step 2 of the calculation procedure are input through NAMELIST $INPUT shown in Figure 18(k). XLEBIP = 18.784 indicates that the body interference shell (also the wing leading edge) start at axial station 18.784. The right wing is attached to the body at coordinates YBOD(1) = 1.5 and ZBOD(1) = 0.0, and the left wing is attached at coordinates YBOD(2) = -1.5 and ZBOD(2) = 0.0. The exposed span, B2, is 8.5, the root chord, CRP is 11.732, and the leading edge sweep, SWLEP, is 44.0°. A 6x6 chordwise by spanwise panel layout is used on the wing, NCW x MSWR. Wing thickness is not modeled for this case, NTDAT = 0. NOUT(5) = 1 indicates that detailed output will be printed from the fin load calculation procedure.

The variables for step 3 of the calculation procedure are shown in Figure 18(l). The values required by step 3 are the same as items 2, 3, 4, and 7 of step 1. Note that the axial

starting location, XI, is set to the wing root chord trailing edge location, and that XF is set to the tail leading edge location.

The variables for step 4 of the calculation procedure are shown in Figure 18(m). These variables are same as those of step 2; only they specify the geometry and paneling information for the tail fins.

This completes the sample case input description. A brief description of the output for this sample case follows.

Sample Cases, Output Description

This section describes a sample case output file corresponding to the model of Reference 23 and shown in Figure 8. The configuration has a monoplane wing and tail fin sections and a noncircular body. The body of the configuration is nearly circular over the ogive nose, then transitions to an elongated (vertical) circular section on the forebody. Before the wing leading edge, the cross section transitions to have a circular bottom and a rectangular top. Over the wing root chord, the cross section transitions back to an elongated (vertical) circle and maintains this shape to the base. Tail fins are located at the rear of the configuration. The input file for this sample case is shown in Figure 18.

Figure 19 depicts the coordinate systems and the force and moment sign conventions used in DEMON3. The normal force is positive up, the side force is positive to the right, the pitching moment is positive nose up, and the yawing moment is positive nose to right.

The sample case output file is shown in Figure 20. The program title page is output page 1, Figure 20(a). Output for step 1 of the calculation procedure (forebody) is shown on pages 2 through 95, Figure 20(b) through 20(v). Output for step 2 of the calculation procedure (wing section) is shown on pages 96 through 119, Figure 20(w) through 20(aq). Output for step 3 of the calculation procedure (afterbody) is shown on pages 120 through 131, Figure 20(ar) through 20(aw). Output for step 4 of the calculation procedure (tail fin section) is shown on pages 132 through 153, Figure 20(ax) through 20(bp). A summary of the total forces and moments acting on the vehicle are shown on page 154, Figure 20(bq). The following is a general description of the sample case output file. Details will be provided for calculation steps 1 and 2. Steps 3 and 4 are similar to steps 1 and 2, respectively, and will be described briefly.

Output page 2 displays the flow conditions and prints the program control variables for step 1. Page 3 contains the input geometry table, x, r, and dr/dx. Output pages 4 through 7 contain the numerical conformal mapping coefficients for the six noncircular body cross sections.

Pages 8 through 13 contain the body paneling geometry information. Additional paneling information is shown on page 14. The panel corner points are printed on pages 15 through 20, and the body centroid points are shown on Pages 21 through 26. The panel areas and inclination angles are shown on pages 27 through 32. The panels source solution for $\alpha_c = 0°$ is printed on pages 32 and 33. Surface velocities on the body are shown on pages 33 through 38. The panel solution at angle of attack is printed on pages 38 and 39.

- 52 -

Output pages 40 through 95 contain the pressure distribution, vortex shedding, and vortex tracking output for the forebody. Page 40 and 41 contain the pressure distribution and sectional loads at the first axial station, x = 1.0. Page 42 is a summary of separation information; it is seen that separation does not occur at this axial station. Pages similar to pages 40 through 42 are printed as the procedure marches down the body. The pressure distribution at the first axial station where separation occurs (x = 7.0) is shown on pages 52 and 53. The separation summary information is shown on page 54. The marching procedure continues down the body to the wing leading edge. A summary of the vortex field at the wing leading edge is shown on page 90. The pressure distribution at this station is printed on pages 91 and 92. A line printer plot of the vortex field is depicted on page 93. New vortices shed at this station are shown on page 94. Page 94 and 95 contain a summary of the total loads and the vortex field at the end of the forebody.

Page 96 begins the output for the wing section force calculation, step 2. The NAMELIST $INPUT is printed on this page. Page 97 contains a summary of the wing planform geometry, sweep angles, and attachment points to the body. Paneling information for the body interference shell is printed on page 98.

Velocities induced at the wing control points by the body triplet panels are shown on page 99. Vortex-induced velocities at the panel control points are shown on page 100. Velocities from the constant u-velocity panel modeling the wing and body interference shell at wing control points are printed on page 102.

The pressure distribution at points on the body interference shell are shown on pages 103 and 104. The results of integration of the pressure distribution are shown on pages 104 through 106. A summary of the sectional loads on the body interference shell is shown on pages 106 and 107.

The total velocities at the fin control points are shown on page 108, and the velocities at panel outboard edges are printed on page 109. Velocities and pressures on the upper and lower wing surfaces are shown on page 111. The pressure loadings at these points is shown on page 112. A summary of the linear pressure wing loads is printed on page 113.

Pages 114 and 115 contain the wing spanwise load distribution information used to determine the leading edge and side edge suction forces on the wing. The wing vorticity from these forces is also determined.

Page 116 contains a summary of the Bernoulli pressure loads acting on the wing.

Pages 117 through 119 contain the spanwise load distributions for the Bernoulli loadings. This information is used to determine the vorticity shed from the wing.

Page 120 begins the output for the afterbody calculation, step 3. This procedure is similar to the forebody calculation (step 1) except the procedure starts with initial vorticity from the forebody and wings. The pressure distribution on the body is calculated, and vorticity is shed and tracked along the afterbody from the wing trailing edge to the tail leading edge. The output is shown on pages 120 through 131. These pages are similar to the forebody pages described earlier.

The output for step 4 of the calculation procedure (tail fin section) is shown on pages 132 through 153. This output is similar to the output described for step 2 of the calculation procedure (wing section).

The final output page is number 154 which contains a summary of the forces and moments acting on the vehicle. Forces and moments are given in both the body rolled and unrolled coordinate systems as depicted in Figure 19.

CONCLUSIONS

Program DEMON3 for the engineering level prediction of pressures, component loads, and overall forces and moments acting on supersonic configurations is described. The addressable configuration consists of a body which may have noncircular cross section and up to two fin sets. Within a fin set, the lifting surfaces may be in cruciform, trifrom, planar, and low profile layouts. The planform of the lifting surfaces may have breaks in sweep, and are not limited to any restrictions in aspect ratio or taper ratio. Program DEMON3 is a combination of proven methodology including low order panel methods, body vortex shedding and tracking schemes, and optional nonlinear pressure calculation methods including effects of interference. The particular methods allow application to nonconventional configurations at angles of attack up to 25 deg, for Mach numbers up to approximately 2.5 if the linear theory/Bernoulli pressure methods are used, or up to Mach 6 if the optional nonlinear shock expansion and/or Newtonian pressure methods are engaged.

Comparisons with experimental data and other predictions for realistic, nonconventional configurations show that the DEMON3 program is capable of predicting overall aerodynamic forces, moments, and pressure distributions to a fair to good degree of accuracy. However, the nonlinear pressure calculation on the body should be extended to second order shock expansion.

On the basis of the findings reported herein, the following recommendations are offered:

- Additional testing needs to be performed to assess the range of applicability of the program further.

- Program DEMON3 can economically generate aerodynamic force distributions acting on the body and the lifting surfaces of nonconventional configurations. This capability makes DEMON3 a useful tool in preliminary structural analysis of the components of the configuration. In this application, DEMON3 should be equipped with a post processor for conversion of forces at aerodynamic control points to forces at user supplied structural analysis node or grid points. This technology is presently available (Refs. 8 and 12).

- The treatment of the center vortex in the vortex tracking scheme should be updated with the methodology very recently developed at NEAR for other aerodynamic prediction methods.

REFERENCES

1. Dillenius, M. F. E. and Nielsen, J. N.: Computer Programs for Calculating Pressure Distributions Including Vortex Effects on Supersonic Monoplane or Cruciform Wing-Body-Tail Combinations With Round or Elliptical Bodies. NASA CR-3122, April 1979.

2. Dillenius, M. F. E.: Improvements to Missile Aerodynamics Program DEMON2. NEAR TR 254, June 1982.

3. Mendenhall, M. R.: Prediction of Vortex Shedding From Circular and Noncircular Bodies in Supersonic Flow. NEAR TR 239, November 1981.

4. Mendenhall, M. R. and Perkins, S. C., Jr.: Prediction of Vortex Shedding From Circular and Noncircular Bodies in Supersonic Flow. NASA CR-3754, January 1984.

5. Lesieutre, D. J., Mendenhall, M. R., and Torres, T. O.: MISSILE STABILITY AND CONTROL METHODS DEVELOPMENT Vol. III, Programs SUBVTX and SUPVTX for Determining Aerodynamic Characteristics of Arbitrary Missile Bodies Including Separation Vorticity. NEAR TR 396, Vol. III, March 1990.

6. Dillenius, M. F. E.: Program LRCDM2, Improved Aerodynamic Prediction Program for Supersonic Canard-Tail Missiles With Axisymmetric Bodies. NASA CR-3883, April 1985.

7. Dillenius, M. F. E., Reed, R. R., and Keirstead, M. M.: Program NWCDM-NSTRN for Calculation of Forces at Nastran Grid Points on Supersonic Missile Configurations. NEAR TR 330, September 1984.

8. Dillenius, M. F. E., Perkins, S. C., Jr., and Lesieutre, D. J.: Modified NWCDM-NSTRN and Supersonic Store Separation Programs for Calculating NASTRAN Forces Acting on Missiles Attached to Supersonic Aircraft. NWC TP 6834, September 1987.

9. Dillenius, M. F. E. and Perkins, S. C., Jr.: Computer Program AMICDM, Aerodynamic Prediction program for Supersonic ARMY Type Missile Configurations With Axisymmetric Bodies. U.S. Army MICOM Technical Report RD-CR-84-15, June 1984.

10. Dillenius, M. F. E. and Keirstead, M. M.: Panel Methods Applied to Supersonic Inlets Alone and To Complete Supersonic Air Breathing Configurations. NASA CR-3979, May 1986.

11. Perkins, S. C., Jr. and Dillenius, M. F. E.: MISSILE STABILITY AND CONTROL METHODS DEVELOPMENT Vol. II, Program INLADD for Estimating Additive Forces and Moments for Supersonic Inlets. NEAR TR 396, Vol. II, March 1990.

12. Lesieutre, D. J., Dillenius, M. F. E., and Whittaker, C. H.: Program SUBSAL and Modified Subsonic Store Separation for Calculating NASTRAN Forces Acting on Missiles Attached to Subsonic Aircraft. NEAR TR 393, December 1991.

13. Woodward, F. A. and Landrum, E. J.: The Supersonic Triplet- A New Aerodynamic Panel Singularity with Directional Properties. AIAA Journal, Vol. 18, No. 2, February 1980.

14. Woodward, F. A.: An Improved Method For The Aerodynamic Analysis of Wing-Body-Tail Configurations in Subsonic and Supersonic Flow. NASA CR-2228. May 1973.

15. Carmichael, R. L. and Woodward, F. A.: An Integrated Approach to the Analysis and Design of Wings and Wing-Body Combinations in Supersonic Flow. NASA TN D-3685, October 1966.

16. Woodward, F. A.: Development of the Triplet Singularity for the Analysis of Wings and Bodies in Supersonic Flow. NASA CR 3466, September 1981.

17. Woodward, F. A.: USSAERO Computer Program Development, Versions B and C. NASA CR 3227, April 1980.

18. Carlson, H. W.: A Modification to Linearized Theory for Prediction of Pressure Loadings on Lifting Surfaces at High Supersonic Mach Numbers and Large Angles of Attack. NASA TP-1406, February 1979.

19. Dillenius, M. F. E. and Allen, J. M.: Paneling Methods with Vorticity Effects and Corrections for Nonlinear Compressibility. Progress in Astronautics and Aeronautics, Volume 104, Chapter XIII, 1986.

20. Hammitt, A. G. and Murthy, K. R. A.: Approximate Solutions for Supersonic Flow Over Wedges and Cones. Journal of the Aero/Space Sciences, January 1960.

21. Pittman, J. L.: Application of Supersonic Linear Theory and Hypersonic Impact Methods to Three Nonslender Hypersonic Airplane Concepts at Mach Numbers From 1.10 to 2.86. NASA TP 1539, December 1979.

22. Blair, A. B., Jr., Allen, J. M., and Hernandez, G.: Effect of Tail Fin Span on Stability and Control Characteristics of a Canard Controlled Missile at Supersonic Mach Numbers, NASA TP 2157, June 1983.

23. Covell, P. F.: Supersonic Aerodynamic Characteristics of Canard, Tailless, and Aft-Tail Configurations for Two Wing Planforms, NASA TP 2434, June 1985.

24. Mendenhall, M. R., Lesieutre, D. J., Caruso, S. C., Dillenius, M. F. E., and Kuhn, G. D.: AERODYNAMIC DESIGN OF PEGASUS[TM] Concept to Flight with CFD, AIAA Paper 91-0190, January 1991.

25. Stallings, R. L. Jr. and Lamb, M.: Wing-Alone Aerodynamic Characteristics for High Angles of Attack at Supersonic Speeds. NASA TP 1889, July 1981.

26. Landrum, E. J. : Wind-Tunnel Pressure Data at MAch Numbers From 1.6 to 4.63 for a Series of Bodies of Revolution at Angles of Attack from -4° to 60°. NASA TM X-3558, October 1977.

27. Lesieutre, D. J., Mendenhall, M. R., Nazario, S. M., and Hemsch, M. J.: Prediction of the Aerodynamic Characteristics of Cruciform Missiles Including Effects of Roll Angle and Control Deflection. NEAR TR-360, Revised August 1987.

28. Vukelich, S. R., and Jenkins, J. E.: Missile DATCOM: Aerodynamic Prediction of Conventional Missiles Using Component Build-Up Techniques, AIAA Paper 84-0388, January 1984.

29. Development, Test, and Verify an Aeroelastic Tailoring Procedure to Optimize the Placement and Control of Missile Fin Center of Pressure to Minimize fin Hinge Moments and Control Fin Actuator Power. Work being preformed under Contract N00019-88-C-0071, Department of the Navy, Naval Air Systems Command.

TABLE I

Routines of program DEMON3

The designation .f signifies routines in source code

1. aicbod.f	17. dphidt.f	33. lubksb.f	49. seprat.f	65. thetin.f
2. aicwgb.f	18. dtable.f	34. ludcmp.f	50. shape.f	66. thkin.f
3. amap.f	19. dzdnu.f	35. matmul.f	51. shkagl.f	67. thklyt.f
4. asum.f	20. edges. f	36. mxout.f	52. shkexp.f	68. thkout.f
5. bdyshl.f	21. elnose.f	37. newrad.f	53. shkxb.f	69. thkvel.f
6. bipan.f	22. f.f	38. panel.f	54. smooth.f	70. tolds.f
7. bmap.f	23. fincon.f	39. pinpnl.f	55. solve.f	71. vcentr.f
8. bodpan.f	24. finsec.f	40. plotv.f	56. sorpan.f	72. velnor.f
9. bodvel.f	25. finvel.f	41. prcor.f	57. specld.f	73. velo.f
10. cmap.f	26. forcep.f	42. prcorb.f	58. specpr.f	74. veloth.f
11. combin.f	27. formom.f	43. prstrt.f	59. spnld.f	75. vlocty.f
12. config.f	28. fpvel.f	44. rhsfin.f	60. srfvel.f	76. volume.f
13. confor.f	29. gaussj.f	45. rotbw.f	61. sum.f	77. vtable.f
14. cpbern.f	30. geom.f	46. rotfw.f	62. suppan.f	78. xlocat.f
15. demon3.f	31. inpt.f	47. rotwb.f	63. thdih.f	79. z.f
16. dfeqkm.f	32. layout.f	48. rotwf.f	64. thetax.f	

TABLE II

```
PROGRAM
DEMON3

   |--TOLDS
   |--INPT ----PRSTRT
   |       |--CONFOR----Z
   |--ELNOSE----F    ----SHAPE
   |       |           |--BMAP ----AMAP ----Z
   |       |           |--CMAP ----DZDNU
   |       |           |       |--Z
   |       |           |--AMAP ---Z
   |       |           |--BODVEL----SUPPAN
   |       |           |       |--SORPAN
   |       |           |--VLOCTY----SUM ----DZDNU
   |       |                   |--SMOOTH
   |       |                   |--ASUM
   |       |--SHAPE
   |       |--BMAP ----AMAP ----Z
   |       |--CMAP ----DZDNU
   |       |       |--Z
   |       |--GEOM ----CONFIG
   |       |       |--NEWRAD
   |       |       |--BODPAN----PANEL
   |       |--AICBOD----BODVEL----SUPPAN
   |       |               |--SORPAN
   |       |--SOLVE ----LUDCMP
   |       |       |--LUBKSB
   |       |       |--MATMUL
   |       |       |--VOLUME
   |       |--SRFVEL
   |       |--VLOCTY----SUM ----DZDNU
   |       |       |--SMOOTH
   |       |       |--ASUM
   |       |--DPHIDT----SMOOTH
   |       |--THETAX----SHAPE
   |       |       |--BMAP ----AMAP ----Z
   |       |--SHKXB ----THDIH
   |       |--PRCORB
   |       |--FORCEP
   |       |--PLOTV ----PLOTA2----PLOTA8----PLOTA6
   |       |               |       |--PLOTA5
   |       |               |--PLOTA7
   |       |--FPVEL ----CMAP ----DZDNU
   |       |       |       |--Z
   |       |       |--BODVEL----SUPPAN
   ↓       ↓       ↓           |--SORPAN
```

- 60 -

```
Y     Y       Y--VLOCTY----SUM  ----DZDNU
|     |         |--SMOOTH
|     |         |--ASUM
|     |--SEPRAT
|     |--VTABLE
|     |--DFEQKM----F   ----SHAPE
|     |           |--BMAP ----AMAP ----Z
|     |           |--CMAP ----DZDNU
|     |           |     |--Z
|     |           |--AMAP ----Z
|     |           |--BODVEL----SUPPAN
|     |           |    |--SORPAN
|     |           |--VLOCTY----SUM  ----DZDNU
|     |                   |--SMOOTH
|     |                   |--ASUM
|     |--AMAP ----Z
|     |--DTABLE
|     |--VCENTR
|     |--COMBIN
|     |--TOLDS
|--FINCON----FINSEC----LAYOUT
|         |       |--THKIN ----EDGES
|         |       |     |--THETIN
|         |       |--THKOUT
|         |       |--THKLYT
|         |       |--XLOCAT
|         |       |--BIPAN
|         |--AICWGB---VELNOR---ROTWF
|         |          |--ROTWB
|         |          |--VELO
|         |          |--ROTFW
|         |          |--ROTBW
|         |--BODVEL---SUPPAN
|         |    |--SORPAN
|         |--CMAP ----DZDNU
|         |     |--Z
|         |--VLOCTY----SUM  ----DZDNU
|         |     |--SMOOTH
|         |     |--ASUM
|         |--RHSFIN----THKVEL---PINPNL
|         |    |      |--ROTWF
|         |    |      |--VELOTH
|         |    |      |--ROTFW
|         |    |--LUDCMP
|         |    |--LUBKSB
|         |    |--MATMUL
|         |--BDYSHL----CPBERN
|         |     |--FORMOM
↓         ↓--TOLDS
```

- 61 -

```
|--FINVEL----VELNOR----ROTWF
|        |        |--ROTWB
|        |        |--VELO
|        |        |--ROTFW
|        |        |--ROTBW
|        |--ROTWF
|        |--ROTFW
|--SPECPR----ROTWF
      |--SHKEXP----ROTWF
      |        |--SHKAGL
      |--VELNOR----ROTWF
      |        |--ROTWB
      |        |--VELO
      |        |--ROTFW
      |        |--ROTBW
      |--THKVEL----PINPNL
      |        |--ROTWF
      |        |--VELOTH
      |        |--ROTFW
      |--PINPNL
      |--CPBERN
      |--PRCOR
      |--SPECLD----ROTWF
      |--ROTFW
      |--TOLDS
      |--SPNLD ----ROTWF
             |--ROTFW
             |--TOLDS
```

PROGRAM
END

TABLE III

PROGRAM STOPS

stop number	explanation	subroutine
20		bodpan
50		bodpan
60		bodpan
unnumbered	normal stop	demon3
201		dtable
202		dtable
unnumbered	bad argument	dtable
40		elnose
41		elnose
44		elnose
45		elnose
46		elnose
5		inpt
unnumbered	too many vorticies	inpt
unnumbered	np dimension to high	ludcmp
unnumbered	singular matrix	ludcmp
120		newrad
130		newrad
90		pinpnl
unnumbered	illegal argument for sqrt	shkagl
unnumbered	illegal argument for acos	shkagl
unnumbered	illegal argument for asin	shkxb
unnumbered	hs is negative	shkxb
unnumbered	to many triplet panels	solve
201		vtable
202		vtable
unnumbered	bad argument	vtable
unnumbered	cannot find triplet panel for interference shell	xlocat

TWO DIMENSIONAL FLOW

CONSTANT SOURCE

CONSTANT VORTEX
(LINEARLY VARYING
DOUBLET SHEET)

CONSTANT TRIPLET
(UNI-DIRECTIONAL)

$u = 0$
$w = 0$

(a)   Supersonic triplet concept.

ELEMENTARY SOURCE / VORTEX FILAMENT

CONTROL POINT

M_∞

A

A

TANGENTIAL VELOCITY DISTRIBUTION
SECTION A-A

X_B
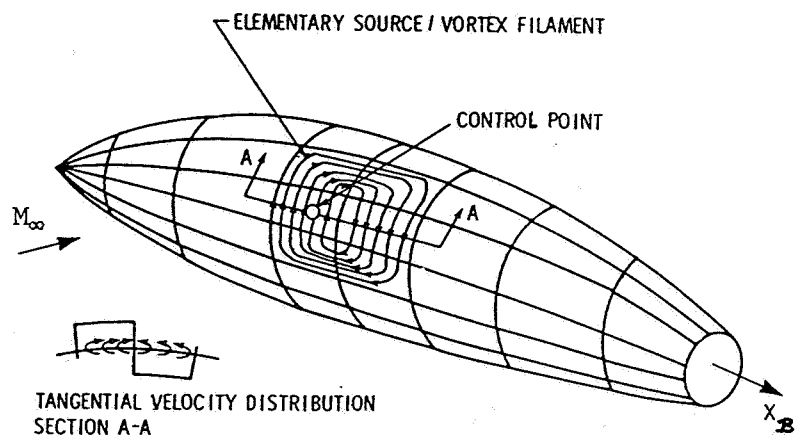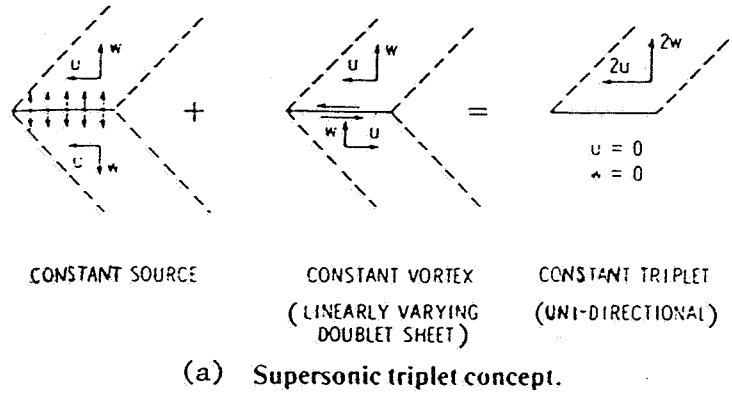
(b)   Triplet panel grouping on arbitrary body at incidence.

Figure 1. – Triplet panel concept and layout on
the body.
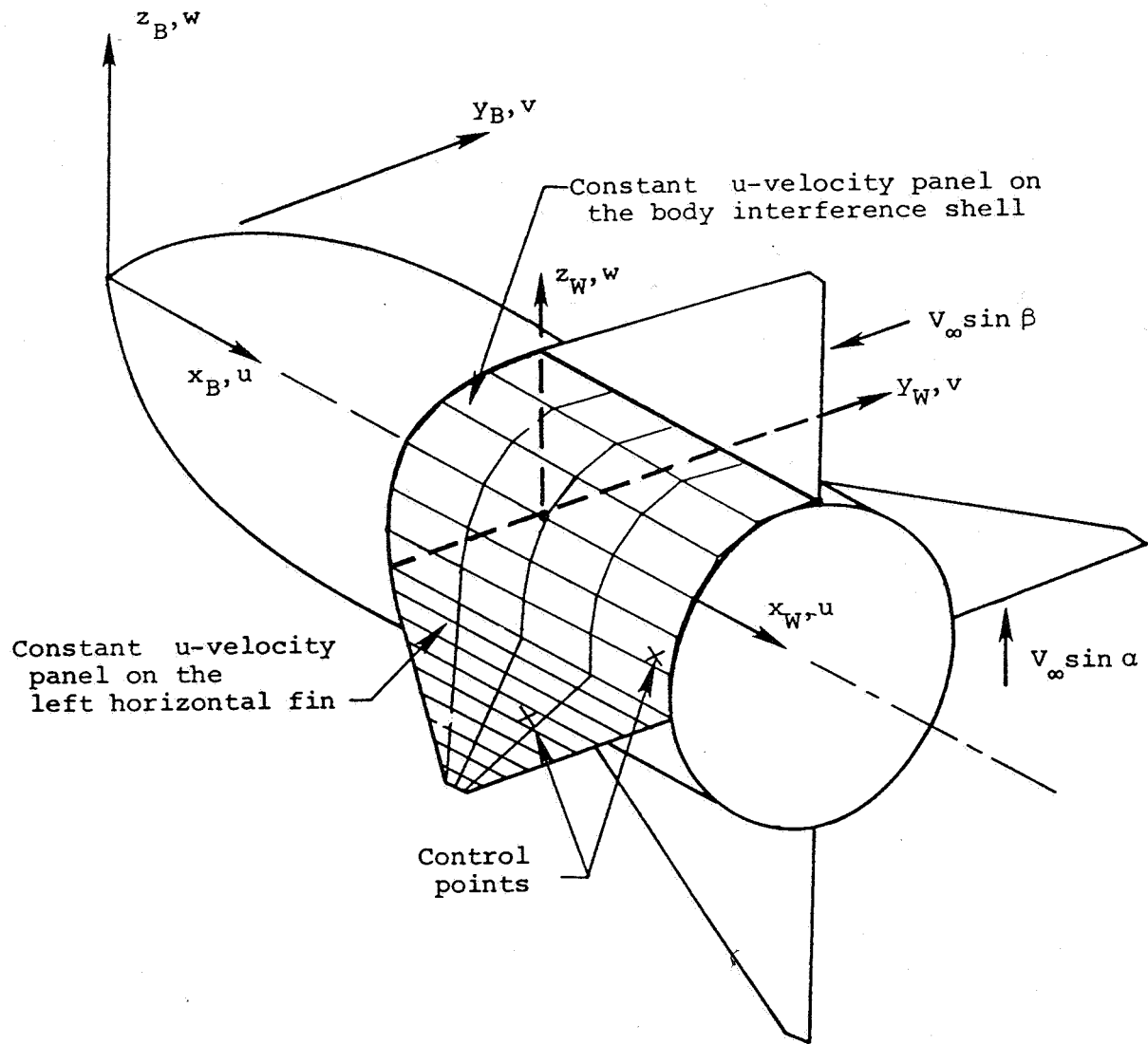
Figure 2. – Coordinate systems and typical panel layout shown for one fin and quarter of the interference shell.

$\dfrac{\Gamma}{2\pi DV_{\infty}} = 0.081$

0.261

0.183

$x/L = 0.32$

$x/L \approx 1.0$

$x/L = 0.64$

0.32

0.64

Vapor screen

$x/L \approx 1.0$

EXPERIMENT

Theory

(a) $\phi = 0°$
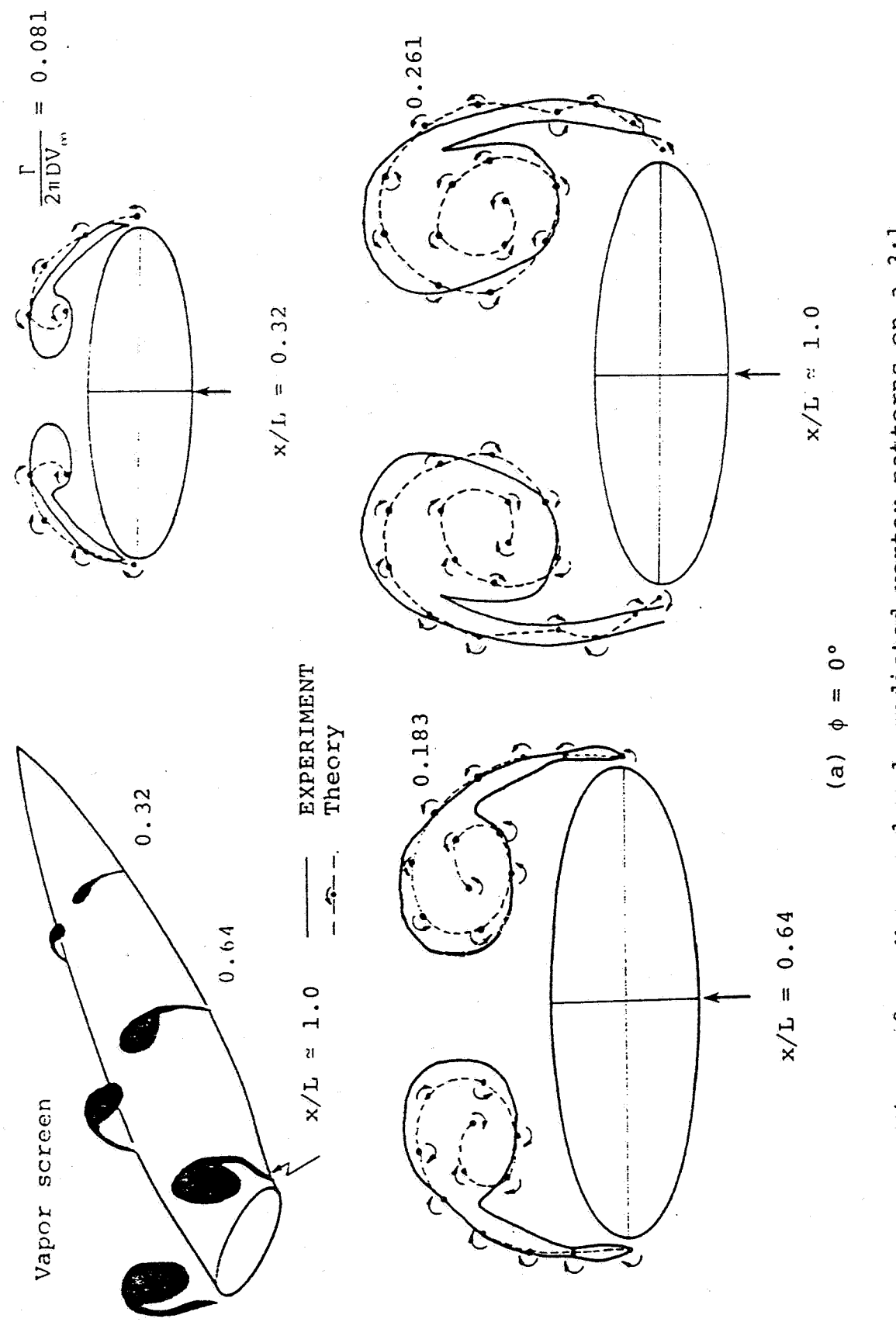
Figure 3. - Measured and predicted vortex patterns on a 3:1 elliptic cross section body at $M_{\infty} = 2.5$ and $\alpha_C = 20°$.

-66-

$$\frac{\Gamma}{2\pi DV_\infty} = 0.080$$

−0.036

x/L = 0.32

0.255

x/L ≃ 1.0

−0.116

EXPERIMENT
Theory

Vapor screen

0.32

0.64

x/L ≃ 1.0

0.183

−0.064

x/L = 0.64

(b) φ = 45°

Figure 3 .−Concluded.

Forebody   Fin   section

                                         Afterbody

Vortex feeding sheet

Mach cone

                                    Leading and
                                    side-edge vortex

                    Trailing-edge vortex
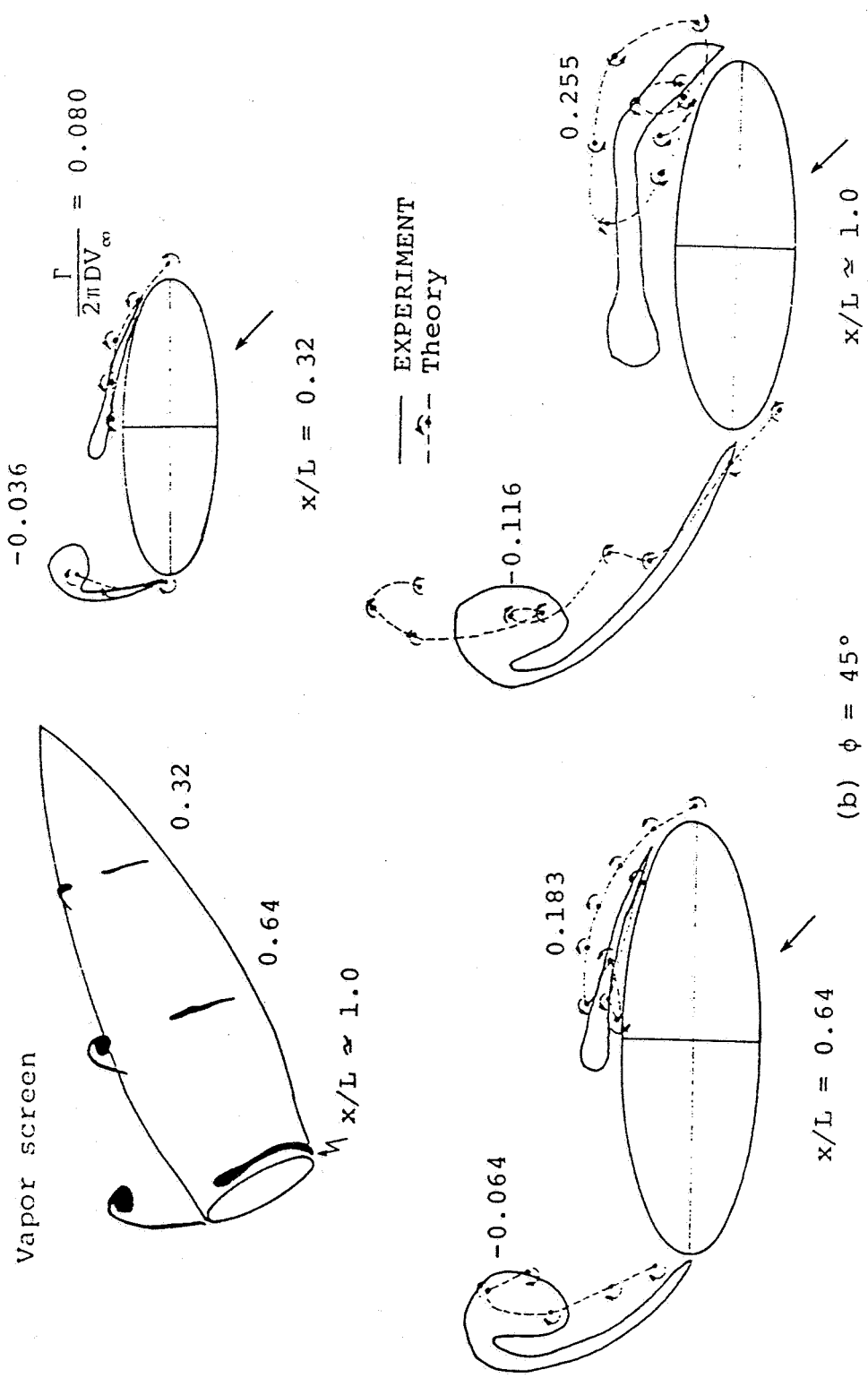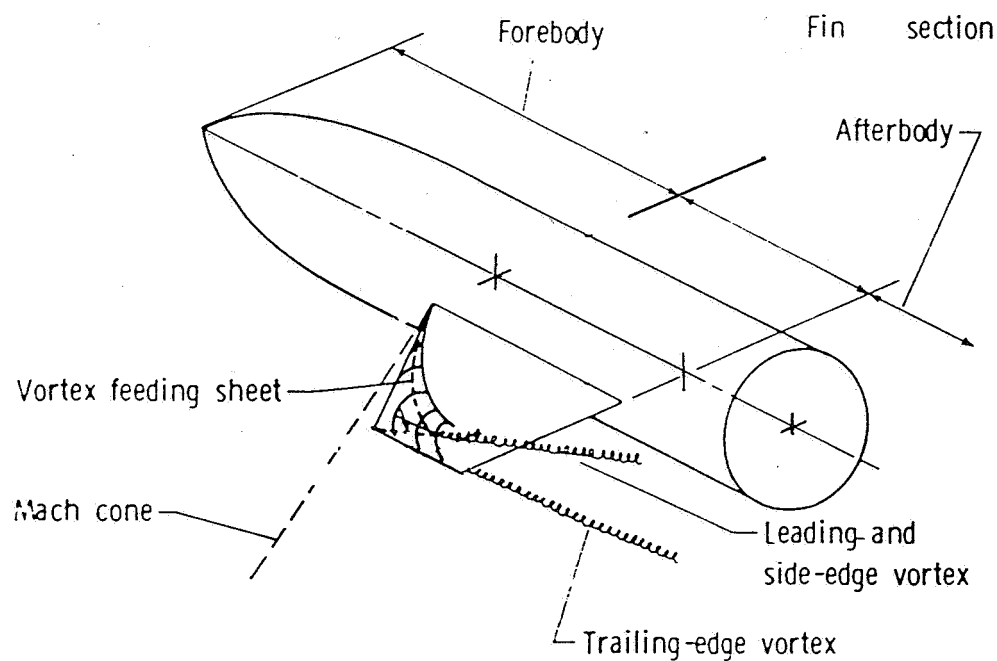
Typical leading- and side-edge vortex development.

Figure 4. - Fin wake model.
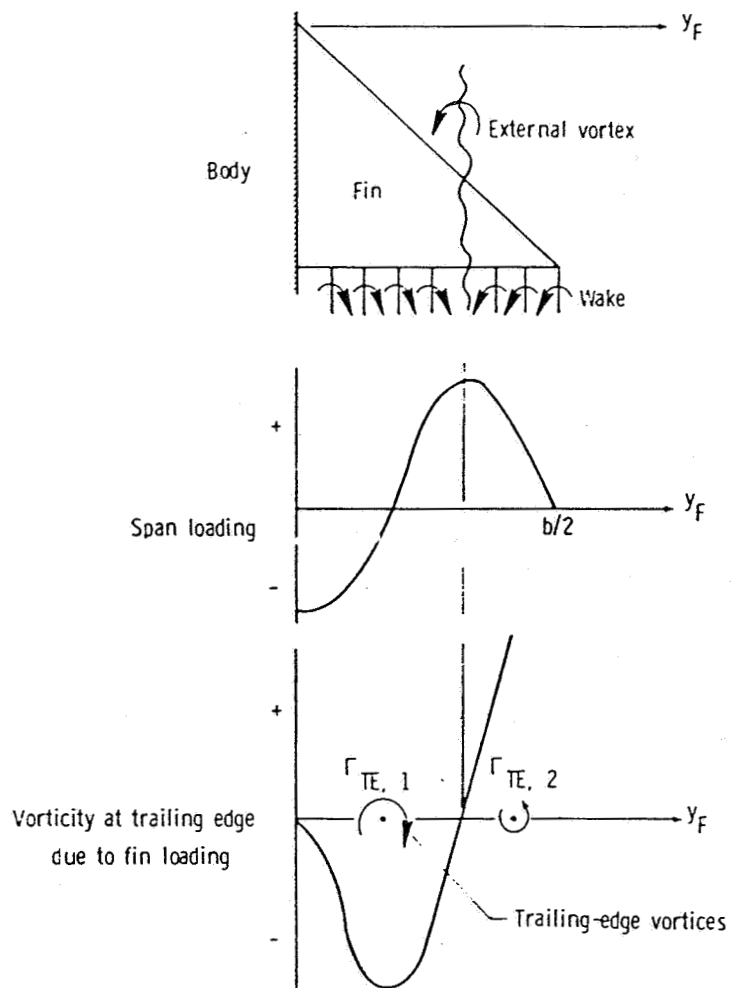
Figure 5. – Span loading and vorticity distribution on a delta wing in the presence of an external vortex.

(b) Pitching-moment coefficient

(a) Normal-force coefficient
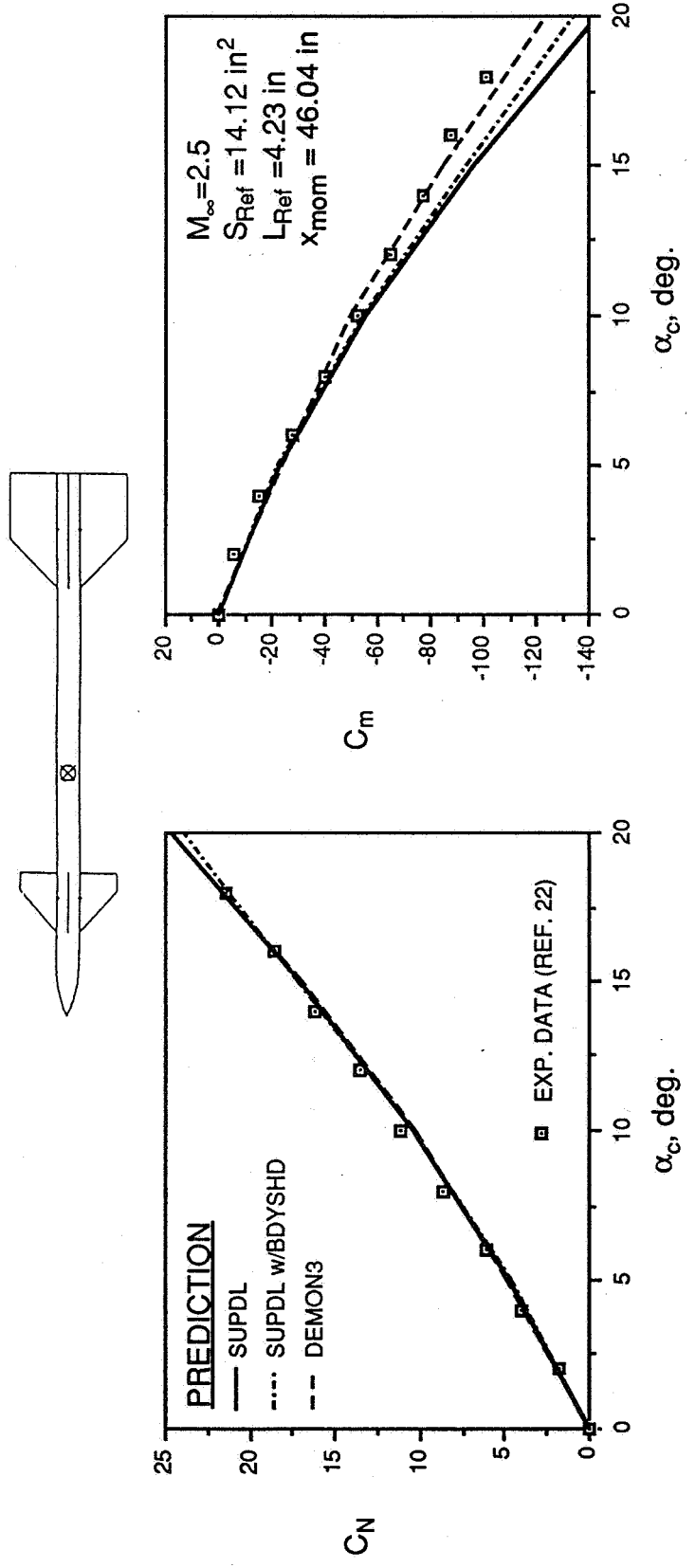
Figure 6. - Comparison of predicted and measured aerodynamic characteristics for the canard-body-tail model in Reference 22, $M_\infty = 2.5$, $\phi = 0°$, and $\delta_{2,4} = \pm5°$ roll control.
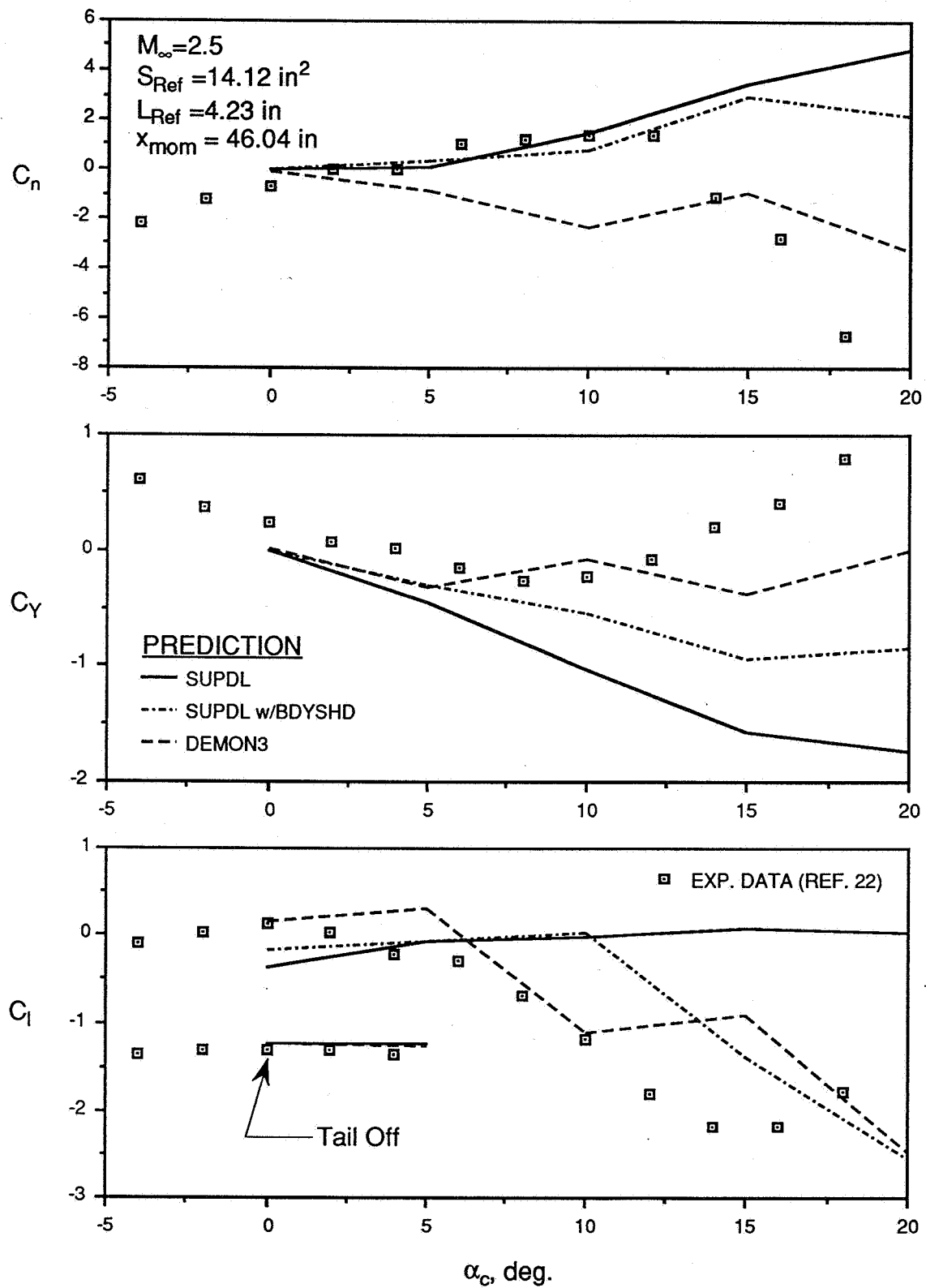
Figure 7. – Comparison of predicted and measured aerodynamic characteristics for the canard-body-tail model in Reference 22, $M_\infty = 2.5$, $\phi = 0°$, and $\delta_{2,4} = \pm 5°$ roll control.

WING PLANE ——————|—+—|—————— AFT-TAIL PLANE

SECT A-A

1.000

1.500

SECT B-B

TRANSITION SECTIONS

SIDE VIEW

MS 0.000   11.850   15.350   20.150   25.150   38.034

A   B

A   B

20.141
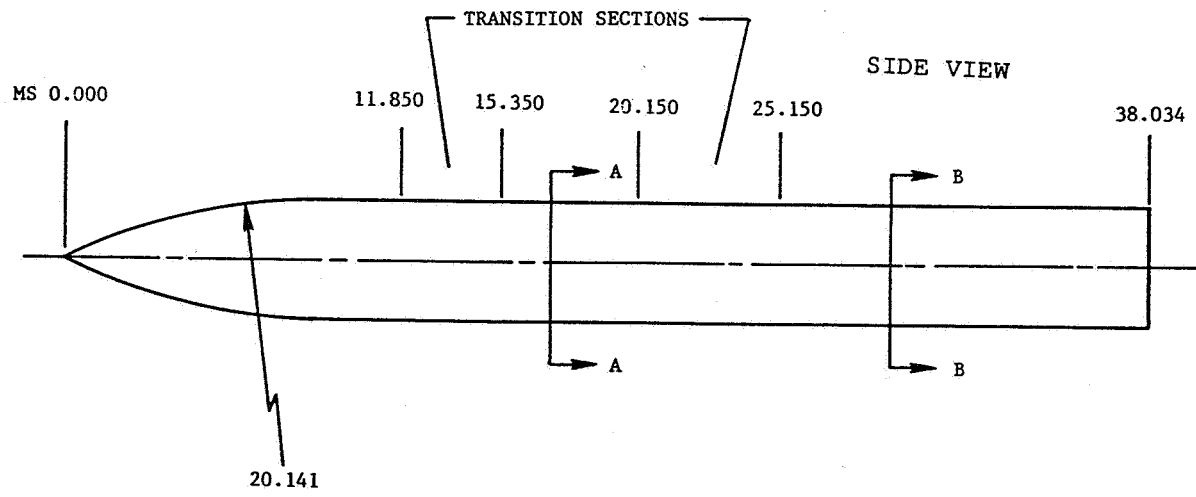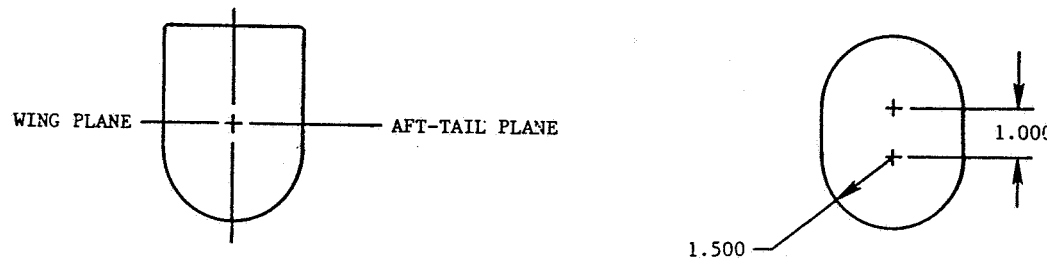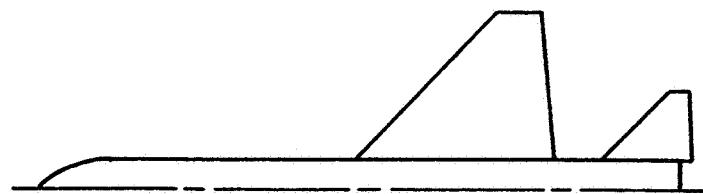
All dimensions in inches

Figure 8. - Configuration geometry of the wind tunnel model of Reference 23.
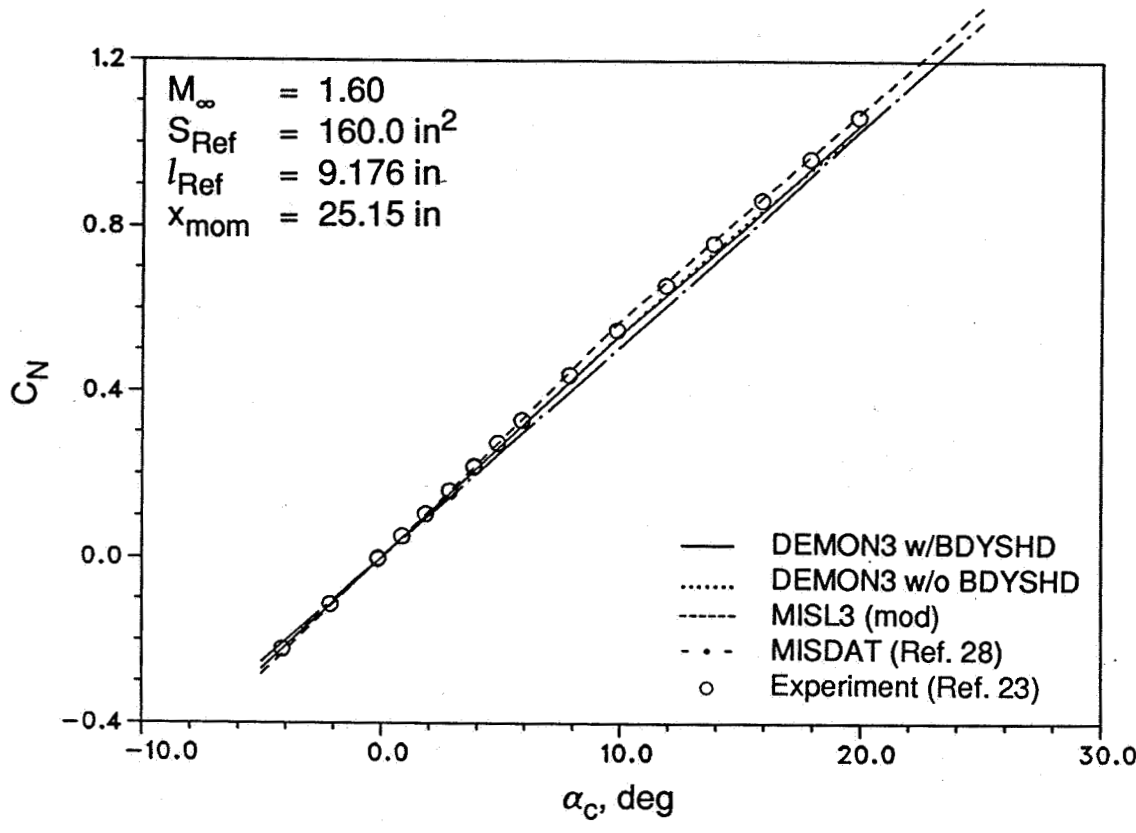
(a) Normal-force coefficient
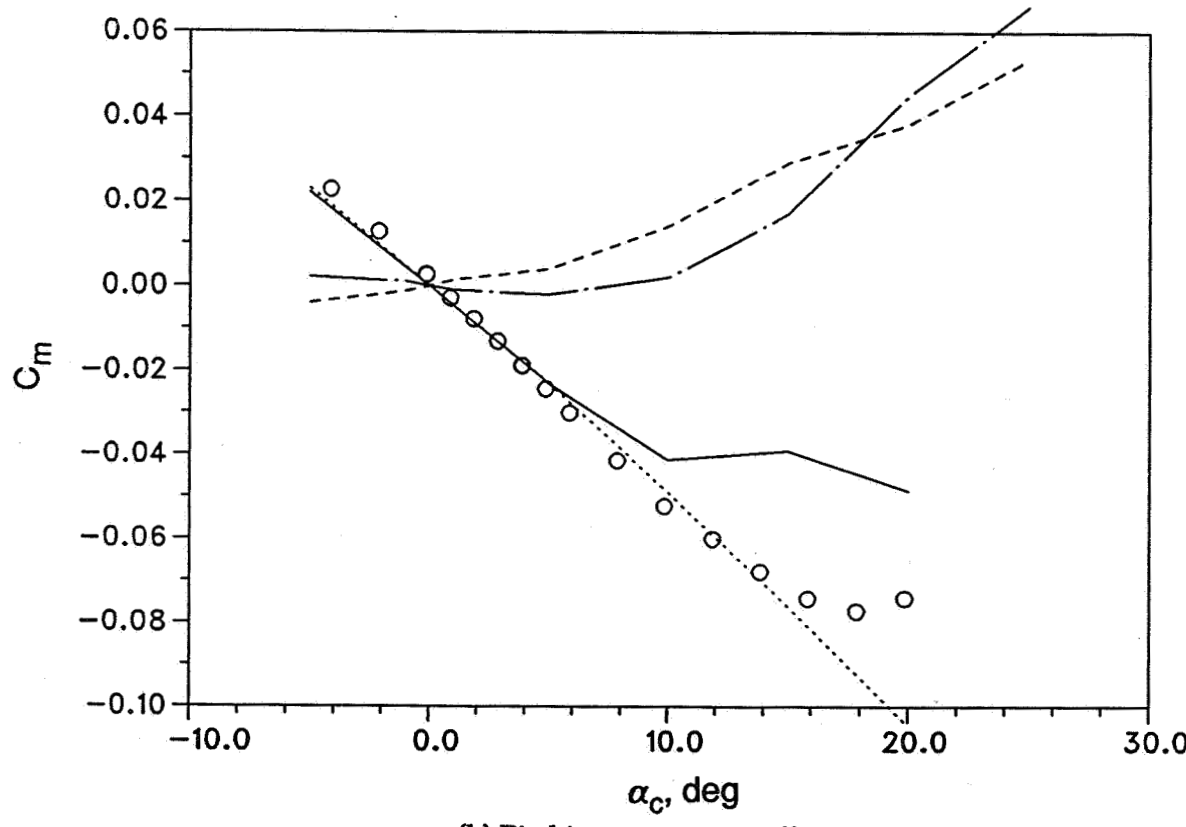
(b) Pitching-moment coefficient

Figure 9. – Comparison of predicted and measured aerodynamic characteristics for the wing-body-tail model in Reference 23, $M_\infty = 1.6$ and $\phi = 0°$.
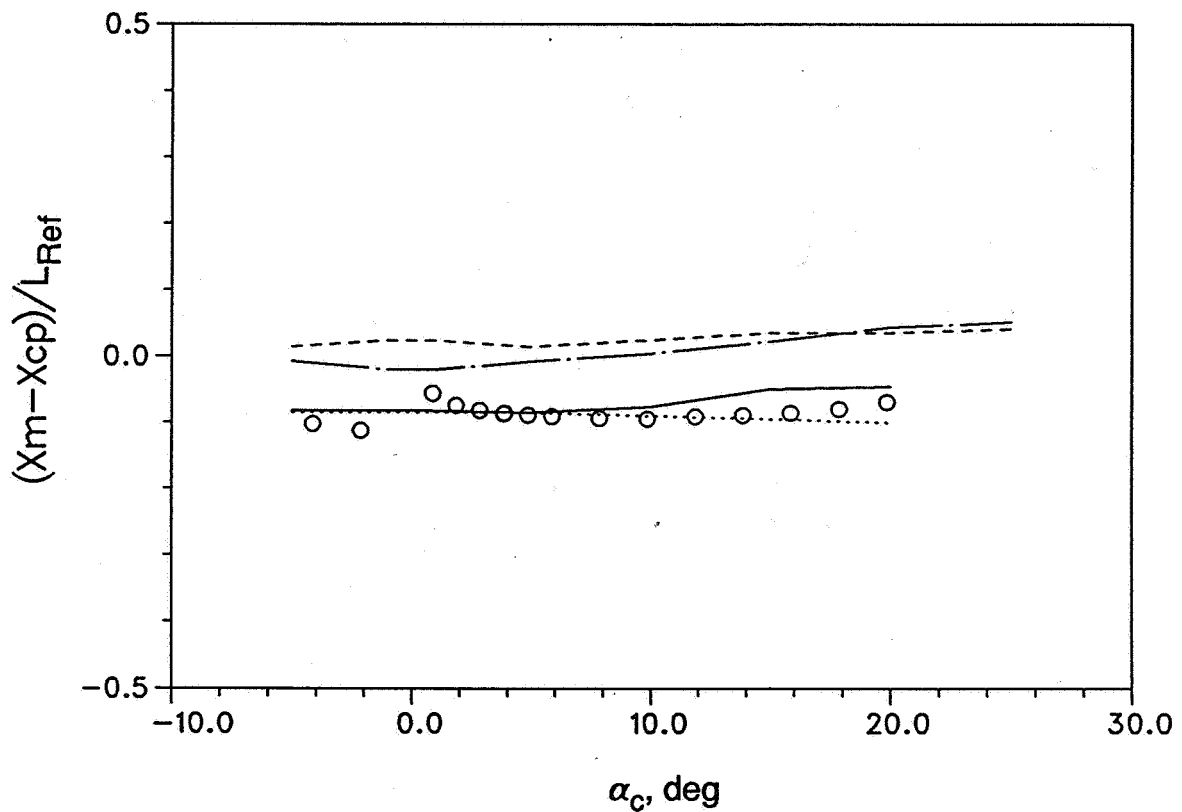
(c) Configuration center of pressure

Figure 9. - Concluded.
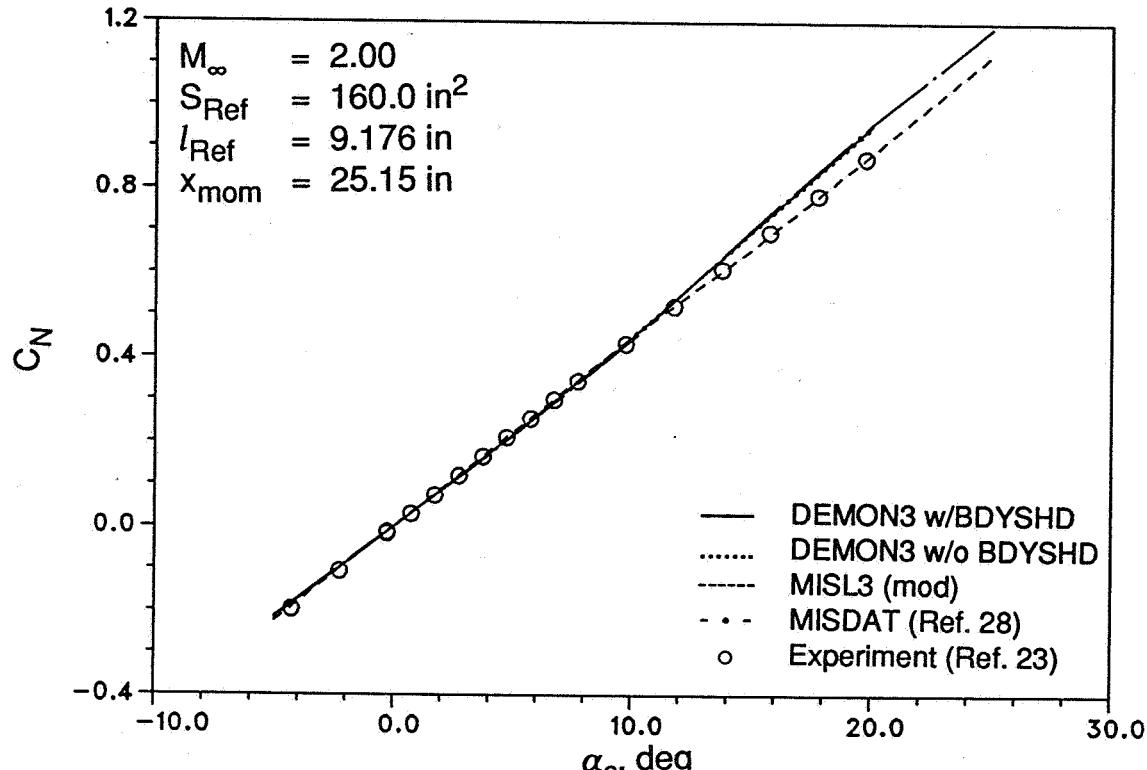
(a) Normal-force coefficient
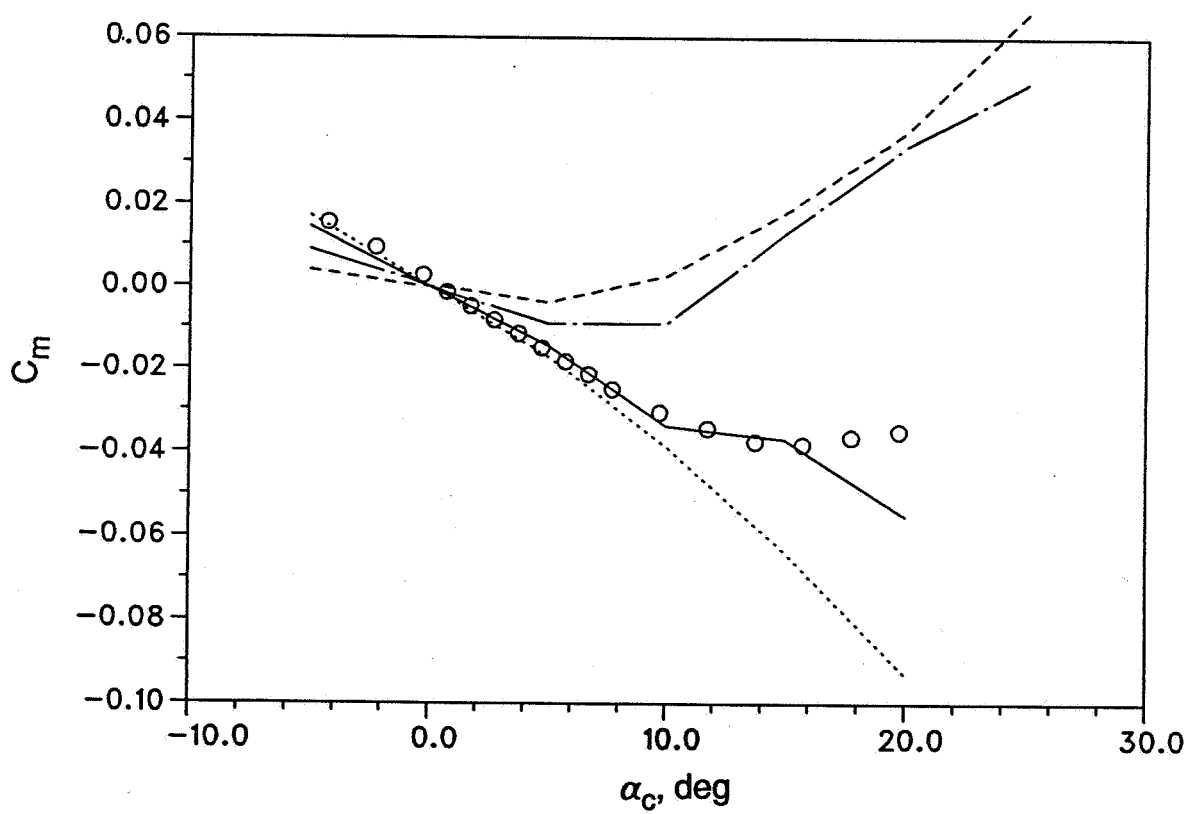
(b) Pitching-moment coefficient

Figure 10. - Comparison of predicted and measured aerodynamic characteristics for the wing-body-tail model in Reference 23, $M_\infty = 2.0$ and $\phi = 0°$.
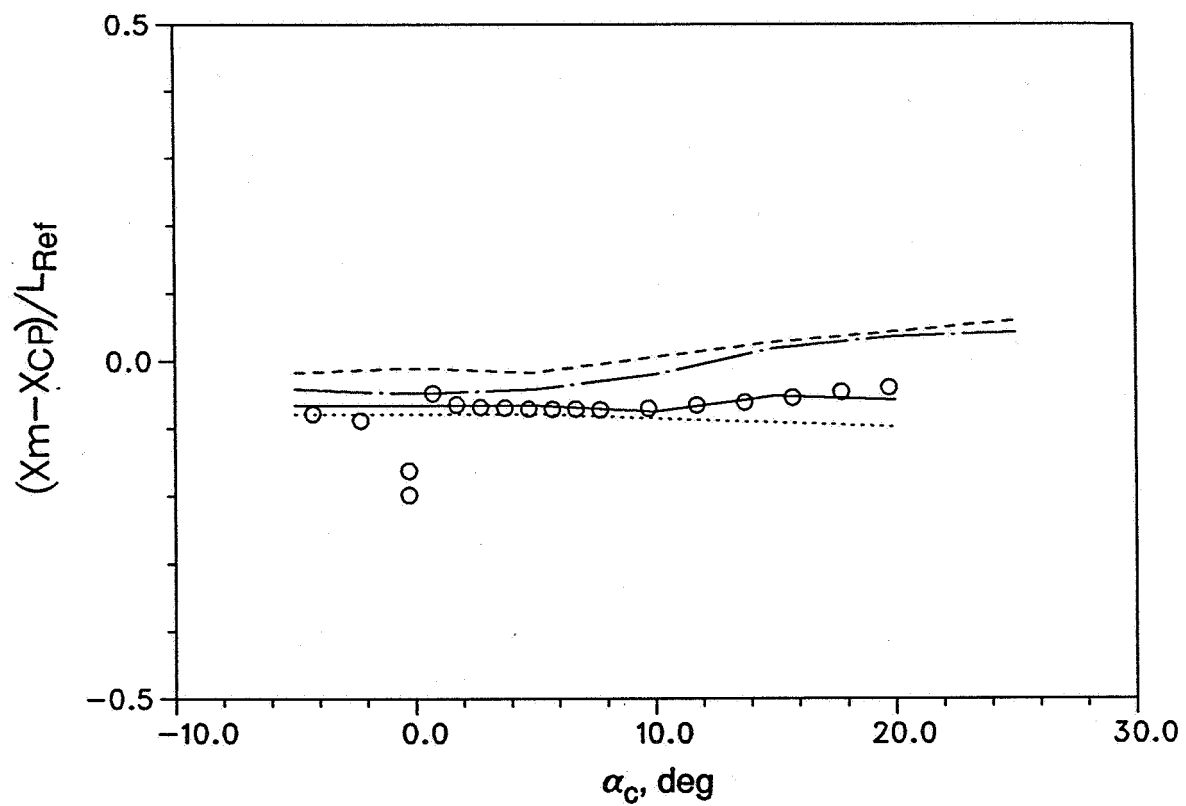
(c) Configuration center of pressure

Figure 10. - Concluded.

49.34

14.17

22
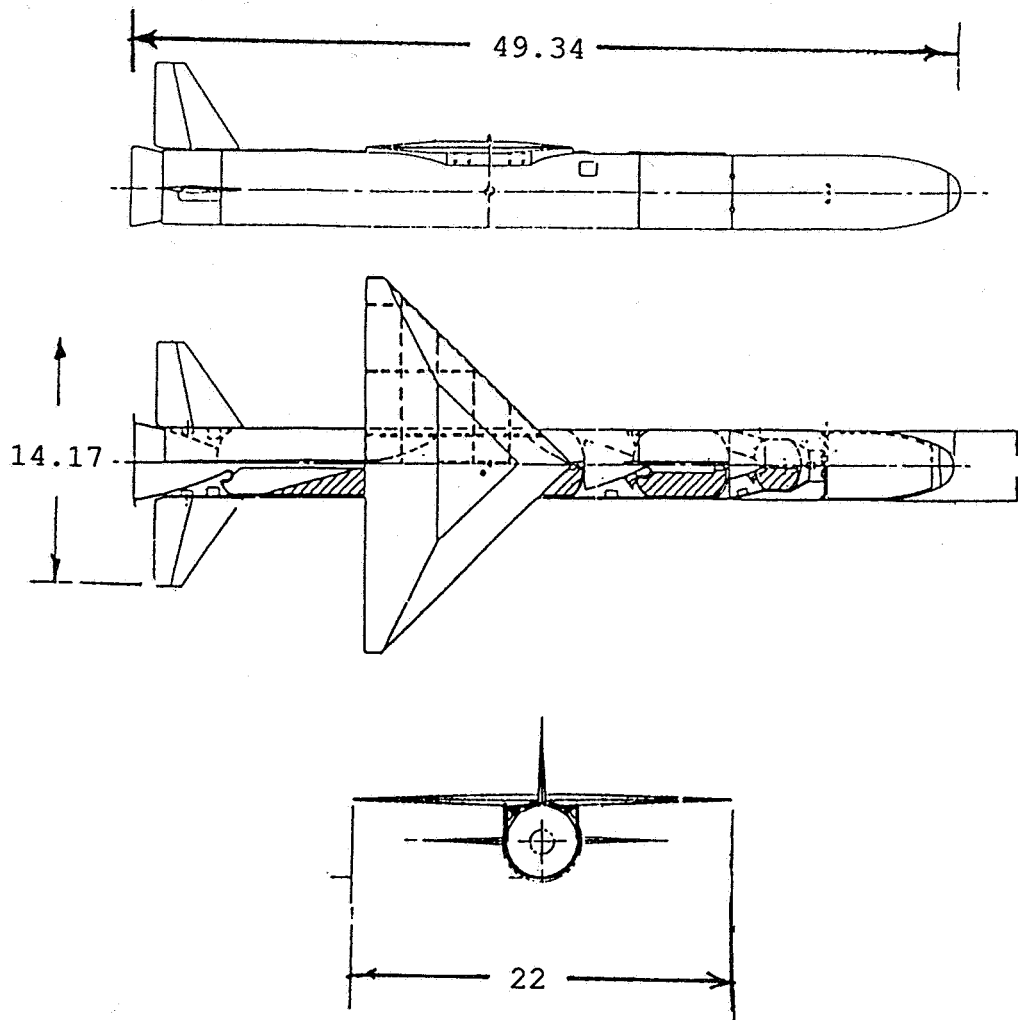
All dimensions in feet

Figure 11.- Configuration geometry of the Pegausus™ launch vehicle, Reference 24.
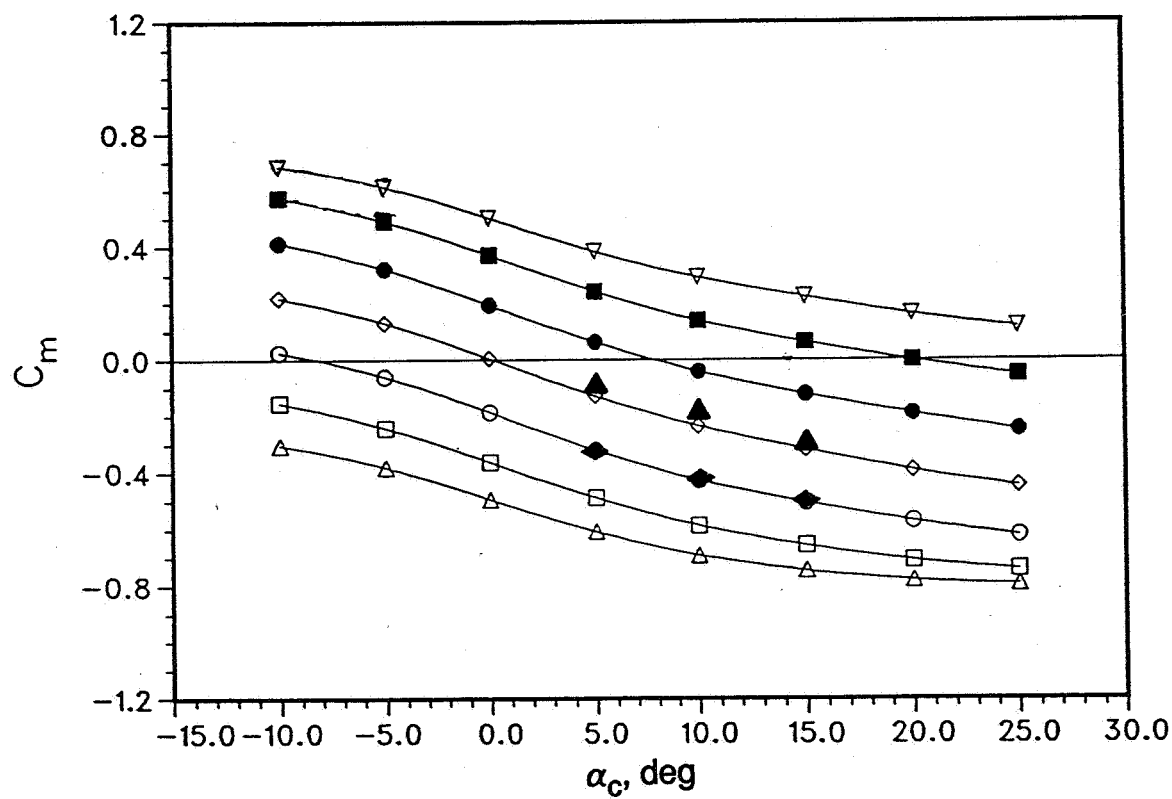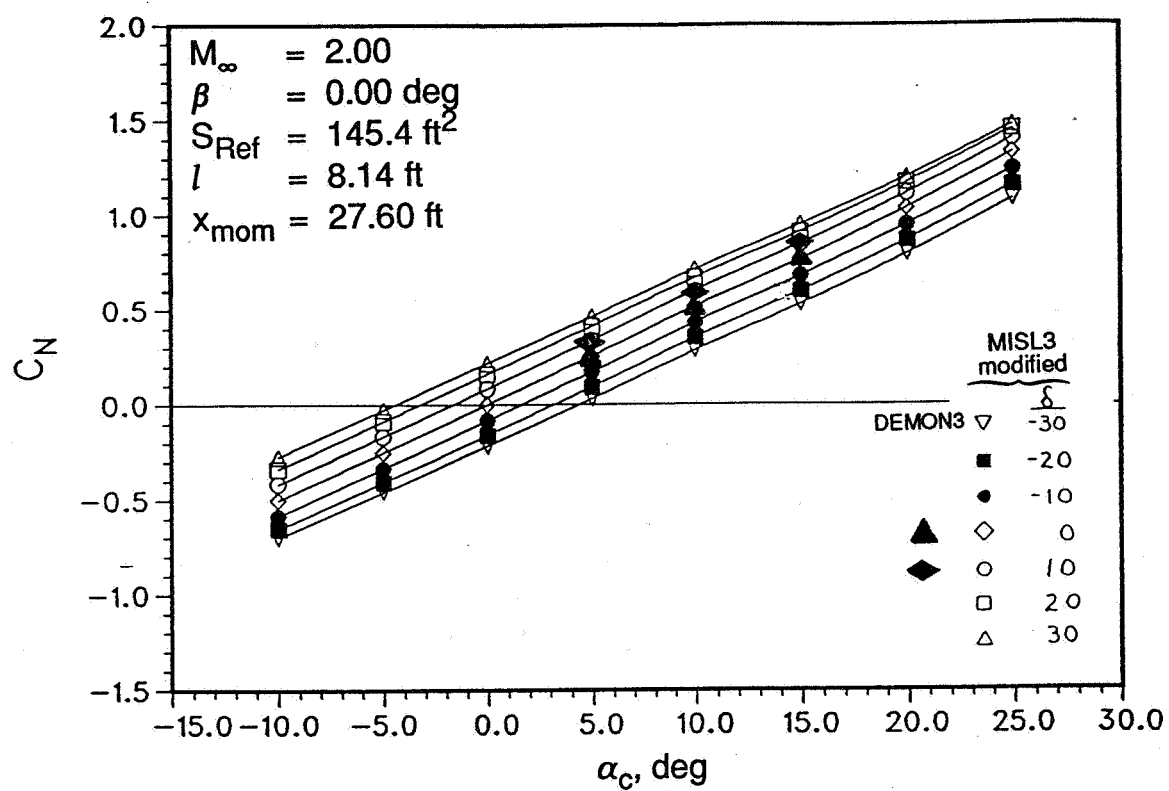
Figure 12. – Comparison of DEMON3 predicted and modified MISL3 predicted aerodynamic characteristics for the Pegasus[TM] launch vehicle, Reference 24, $M_\infty = 2.0$, $\phi = 0°$ with and without pitch deflection.
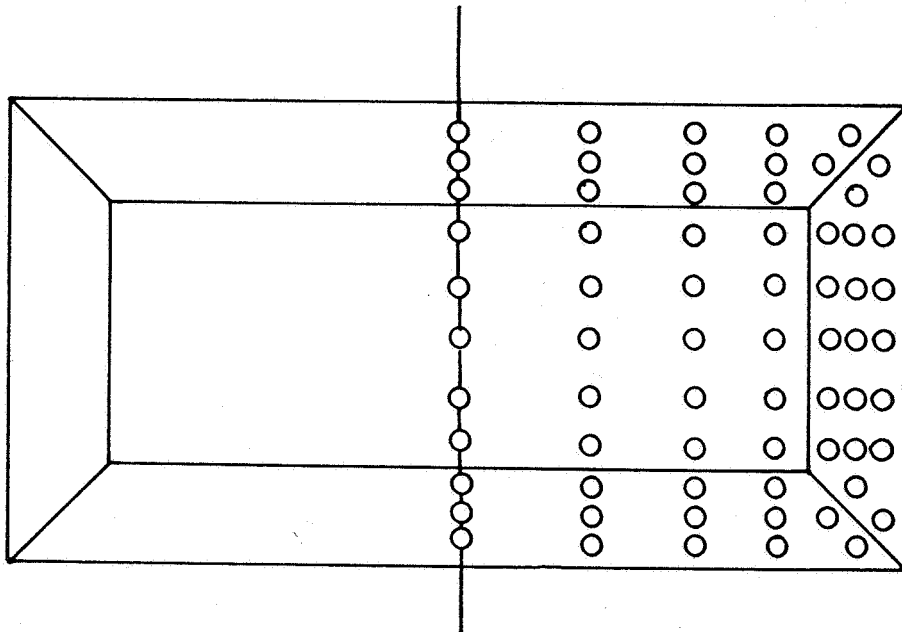
Pressure tap layout (Ref. 25)

All dimensions in centimeters
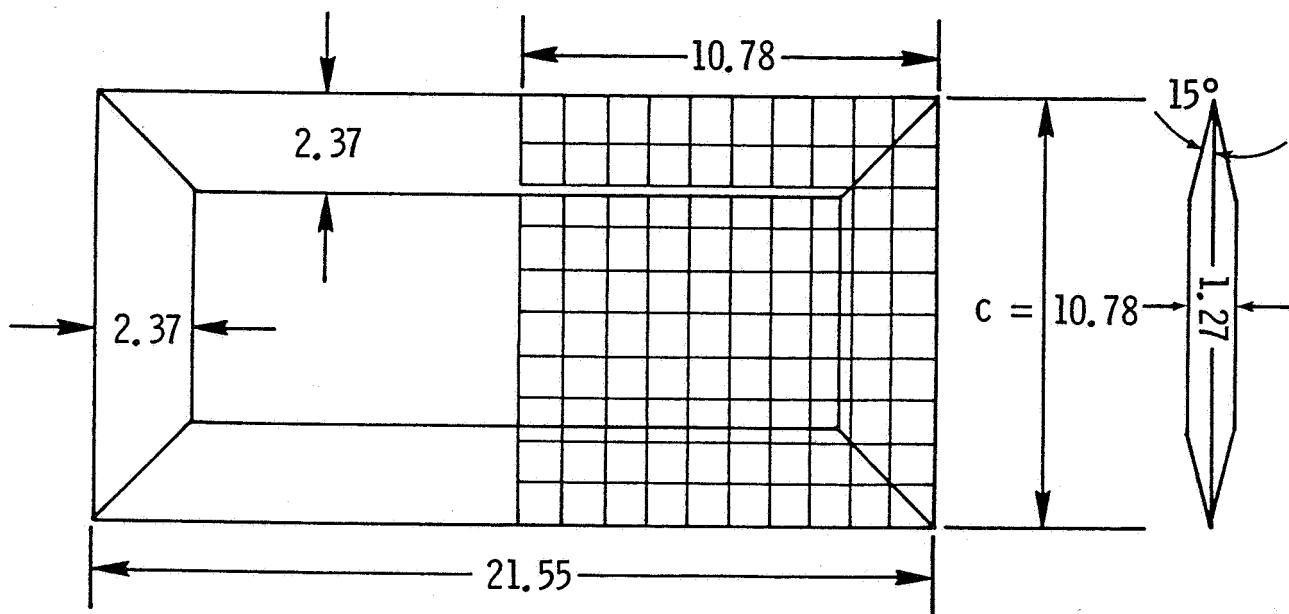
Paneling layout

Figure 13. – Panel and pressure tap layout on a rectangular wing.

Figure 14.— Theoretical and experimental chordwise pressure distribution on a rectangular wing at M_∞=2.86 and α_c=10.3 deg.
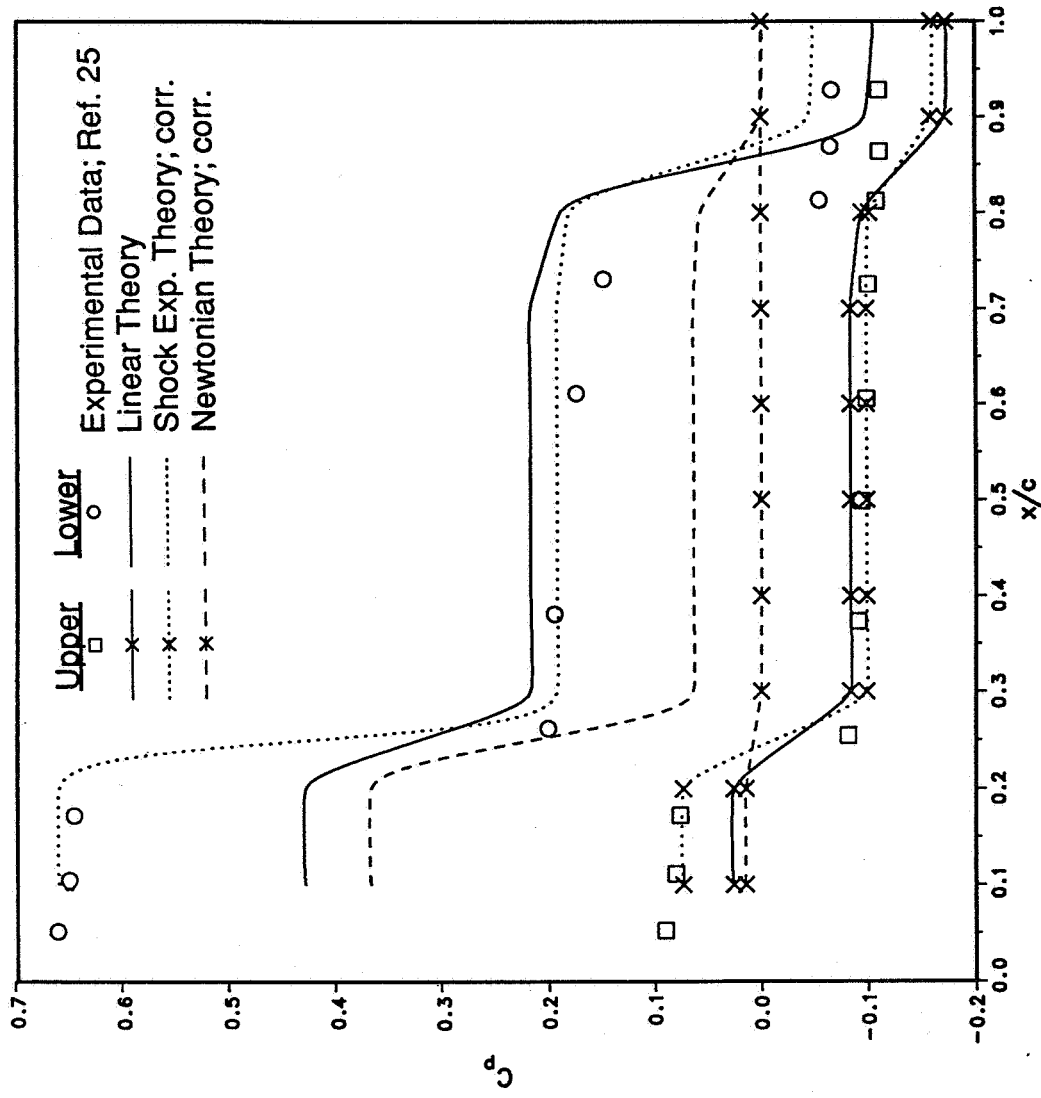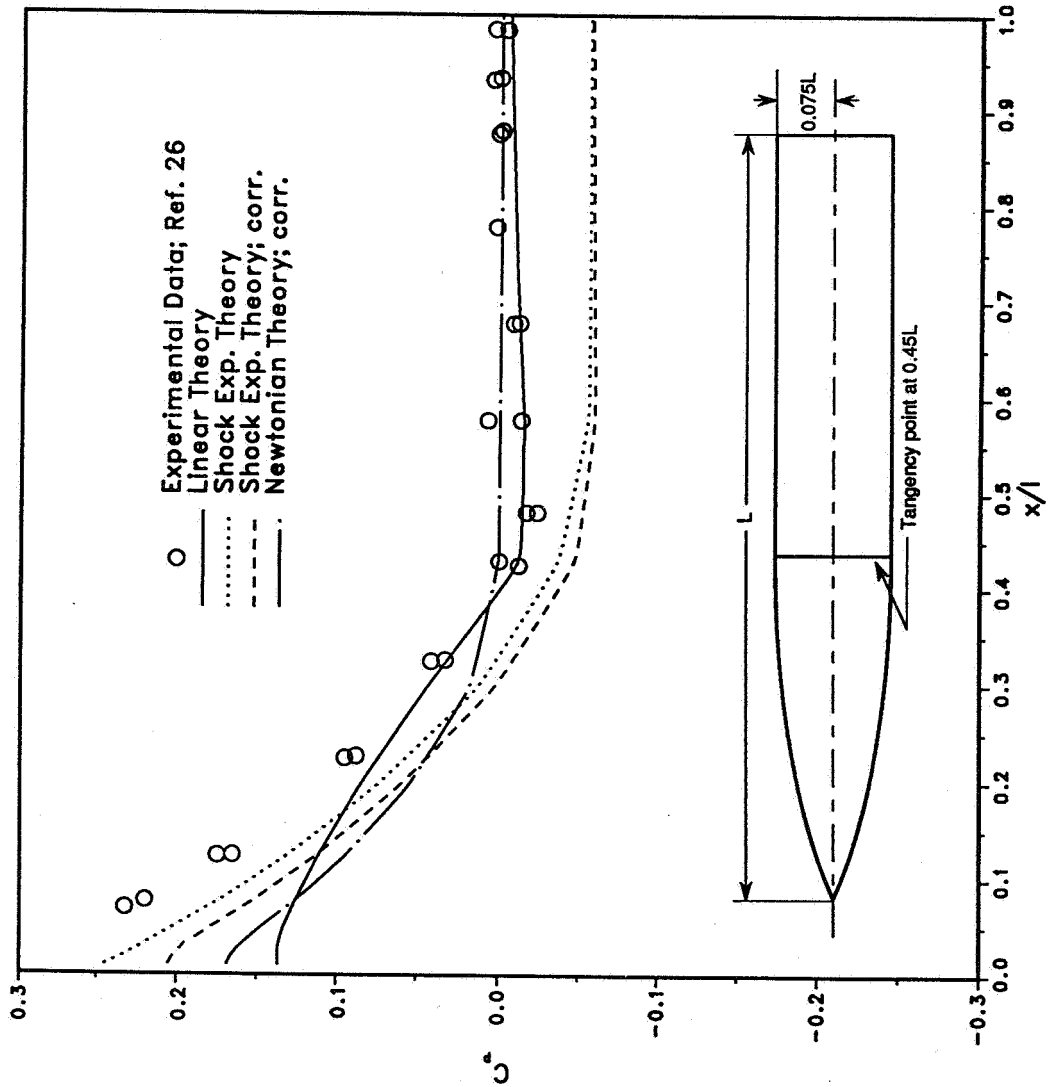
Figure 15.— Pressure distributions acting on upper and lower meridians of an ogive-cylinder at $M_\infty = 2.96$ and $\alpha_c = 0.0$ deg.
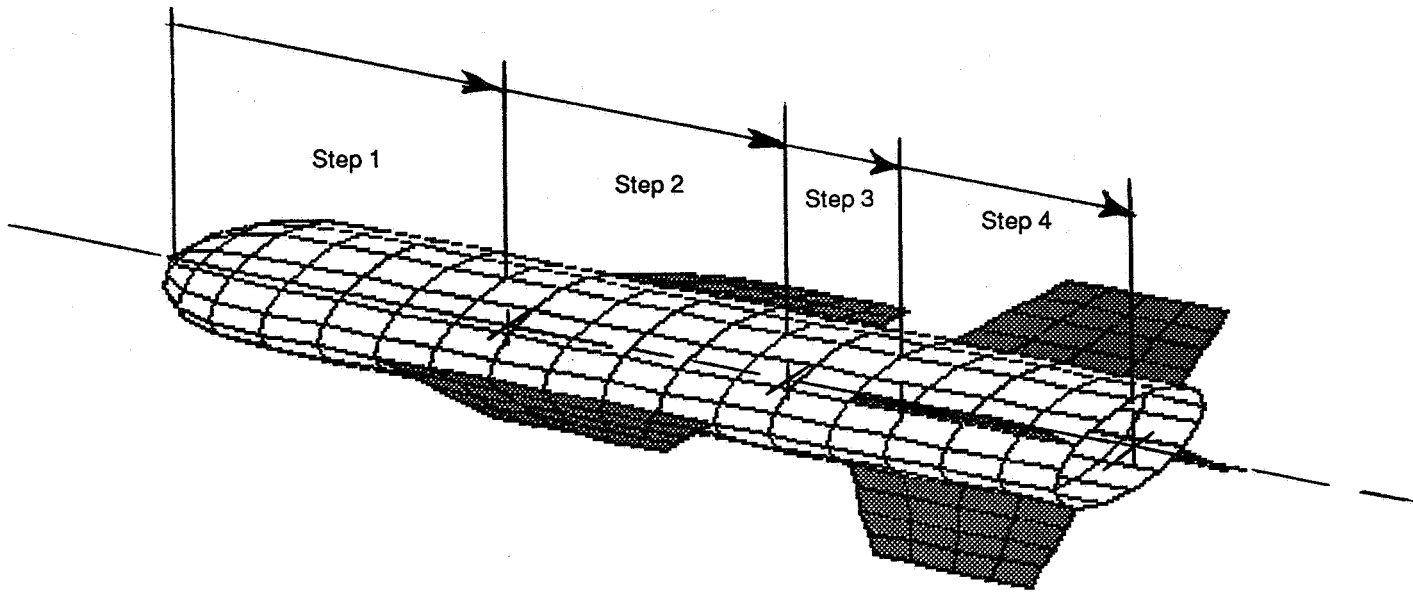
Figure 16. – Stepwise procedure in DEMON3.
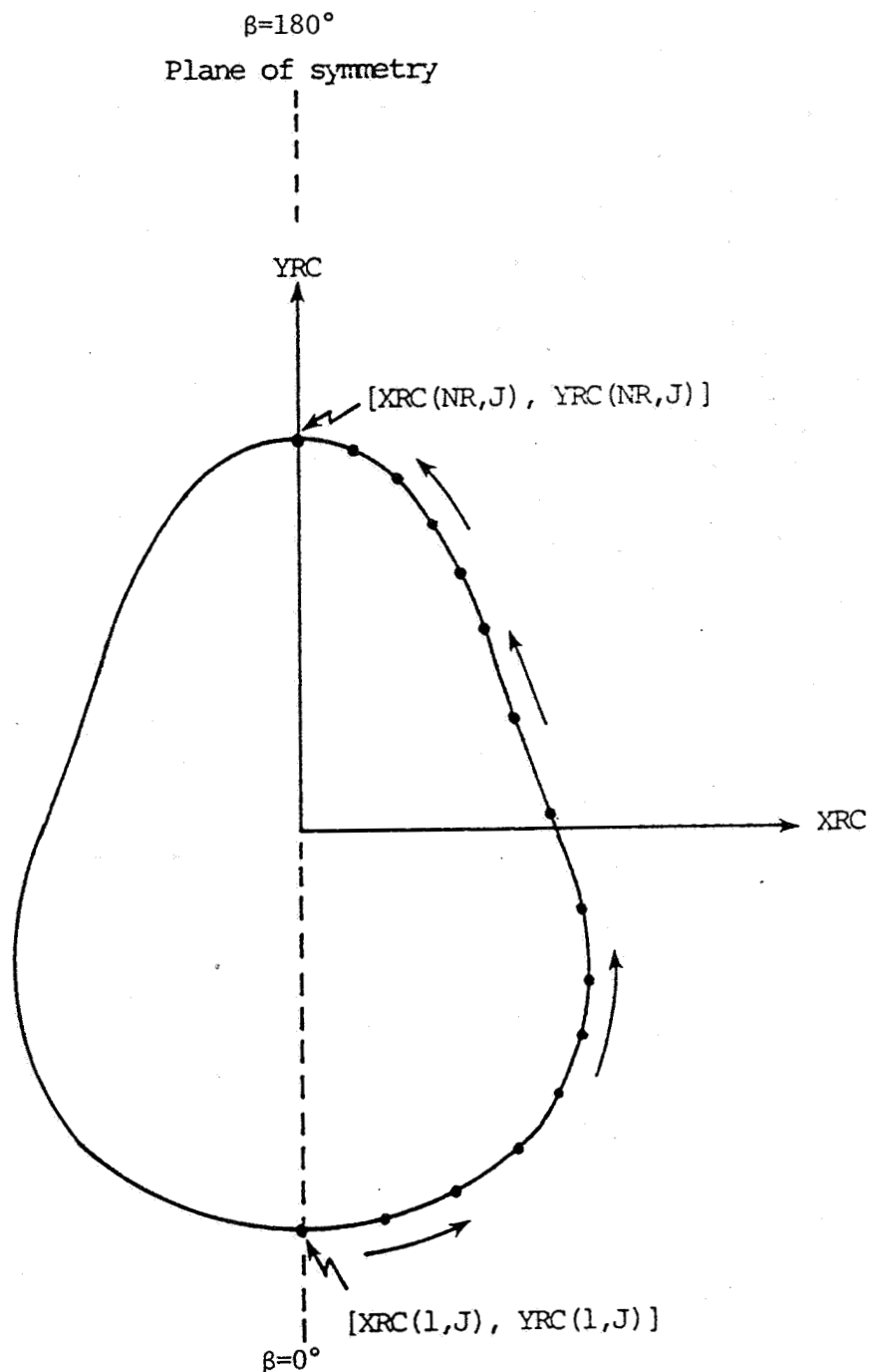
Figure 17. – Convention for ordering coordinates for a noncircular cross section at X = XFC(J).

Input for Step 1

```
1    4    0    1    1    0    0    0    1    1    0    0    0    0    0    0    0    Item 1
3    1                                                                             Item 2
1    1                                                                             Item 3
SAMPLE DEMON3 RUN FOR NONCIRCULAR NASA MODEL:  TR 2434 --  DIMENSIONS IN INCHES    Item 4
159.9984   9.176    25.15    1.26E+08  38.462   3.0     0.0    0                   Item 5
10.0       0.0      0.0      0.025     1.6      1.0                                Item 6
1.0        18.784   1.5      1.05      0.0      0.0                                Item 7
0.05       0.0      0.0      0.0                                                   Item 8
14                                                                                Item 9
0.00000    0.00000  0.25729                                                       Item 10
0.65833    0.16438  0.24213
1.31667    0.31884  0.22713
1.97500    0.46346  0.21227
2.63333    0.59835  0.19755
3.29167    0.72359  0.18294
3.95000    0.83926  0.16846
11.85000   1.65150  0.00000
15.35000   1.87400  0.00000
20.15000   1.87400  0.00000
25.16000   1.87400 -0.04450
25.14000   1.65150 -0.04450
25.15150   1.65150  0.00000
38.46200   1.65150  0.00000
25
6
4.00000    8.75000  11.85000  15.35000  20.150   25.150                           Item 11
21                                                                                Item 12
0.00000   -1.40000                                                                Item 13
0.24311   -1.37873                                                                Item 14
0.47883   -1.31557
0.70000   -1.21244
0.89990   -1.07246
1.07246   -0.89990
1.21244   -0.70000
1.31557   -0.47883
1.37873   -0.24311
1.40000   -0.07000
1.40000    0.00000
1.40000    0.07000
1.37873    0.24311
1.31557    0.47883
1.21244    0.70000
1.07246    0.89990
0.89990    1.07246
0.70000    1.21244
0.47883    1.31557
0.24311    1.37873
0.00000    1.40000
```

(a) Page 1

Figure 18.- Sample case input for program DEMON3

```
21
0.00000   -2.00000
0.26047   -1.97721
0.51303   -1.90954
0.75000   -1.79904
0.96418   -1.64907
1.14907   -1.46418
1.29904   -1.25000
1.40954   -1.01303
1.47721   -0.76047
1.50000   -0.50000
1.50000    0.00000
1.50000    0.50000
1.47721    0.76047
1.40954    1.01303
1.29904    1.25000
1.14907    1.46418
0.96418    1.64907
0.75000    1.79904
0.51303    1.90954
0.26047    1.97721
0.00000    2.00000
```

```
21
0.00000   -2.00000
0.26047   -1.97721
0.51303   -1.90954
0.75000   -1.79904
0.96418   -1.64907
1.14907   -1.46418
1.29904   -1.25000
1.40954   -1.01303
1.47721   -0.76047
1.50000   -0.50000
1.50000    0.00000
1.50000    0.50000
1.47721    0.76047
1.40954    1.01303
1.29904    1.25000
1.14907    1.46418
0.96418    1.64907
0.75000    1.79904
0.51303    1.90954
0.26047    1.97721
0.00000    2.00000
```

(b) Page 2

Figure 18.- Continued.

- 85 -

Item 13
Item 14

21	
0.00000	-2.00000
0.26047	-1.97721
0.51303	-1.90954
0.75000	-1.79904
0.96418	-1.64907
1.14907	-1.46418
1.29904	-1.25000
1.40954	-1.01303
1.47721	-0.76047
1.50000	-0.50000
1.50000	0.00000
1.50000	0.50000
1.50000	0.76449
1.50000	1.04596
1.50000	1.36603
1.50000	1.75865
1.25865	2.00000
0.86603	2.00000
0.54596	2.00000
0.26449	2.00000
0.00000	2.00000

Item 13
Item 14

21	
0.00000	-2.00000
0.26047	-1.97721
0.51303	-1.90954
0.75000	-1.79904
0.96418	-1.64907
1.14907	-1.46418
1.29904	-1.25000
1.40954	-1.01303
1.47721	-0.76047
1.50000	-0.50000
1.50000	0.00000
1.50000	0.50000
1.50000	0.76449
1.50000	1.04596
1.50000	1.36603
1.50000	1.75865
1.25865	2.00000
0.86603	2.00000
0.54596	2.00000
0.26449	2.00000
0.00000	2.00000

(c) Page 3

Figure 18.- Continued.

```
21
0.00000    -2.00000                                              Item 13
0.26047    -1.97721                                              Item 14
0.51303    -1.90954
0.75000    -1.79904
0.96418    -1.64907
1.14907    -1.46418
1.29904    -1.25000
1.40954    -1.01303
1.47721    -0.76047
1.50000    -0.50000
1.50000     0.00000
1.50000     0.50000
1.47721     0.76047
1.40954     1.01303
1.29904     1.25000
1.14907     1.46418
0.96418     1.64907
0.75000     1.79904
0.51303     1.90954
0.26047     1.97721
0.00000     2.00000
TRIPLET PANEL INPUT FOR NONCIRCULAR NASA MODEL
0    -1            15       24
1    -1
0.00000     2.00000    4.00000    5.58333    7.16667    8.75000   10.30000   11.85000
13.60000   15.35000   17.06700   18.78400   20.73933   22.69467   24.65000   26.60533
28.56067   30.51600   31.82300   33.13000   34.46300   35.79600   37.12900   38.46200
0.00000     0.00000
0.00000     0.00000
0.00000     0.00000
0.00000     0.00000                                              Item 23
0.00000     0.00000                                              Item 24
0.00000     0.00000                                              Item 25
0.00000     0.00000                                              Item 26
0.00000     0.00000
0.00000    -0.83400                                              Item 31
0.21586    -0.80558
0.41700    -0.72227
0.58973    -0.58973
0.72227    -0.41700
0.80558    -0.21586
0.83400    -0.04000
0.83400     0.04000
0.80558     0.21586
0.72227     0.41700
0.58973     0.58973
0.41700     0.72227
0.21585     0.80558                                              Item 31
0.00000     0.83400
```

(d) Page 4

Figure 18.- Continued.

0.00000	-1.40000
0.36235	-1.35230
0.70000	-1.21244
0.98995	-0.98995
1.21244	-0.70000
1.35230	-0.36235
1.40000	-0.07000
1.40000	0.00000
1.35230	0.07000
1.21244	0.36235
0.98995	0.70000
0.70000	0.98995
0.36235	1.21244
0.00000	1.35230
0.00000	1.40000
0.37098	-1.60000
0.71667	-1.55116
1.01352	-1.40797
1.24131	-1.18019
1.38450	-0.88333
1.43333	-0.53764
1.43333	-0.21333
1.38450	0.00000
1.24131	0.21333
1.01352	0.53764
0.71667	0.88333
0.37098	1.18019
0.00000	1.40797
0.00000	1.55116
0.37960	1.60000
0.73333	-1.80000
1.03709	-1.75003
1.27017	-1.60351
1.41669	-1.37042
1.46667	-1.06667
1.46667	-0.71294
1.41669	-0.35667
1.27017	0.00000
1.03709	0.35667
0.73333	0.71294
0.37960	1.06667
0.00000	1.37042
0.00000	1.60351
0.38823	1.75003
0.75000	1.80000
1.06066	-2.00000
1.29904	-1.94889
1.44889	-1.79904
1.50000	-1.56066
1.50000	-1.25000
1.44889	-0.88823
1.29904	-0.50000
1.06066	0.00000
0.75000	0.50000
0.38823	0.88823
0.00000	1.25000
	1.56066
	1.79904
	1.94889
	2.00000

(e) Page 5

Figure 18.- Continued.

Item 31

Item 31

Item 31

Item 31

```
0.00000   -2.00000
0.38823   -1.94889
0.75000   -1.79904
1.06066   -1.56066
1.29904   -1.25000
1.44889   -0.88823
1.50000   -0.50000
1.50000    0.00000
1.44889    0.50000
1.29904    0.88823
1.06066    1.25000
0.75000    1.56066
0.38823    1.79904
0.00000    1.94889
0.00000    2.00000
0.38823   -2.00000
0.75000   -1.94889
1.06066   -1.79904
1.29904   -1.56066
1.44889   -1.25000
1.50000   -0.88823
1.50000   -0.50000
1.44889    0.00000
1.29904    0.50000
1.06066    0.88823
0.75000    1.25000
0.38823    1.56066
0.00000    1.79904
0.00000    1.94889
0.38823    2.00000
0.75000   -2.00000
1.06066   -1.94889
1.29904   -1.79904
1.44889   -1.56066
1.50000   -1.25000
1.50000   -0.88823
1.47444   -0.50000
1.39952    0.00000
1.28033    0.50000
0.80801    0.89508
0.39507    1.30801
0.00000    1.78033
0.00000    1.89952
0.38823    1.97444
0.75000    2.00000
1.06066   -2.00000
1.29904   -1.94889
1.44889   -1.79904
1.50000   -1.56066
1.50000   -1.25000
1.50000   -0.88823
1.50000   -0.50000
1.50000    0.00000
0.86603    0.50000
0.40192    0.50000
0.00000    0.90192
           1.36603
           2.00000
           2.00000
           2.00000
```

(f) Page 6

Figure 18.- Continued.

Item 31

Item 31

Item 31

Item 31

0.00000	-2.00000
0.38823	-1.94889
0.75000	-1.79904
1.06066	-1.56066
1.29904	-1.25000
1.44889	-0.88823
1.50000	-0.50000
1.50000	0.00000
1.50000	0.50000
1.50000	0.90192
1.50000	1.36603
0.86603	2.00000
0.40192	2.00000
0.00000	2.00000
0.00000	-2.00000
0.38823	-1.94889
0.75000	-1.79904
1.06066	-1.56066
1.29904	-1.25000
1.44889	-0.88823
1.50000	-0.50000
1.50000	0.00000
1.50000	0.50000
1.50000	0.90192
1.50000	1.36603
0.86603	2.00000
0.40192	2.00000
0.00000	2.00000
0.00000	-2.00000
0.38823	-1.94889
0.75000	-1.79904
1.06066	-1.56066
1.29904	-1.25000
1.44889	-0.88823
1.50000	-0.50000
1.50000	0.00000
1.50000	0.50000
1.49398	0.90031
1.47631	1.35235
1.44822	1.94822
0.85235	1.97631
0.40031	1.99398
0.00000	2.00000
0.00000	-2.00000
0.38823	-1.94889
0.75000	-1.79904
1.06066	-1.56066
1.29904	-1.25000
1.44889	-0.88823
1.50000	-0.50000
1.50000	0.00000
1.50000	0.50000
1.47399	0.89495
1.39772	1.30698
1.27640	1.77640
0.80698	1.89772
0.39495	1.97399
0.00000	2.00000

(g) Page 7

Figure 18.- Continued.

```
-2.00000   0.00000
-1.94889   0.38823
-1.79904   0.75000
-1.56066   1.06066
-1.25000   1.29904
-0.88823   1.44889
-0.50000   1.50000
 0.00000   1.50000
 0.50000   1.50000
 0.88960   1.45400
 1.26160   1.31914
 1.31914   1.10459
 1.45400   0.81914
 1.10459   1.60459
 1.60459   0.76160
 1.81914   0.38960
 0.76160
 1.95400
 0.38960
 2.00000   0.00000
-2.00000   0.38823
-1.94889   0.75000
-1.79904   1.06066
-1.56066   1.29904
-1.25000   1.44889
-0.88823   1.50000
-0.50000   1.50000
 0.00000   1.50000
 0.50000   1.44889
 0.88823   1.29904
 1.25000   1.06066
 1.56066   0.75000
 1.79904   0.38823
 1.94889   0.00000
 2.00000   0.38823
-2.00000   0.75000
-1.94889   1.06066
-1.79904   1.29904
-1.56066   1.44889
-1.25000   1.50000
-0.88823   1.50000
-0.50000   1.50000
 0.00000   1.44889
 0.50000   1.29904
 0.88823   1.06066
 1.25000   0.75000
 1.56066   0.38823
 1.79904   0.00000
 1.94889   0.38823
 2.00000   0.75000
-2.00000   1.06066
-1.94889   1.29904
-1.79904   1.44889
-1.56066   1.50000
-1.25000   1.50000
-0.88823   1.50000
-0.50000   1.44889
 0.00000   1.29904
 0.50000   1.06066
 0.88823   0.75000
 1.25000   0.38823
 1.56066   0.00000
 1.79904
 1.94889
 2.00000
```

(h) Page 8

Figure 18.- Continued.

```
Item 31
0.00000   -2.00000
0.38823   -1.94889
0.75000   -1.79904
1.06066   -1.56066
1.29904   -1.25000
1.44889   -0.88823
1.50000   -0.50000
1.50000    0.00000
1.50000    0.50000
1.44889    0.88823
1.29904    1.25000
1.06066    1.56066
0.75000    1.79904
0.38823    1.94889
0.00000    2.00000

Item 31
0.00000   -2.00000
0.38823   -1.94889
0.75000   -1.79904
1.06066   -1.56066
1.29904   -1.25000
1.44889   -0.88823
1.50000   -0.50000
1.50000    0.00000
1.50000    0.50000
1.44889    0.88823
1.29904    1.25000
1.06066    1.56066
0.75000    1.79904
0.38823    1.94889
0.00000    2.00000

Item 31
0.00000   -2.00000
0.38823   -1.94889
0.75000   -1.79904
1.06066   -1.56066
1.29904   -1.25000
1.44889   -0.88823
1.50000   -0.50000
1.50000    0.00000
1.50000    0.50000
1.44889    0.88823
1.29904    1.25000
1.06066    1.56066
0.75000    1.79904
0.38823    1.94889
0.00000    2.00000

Item 31
0.00000   -2.00000
0.38823   -1.94889
0.75000   -1.79904
1.06066   -1.56066
1.29904   -1.25000
1.44889   -0.88823
1.50000   -0.50000
1.50000    0.00000
1.50000    0.50000
1.44889    0.88823
1.29904    1.25000
1.06066    1.56066
0.75000    1.79904
0.38823    1.94889
0.00000    2.00000
```

(i) Page 9

Figure 18.- Continued.

Item 31

Item 31

Item 32
Item 33
Item 34

```
0.00000   -2.00000
0.38823   -1.94889
0.75000   -1.79904
1.06066   -1.56066
1.29904   -1.25000
1.44889   -0.88823
1.50000   -0.50000
1.50000    0.00000
1.44889    0.50000
1.29904    0.88823
1.06066    1.25000
0.75000    1.56066
0.38823    1.79904
0.00000    2.00000
0.00000   -2.00000
0.38823   -1.94889
0.75000   -1.79904
1.06066   -1.56066
1.29904   -1.25000
1.44889   -0.88823
1.50000   -0.50000
1.50000    0.00000
1.44889    0.50000
1.29904    0.88823
1.06066    1.25000
0.75000    1.56066
0.38823    1.79904
0.00000    2.00000
PANELING GEOMETRY FOR NONCIRCULAR NASA MODEL
1   0    0    0    0    0
0
```

(j) Page 10
Figure 18.- Continued.

-93-

Input for Step 2

```
$INPUT
 XLEBIP=18.784,
 YBOD(1)=1.5,  ZBOD(1)=0.0,
 YBOD(2)=-1.5,  ZBOD(2)=0.0,
 B2=8.5,  CRP=11.732,  SWLEP=44.0,  SWTEP=-5.76,
 MSWR=6,  MSWL=0,  NCW=6,  NCWT=0,  NTDAT=0,
 NOUT(1)=0,  NOUT(2)=0,  NOUT(3)=0,  NOUT(4)=0,  NOUT(5)=1,
 TOLFAC=1.0000,
$END
```

(k) Page 11

Figure 18.- Continued.

Input for Step 3

```
3    1    0    1    0    0    0    0    0    0    0    0         Item 2
1    1    0    1    3    2    0    1    1    0    0    0         Item 3
SAMPLE DEMON3 RUN FOR NONCIRCULAR NASA MODEL:                   Item 4
30.516   33.130   1.5   1.05   0.0   1.0   TR 2434 -- DIMENSIONS IN INCHES    Item 7
                                     0.0
```

(l) Page 12

Figure 18.- Continued.

Input for Step 4

```
$INPUT
XLEBIP=33.130,
YBOD(1)=1.5,  ZBOD(1)=0.0,
YBOD(2)=-1.5,  ZBOD(2)=0.0,
B2=4.0,  CRP=5.332,  SWLEP=44.0,  SWTEP=-5.76,
MSWR=6,  MSWL=0,  MSWU=0,  NCW=4,
NOUT(1)=0, NOUT(2)=0, NOUT(3)=0, NOUT(4)=0, NOUT(5)=1,
TOLFAC=1.0000,
$END
```

(m) Page 13

Figure 18.- Concluded.
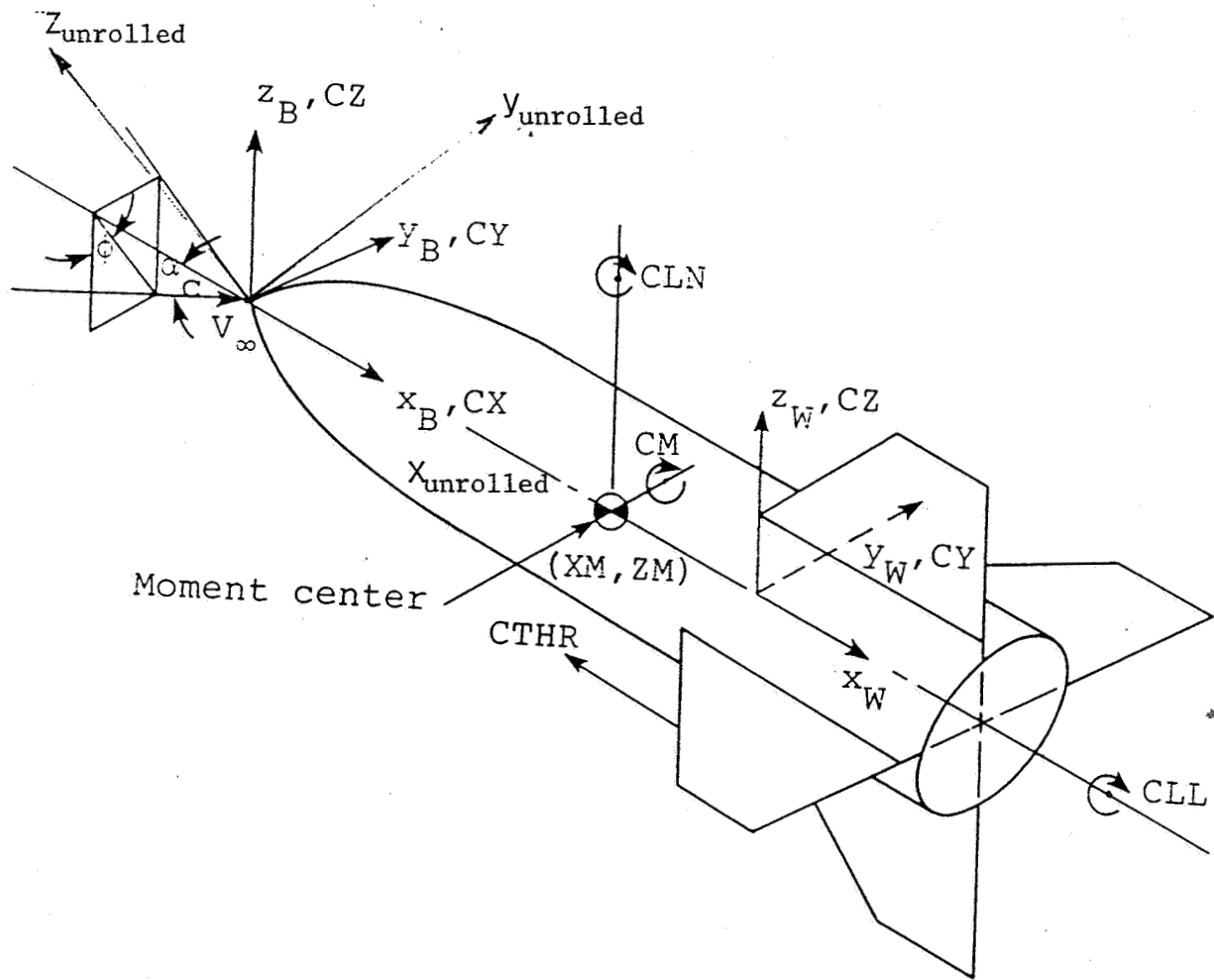
Figure 19. – Coordinate systems and force/moment conventions used in DEMON3.

```
**********************************************************
*                                                        *
*   ddd    ccccc    m    m    ooo    n   n    33333       *
*   d   d  e        mm  mm   o   o   nn  n        3       *
*   d   d  eee      m  m m   o   o   n n n      333       *
*   d   d  e        m    m   o   o   n  nn        3       *
*   ddd    eeeee    m    m    ooo    n   n    33333       *
*                                                        *
*              program demon3                            *
*           dated:    september 1991                     *
*                                                        *
*          prepared for:  nasa langley                   *
*                    by                                  *
*        nielsen engineering & research, inc.            *
*          510 clyde ave, mt. view, ca 94043             *
*                                                        *
**********************************************************
```

(a) Page 1

Figure 20.- Sample case output from program DEMON3

-98-

SAMPLE DEMON3 RUN FOR NONCIRCULAR NASA MODEL: TR 2434 -- DIMENSIONS IN INCHES

```
reference quantities
  ref. area ........ 160.00
  ref. length ...... 9.18
  x(moment center) . 25.15
  z(moment center) . 0.00
  body length (l)... 38.46
  base diameter (d). 3.00

flow conditions
  mach number....... 1.60
  alpha c (deg.) ... 10.00
  phi (deg.) ....... 0.00
  reynolds no. (d).. 1.260E+08
  vortex factor .... 1.00
  rcore ............ 0.03

  alpha (deg.) ..... 10.00
  beta (deg.) ...... 0.00
  u/v .............. 0.985
  re(2-dim.)........ 2.188E+07
  f(re) crossflow... 7.293E+06
```

initial conditions						
xi	xf	dx	tol	emkf	rgam	fdx
1.000	18.784	1.500	0.05000	1.050	0.000	0.000

options...

ncir	ncf	isym	nblsep	nsepr	nsmoth	ndfus	ndphi	inp	nxfv	nfv	nvp	nvr	nvm	nva	nasym
3	1	0	1	0	0	1	1	0	0	0	0	0	0	0	0

nprntp	nprnts	nprntv	nplota	nprtvl	nplotv	ncntr	ncore	nvtrns	nrstrt	n2dprb
1	1	1	2	0	3	0	0	1	0	0

```
definitions of output quantities in rolled coordinate system
  cn(x)    (dcn/dx)/(q*d), positive up
  cy(x)    (dcy/dx)/(q*d), positive right
  cn       n/(q*refs), positive up
  cy       y/(q*refs), positive right
  cm       m/(q*refs*refl), positive nose up
  cln      r/(q*refs*refl), positive nose right
  cll      l/(q*refs*refl), positive counterclockwise
```

(b) Page 2

Figure 20.- Continued.

input geometry characteristics
nxr = 14

x	r	dr/dx
0.0000	0.0000	0.2573
0.6583	0.1644	0.2421
1.3167	0.3188	0.2271
1.9750	0.4635	0.2123
2.6333	0.5983	0.1975
3.2917	0.7236	0.1829
3.9500	0.8393	0.1685
11.8500	1.6515	0.0000
15.3500	1.8740	0.0000
20.1500	1.8740	0.0000
20.1600	1.8740	-0.0445
25.1400	1.6515	-0.0445
25.1500	1.6515	0.0000
38.4620	1.6515	0.0000

(c) Page 3

Figure 20.- Continued.

inputted coefficients for numerical mapping,   mnfc = 25   mxfc = 6

xfc
4.000

body axis shift, zz = -0.0003377

body equivalent radius, rr = 1.4000713

xrc
```
0.00000E+00  2.43105E-01  4.78795E-01  6.99995E-01  8.99955E-01  1.07243E+00
1.21228E+00  1.31564E+00  1.37977E+00  1.40209E+00  1.40411E+00  1.40209E+00
1.37977E+00  1.31564E+00  1.21228E+00  1.07242E+00  8.99946E-01  6.99984E-01
4.78783E-01  2.43091E-01 -1.22237E-07
```

yrc
```
-1.39932E+00 -1.37797E+00 -1.31473E+00 -1.21169E+00 -1.07179E+00 -8.99132E-01
-6.99153E-01 -4.78087E-01 -2.42403E-01 -6.95253E-02 -3.40180E-04  7.02057E-02
-2.43083E-01  4.78767E-01  6.99833E-01  8.99813E-01  1.07247E+00  1.21237E+00
 1.31541E+00  1.37865E+00  1.40000E+00
```

thc
```
0.00000E+00  1.74461E-01  3.49015E-01  5.23566E-01  6.97994E-01  8.72391E-01
1.04691E+00  1.22135E+00  1.39448E+00  1.52004E+00  1.57080E+00  1.62156E+00
1.74712E+00  1.92025E+00  2.09469E+00  2.26921E+00  2.44360E+00  2.61803E+00
2.79258E+00  2.96714E+00  3.14159E+00
```

afc
```
-6.10546E-04 -8.72784E-07  4.93871E-04 -2.90119E-07 -4.44486E-04 -1.11750E-07
 3.93286E-04 -7.28950E-08 -3.29862E-04 -2.85693E-08  2.74567E-04 -2.75570E-08
-2.13063E-04 -5.39553E-09  1.51618E-04 -9.69766E-09 -9.22930E-05  4.62253E-09
 3.66242E-05  6.01620E-09  1.26772E-05  8.33390E-09 -5.44624E-05  1.93033E-08
 8.85858E-05
```

. . .

(d) Page 4

Figure 20.- Continued.

xfc
25.150

body axis shift, zz = 0.0000131

body equivalent radius, rr = 1.8074082

```
xrc
   0.00000E+00   2.60466E-01   5.13019E-01   7.49988E-01   9.64153E-01   1.14903E+00
   1.29901E+00   1.40945E+00   1.47711E+00   1.50169E+00   1.50349E+00   1.50168E+00
   1.47709E+00   1.40941E+00   1.29896E+00   1.14896E+00   9.64044E-01   7.49828E-01
   5.12758E-01   2.60037E-01  -1.45504E-07

yrc
  -1.99991E+00  -1.97711E+00  -1.90944E+00  -1.79895E+00  -1.64897E+00  -1.46409E+00
  -1.24993E+00  -1.01296E+00  -7.60414E-01  -5.00097E-01  -2.93238E-05   5.00042E-01
  -7.60360E-01   1.01291E+00   1.24990E+00   1.46407E+00   1.64898E+00   1.79899E+00
   1.90952E+00   1.97724E+00   2.00000E+00

thc
   0.00000E+00   1.57182E-01   3.14043E-01   4.70217E-01   6.25286E-01   7.78734E-01
   9.29788E-01   1.07735E+00   1.21963E+00   1.35137E+00   1.57080E+00   1.79023E+00
   1.92197E+00   2.06425E+00   2.21182E+00   2.36288E+00   2.51635E+00   2.67144E+00
   2.82767E+00   2.98463E+00   3.14159E+00

afc
   1.25105E-01  -1.63454E-05  -2.54414E-02  -7.16568E-06   9.94031E-03  -4.19867E-06
  -4.53296E-03  -2.41251E-06   2.11281E-03  -1.58215E-06  -9.10139E-04  -9.46812E-07
   3.14069E-04  -5.18109E-07  -3.47687E-05  -2.31712E-07  -6.83463E-05  -8.00648E-08
   8.28889E-05   7.87331E-08  -5.86698E-05   1.97523E-07   2.65776E-05   3.05097E-07
  -4.15689E-06
```

(e) Page 7

Figure 20.- Continued.

TRIPLET PANEL INPUT FOR NONCI

print options and panel symmetry
iprt(1)   ixzsym   itbsym
   1   0   1

geometry option information
 j2 j6 nfus nradx nforx
  1 -1   1   15   24

vehicle geometry defintion

nfu
 1
xfus - fuselage x-stations
0.00000   2.00000   4.00000   5.58333   7.16667   8.75000 10.30000 11.85000 13.60000 15.35000
17.06700 18.78400 20.73933 22.69467 24.65000 26.60533 28.56067 30.51600 31.82300 33.13000
34.46300 35.79600 37.12900 38.46200

y- and z-coordinates of arbitrary fuselage cross sections

**** axial station x =   0.00000 ****

    y-coordinates
0.00000 0.00000 0.00000 0.00000 0.00000 0.00000 0.00000 0.00000
0.00000 0.00000 0.00000 0.00000

    z-coordinates
0.00000 0.00000 0.00000 0.00000 0.00000 0.00000 0.00000 0.00000
0.00000 0.00000 0.00000 0.00000

 . .

**** axial station x =   38.46200 ****

    y-coordinates
0.00000 0.38823 0.75000 1.06066 1.29904 1.44889 1.50000 1.50000 1.44889
1.29904 1.06066 0.75000 0.38823 0.00000

    z-coordinates
-2.00000 -1.94889 -1.79904 -1.56066 -1.25000 -0.88823 -0.50000 0.00000
1.25000 1.56066 1.79904 1.94889 0.50000 0.88823

(f) Pages 8 through 13
Figure 20.- Continued.

PANELING GEOMETRY FOR NONCIRCUL

output option, iprint = 1

additional paneling information
  k2   kfus kradx kforx
  1   1   0   0.

(g) Page 14
Figure 20.- Continued.

body panel corner point coordinates

panel   1 and 3 indicate body panel leading-edge points, 2 and 4 indicate trailing-edge points

panel	x_1	y_1	z_1	x_2	y_2	z_2	x_3	y_3	z_3	x_4	y_4	z_4
1	0.00000	0.00000	0.00000	2.00000	0.00000	-0.83400	0.00000	0.00000	0.00000	2.00000	0.21586	-0.80558
2	0.00000	0.00000	0.00000	2.00000	0.21586	-0.80558	0.00000	0.00000	0.00000	2.00000	0.41700	-0.72227
3	0.00000	0.00000	0.00000	2.00000	0.41700	-0.72227	0.00000	0.00000	0.00000	2.00000	0.58973	-0.58973
4	0.00000	0.00000	0.00000	2.00000	0.58973	-0.58973	0.00000	0.00000	0.00000	2.00000	0.72227	-0.41700
5	0.00000	0.00000	0.00000	2.00000	0.72227	-0.41700	0.00000	0.00000	0.00000	2.00000	0.80558	-0.21586
6	0.00000	0.00000	0.00000	2.00000	0.80558	-0.21586	0.00000	0.00000	0.00000	2.00000	0.83400	-0.04000
7	0.00000	0.00000	0.00000	2.00000	0.83400	-0.04000	0.00000	0.00000	0.00000	2.00000	0.83400	0.04000
8	0.00000	0.00000	0.00000	2.00000	0.83400	0.04000	0.00000	0.00000	0.00000	2.00000	0.80558	0.21586
9	0.00000	0.00000	0.00000	2.00000	0.80558	0.21586	0.00000	0.00000	0.00000	2.00000	0.72227	0.41700
10	0.00000	0.00000	0.00000	2.00000	0.72227	0.41700	0.00000	0.00000	0.00000	2.00000	0.58973	0.58973
11	0.00000	0.00000	0.00000	2.00000	0.58973	0.58973	0.00000	0.00000	0.00000	2.00000	0.41700	0.72227
12	0.00000	0.00000	0.00000	2.00000	0.41700	0.72227	0.00000	0.00000	0.00000	2.00000	0.21585	0.80558
13	0.00000	0.00000	0.00000	2.00000	0.21585	0.80558	0.00000	0.00000	0.00000	2.00000	0.00000	0.83400
14	0.00000	0.00000	0.00000	2.00000	0.00000	0.83400	0.00000	0.00000	0.00000	2.00000	0.00000	-0.83400
. . .												
295	35.79600	0.00000	-2.00000	37.12900	0.00000	-2.00000	35.79600	0.38823	-1.94889	37.12900	0.38823	-1.94889
296	35.79600	0.38823	-1.94889	37.12900	0.38823	-1.94889	35.79600	0.75000	-1.79904	37.12900	0.75000	-1.79904
297	35.79600	0.75000	-1.79904	37.12900	0.75000	-1.79904	35.79600	1.06066	-1.56066	37.12900	1.06066	-1.56066
298	35.79600	1.06066	-1.56066	37.12900	1.06066	-1.56066	35.79600	1.29904	-1.25000	37.12900	1.29904	-1.25000
299	35.79600	1.29904	-1.25000	37.12900	1.29904	-1.25000	35.79600	1.44889	-0.88823	37.12900	1.44889	-0.88823
300	35.79600	1.44889	-0.88823	37.12900	1.44889	-0.88823	35.79600	1.50000	-0.50000	37.12900	1.50000	-0.50000
301	35.79600	1.50000	-0.50000	37.12900	1.50000	-0.50000	35.79600	1.50000	0.50000	37.12900	1.50000	0.50000
302	35.79600	1.50000	0.50000	37.12900	1.50000	0.50000	35.79600	1.44889	0.88823	37.12900	1.44889	0.88823
303	35.79600	1.44889	0.88823	37.12900	1.44889	0.88823	35.79600	1.29904	1.25000	37.12900	1.29904	1.25000
304	35.79600	1.29904	1.25000	37.12900	1.29904	1.25000	35.79600	1.06066	1.56066	37.12900	1.06066	1.56066
305	35.79600	1.06066	1.56066	37.12900	1.06066	1.56066	35.79600	0.75000	1.79904	37.12900	0.75000	1.79904
306	35.79600	0.75000	1.79904	37.12900	0.75000	1.79904	35.79600	0.38823	1.94889	37.12900	0.38823	1.94889
307	35.79600	0.38823	1.94889	37.12900	0.38823	1.94889	35.79600	0.00000	2.00000	37.12900	0.00000	2.00000
308	35.79600	0.00000	2.00000	37.12900	0.00000	2.00000	35.79600	0.00000	-2.00000	37.12900	0.00000	-2.00000
309	37.12900	0.00000	-2.00000	38.46200	0.00000	-2.00000	37.12900	0.38823	-1.94889	38.46200	0.38823	-1.94889
310	37.12900	0.38823	-1.94889	38.46200	0.38823	-1.94889	37.12900	0.75000	-1.79904	38.46200	0.75000	-1.79904
311	37.12900	0.75000	-1.79904	38.46200	0.75000	-1.79904	37.12900	1.06066	-1.56066	38.46200	1.06066	-1.56066
312	37.12900	1.06066	-1.56066	38.46200	1.06066	-1.56066	37.12900	1.29904	-1.25000	38.46200	1.29904	-1.25000
313	37.12900	1.29904	-1.25000	38.46200	1.29904	-1.25000	37.12900	1.44889	-0.88823	38.46200	1.44889	-0.88823
314	37.12900	1.44889	-0.88823	38.46200	1.44889	-0.88823	37.12900	1.50000	-0.50000	38.46200	1.50000	-0.50000
315	37.12900	1.50000	-0.50000	38.46200	1.50000	-0.50000	37.12900	1.50000	0.50000	38.46200	1.50000	0.50000
316	37.12900	1.50000	0.50000	38.46200	1.50000	0.50000	37.12900	1.44889	0.88823	38.46200	1.44889	0.88823
317	37.12900	1.44889	0.88823	38.46200	1.44889	0.88823	37.12900	1.29904	1.25000	38.46200	1.29904	1.25000
318	37.12900	1.29904	1.25000	38.46200	1.29904	1.25000	37.12900	1.06066	1.56066	38.46200	1.06066	1.56066
319	37.12900	1.06066	1.56066	38.46200	1.06066	1.56066	37.12900	0.75000	1.79904	38.46200	0.75000	1.79904
320	37.12900	0.75000	1.79904	38.46200	0.75000	1.79904	37.12900	0.38823	1.94889	38.46200	0.38823	1.94889
321	37.12900	0.38823	1.94889	38.46200	0.38823	1.94889	37.12900	0.00000	2.00000	38.46200	0.00000	2.00000
322	37.12900	0.00000	2.00000	38.46200	0.00000	2.00000	37.12900	0.00000	-2.00000	38.46200	0.00000	-2.00000

(h) Pages 15 through 20

Figure 20.- Continued.

body panel centroid point coordinates

point	x cp	y cp	z cp
1	1.33333	0.07195	-0.54653
2	1.33333	0.21095	-0.50928
3	1.33333	0.33558	-0.43733
4	1.33333	0.43733	-0.33558
5	1.33333	0.50928	-0.21095
6	1.33333	0.54653	-0.08529
7	1.33333	0.55600	-0.01333
8	1.33333	0.55600	-0.01333
9	1.33333	0.54653	0.08529
10	1.33333	0.50928	0.21095
11	1.33333	0.43733	0.33558
12	1.33333	0.33558	0.43733
13	1.33333	0.21095	0.50928
14	1.33333	0.07195	0.54653
.			
.			
.			
295	36.46250	0.19411	-1.97444
296	36.46250	0.56911	-1.87396
297	36.46250	0.90533	-1.67985
298	36.46250	1.17985	-1.40533
299	36.46250	1.37397	-1.06912
300	36.46250	1.47444	-0.69412
301	36.46250	1.50000	-0.25000
302	36.46250	1.50000	0.25000
303	36.46250	1.47444	0.69412
304	36.46250	1.37396	1.06912
305	36.46250	1.17985	1.40533
306	36.46250	0.90533	1.67985
307	36.46250	0.56911	1.87397
308	36.46250	0.19411	1.97444
309	37.79550	0.19411	-1.97444
310	37.79550	0.56911	-1.87396
311	37.79550	0.90533	-1.67985
312	37.79550	1.17985	-1.40533
313	37.79550	1.37397	-1.06912
314	37.79550	1.47444	-0.69412
315	37.79550	1.50000	-0.25000
316	37.79550	1.50000	0.25000
317	37.79550	1.47444	0.69412
318	37.79550	1.37396	1.06912
319	37.79550	1.17985	1.40533
320	37.79550	0.90533	1.67985
321	37.79550	0.56911	1.87397
322	37.79550	0.19411	1.97444

(i) Pages 21 through 26
Figure 20.- Continued.

body panel areas and inclination angles

panel	area	delta rad	theta rad	delta deg	theta deg
1	0.23560	0.39203	-3.01069	22.46177	-172.500
2	0.23558	0.39203	-2.74891	22.46184	-157.501
3	0.23559	0.39203	-2.48710	22.46189	-142.500
4	0.23559	0.39203	-2.22529	22.46189	-127.500
5	0.23558	0.39203	-1.96347	22.46184	-112.499
6	0.19286	0.39324	-1.73102	22.53111	-99.180
7	0.04334	0.39508	-1.57080	22.63614	-90.000
8	0.04334	0.39508	-1.57080	22.63614	-90.000
9	0.19286	0.39324	-1.41058	22.53111	-80.820
10	0.23558	0.39203	-1.17812	22.46184	-67.501
11	0.23559	0.39203	-0.91630	22.46189	-52.500
12	0.23559	0.39203	-0.65450	22.46189	-37.500
13	0.23559	0.39203	-0.39266	22.46180	-22.498
14	0.23559	0.39203	-0.13091	22.46176	-7.501
. . .					
295	0.52198	0.00000	-3.01070	0.00000	-172.500
296	0.52197	0.00000	-2.74889	0.00000	-157.500
297	0.52198	0.00000	-2.48709	0.00000	-142.500
298	0.52198	0.00000	-2.22530	0.00000	-127.500
299	0.52197	0.00000	-1.96350	0.00000	-112.500
300	0.52198	0.00000	-1.70169	0.00000	-97.500
301	0.66650	0.00000	-1.57080	0.00000	-90.000
302	0.52198	0.00000	-1.57080	0.00000	-90.000
303	0.52197	0.00000	-1.43990	0.00000	-82.500
304	0.52198	0.00000	-1.17810	0.00000	-67.500
305	0.52198	0.00000	-0.91629	0.00000	-52.500
306	0.52197	0.00000	-0.65450	0.00000	-37.500
307	0.52198	0.00000	-0.39270	0.00000	-22.500
308	0.52198	0.00000	-0.13090	0.00000	-7.500
309	0.52197	0.00000	-3.01070	0.00000	-172.500
310	0.52198	0.00000	-2.74889	0.00000	-157.500
311	0.52198	0.00000	-2.48709	0.00000	-142.500
312	0.52197	0.00000	-2.22530	0.00000	-127.500
313	0.52198	0.00000	-1.96350	0.00000	-112.500
314	0.52198	0.00000	-1.70169	0.00000	-97.500
315	0.66650	0.00000	-1.57080	0.00000	-90.000
316	0.66650	0.00000	-1.57080	0.00000	-90.000
317	0.52198	0.00000	-1.43990	0.00000	-82.500
318	0.52197	0.00000	-1.17810	0.00000	-67.500
319	0.52198	0.00000	-0.91629	0.00000	-52.500
320	0.52198	0.00000	-0.65450	0.00000	-37.500
321	0.52197	0.00000	-0.39270	0.00000	-22.500
322	0.52198	0.00000	-0.13090	0.00000	-7.500

(j) Pages 27 through 32
Figure 20.- Continued.

entering subroutine - aicbod

alpha=0 source strengths

```
 1   14   0.01304  0.01304  0.01302  0.01301  0.01301  0.01304      0.01304  0.01299  0.01286  0.01286  0.01299  0.01304
          0.01304  0.01301  0.01304  0.01303  0.01303
15   28   0.02587  0.02581  0.02584  0.02579  0.02579  0.02586      0.02586  0.02578  0.02565  0.02565  0.02578  0.02586
          0.02581  0.02587  0.02584  0.02579  0.02584
29   42   0.04044  0.04054  0.03877  0.04111  0.02584  0.03835      0.03835  0.03559  0.03559  0.03559  0.03559  0.03835
          0.04054  0.04044  0.04111  0.03878  0.03878
43   56   0.04774  0.04872  0.04563  0.04941  0.04111  0.04370      0.04370  0.04118  0.04022  0.04022  0.04119  0.04370
          0.04872  0.04774  0.04941  0.04563  0.04563
57   70   0.05446  0.05577  0.05199  0.05669  0.04941  0.04996      0.04996  0.04702  0.04545  0.04545  0.04702  0.04996
          0.05577  0.05446  0.05669  0.05199  0.05199
71   84   0.05530  0.05397  0.05561  0.05337  0.05669  0.05144      0.05144  0.05159  0.05049  0.05049  0.05159  0.05144
          0.05397  0.05530  0.05337  0.05561  0.05337
85   98   0.05394  0.05395  0.05366  0.05410  0.05561  0.05396      0.05396  0.05365  0.05384  0.05384  0.05365  0.05395
          0.05395  0.05394  0.05410  0.05366  0.05410
99  112   0.04872  0.05020  0.04743  0.04755  0.05366  0.04834      0.04834  0.05173  0.04676  0.05078  0.04746  0.04981
          0.05020  0.04872  0.04755  0.04762  0.04755
113 126   0.04794  0.04925  0.04843  0.04762  0.04762  0.05338      0.05338  0.05383  0.04843  0.05113  0.04736  0.05016
          0.04925  0.04794  0.05505  0.05265  0.05265
127 140   0.05505  0.05017  0.06097  0.05265  0.05265  0.05607      0.05607  0.05501  0.05332  0.05203  0.05057  0.05035
          0.05017  0.05505  0.05659  0.05891  0.05891
141 154   0.05659  0.06087  0.04931  0.04966  0.05891  0.05995      0.05995  0.04969  0.05852  0.04869  0.05499  0.04907
          0.06087  0.05659  0.04966  0.05275  0.05275
155 168   0.04907  0.05077  0.04985  0.05131  0.05880  0.04650      0.04650  0.04960  0.04612  0.04799  0.04557  0.04655
          0.05077  0.04907  0.05116  0.04539  0.04539
169 182   0.05614  0.04576  0.04500  0.04956  0.04956  0.04925      0.04925  0.04404  0.05042  0.04452  0.04891  0.04502
          0.04576  0.05614  0.04670  0.04776  0.04776
183 196   0.05007  0.04517  0.04950  0.04776  0.04756  0.04514      0.04514  0.04389  0.04728  0.04624  0.04750  0.04662
          0.04517  0.05007  0.04676  0.04756  0.04718
197 210   0.04620  0.04677  0.04590  0.04327  0.04382  0.04259      0.04259  0.04470  0.04487  0.04613  0.04634  0.04662
          0.04677  0.04620  0.04681  0.04718  0.04725
211 224   0.04681  0.03959  0.04673  0.04382  0.04240  0.04495      0.04495  0.04355  0.04518  0.04442  0.04622  0.04449
          0.03959  0.04681  0.03952  0.04725  0.04674
225 238   0.04775  0.04240  0.04726  0.04240  0.04349  0.04426      0.04426  0.04449  0.04442  0.04494  0.04481  0.04533
          0.04240  0.04775  0.04338  0.04674  0.04479
239 252   0.04593  0.04693  0.04612  0.04335  0.04452  0.06654      0.06654  0.06719  0.06617  0.06758  0.06637  0.06740
          0.04693  0.04593  0.04298  0.04479  0.04595
253 266   0.04335  0.04392  0.04507  0.04486  0.06595  0.06756      0.06756  0.06633  0.06759  0.06613  0.06716  0.06590
          0.04392  0.04335  0.04462  0.04452  0.06701
267 280   0.04486  0.04411  0.06645  0.06610  0.06772  0.06553      0.06553  0.06631  0.06487  0.06591  0.06464  0.06539
          0.04411  0.04486  0.06726  0.06670  0.06426
281 294   0.06704  0.06754  0.06581  0.06617  0.06625  0.06633      0.06633  0.06530  0.06603  0.06477  0.06553  0.06441
          0.06754  0.06564  0.06442  0.06423  0.06650
295 308   0.06564  0.06710  0.06651  0.06595  0.06436  0.06567      0.06567  0.06605  0.06515  0.06563  0.06470  0.06519
          0.06490  0.06661  0.06432  0.06455  0.06636
309 322   0.06490  0.06415  0.06588  0.06619  0.06635  0.06603      0.06603  0.06546  0.06575  0.06499  0.06531  0.06467
          0.06595  0.06512  0.06630  0.06655  0.06616
          0.06434  0.06480  0.06444  0.06605
          0.06636  0.06649  0.06462  0.06497
          0.06616  0.06635  0.06447  0.06629  0.06589
```

(k) Pages 32 and 33

Figure 20.- Continued.

-108-

entering subroutine - alcbod

velocity on body

mach= 1.600   alpha= 10.000   phi=   0.000

panel no.	source strength	axial velocity	lateral velocity	vertical velocity	normal
1	0.01698	-0.28505	0.65903E-01	-0.45677	0.53536
2	0.01678	-0.27941	0.19505	-0.40852	0.52452
3	0.01606	-0.26851	0.29054	-0.32399	0.50358
4	0.01553	-0.25310	0.35277	-0.21084	0.47395
5	0.01425	-0.23424	0.36762	-0.97006E-01	0.43767
6	0.01359	-0.21607	0.35265	0.95235E-02	0.40295
7	0.01223	-0.20312	0.32596	0.71742E-01	0.37903
8	0.01311	-0.20314	0.32596	0.48538E-01	0.37903
9	0.01199	-0.18926	0.28969	0.10246	0.35178
10	0.01144	-0.17025	0.23039	0.15016	0.31486
11	0.01009	-0.15140	0.16039	0.18333	0.27857
12	0.00961	-0.13600	0.10371	0.18910	0.24895
13	0.00887	-0.12510	0.52212E-01	0.18944	0.22800
14	0.00868	-0.11946	0.18965E-01	0.18470	0.21716
. . .					
295	0.11276	-0.16567E-02	0.41693E-01	-0.16816	0.17216
296	0.10994	-0.18441E-02	0.11917	-0.12429	0.16043
297	0.10503	-0.16894E-02	0.15924	-0.51459E-01	0.13776
298	0.09741	-0.11993E-02	0.16012	-0.35025E-01	0.10571
299	0.08881	-0.85131E-03	0.11342	0.10016	0.66452E-01
300	0.07912	-0.58332E-03	0.40162E-01	0.13141	0.22665E-01
301	0.06960	-0.15136E-03	-0.17276E-06	0.92085E-01	0.75904E-08
302	0.05933	0.55010E-03	-0.23516E-06	0.92044E-01	0.75904E-08
303	0.04986	0.85754E-03	-0.40296E-01	0.13244	-0.22665E-01
304	0.04006	0.11871E-02	-0.11428	0.10224	-0.66452E-01
305	0.03130	0.13644E-02	-0.16156	0.36900E-01	-0.10571
306	0.02371	0.13468E-02	-0.16087	-0.50210E-01	-0.13776
307	0.01866	0.13545E-02	-0.12074	-0.12364	-0.16043
308	0.01582	0.12692E-02	-0.42461E-01	-0.16806	-0.17216
309	0.11274	0.12187E-02	0.41134E-01	0.16823	0.16043
310	0.11056	-0.10396E-02	0.12035	-0.12380	0.13776
311	0.10434	-0.92142E-03	0.15899	-0.51645E-01	0.10571
312	0.09850	-0.83901E-03	0.16064	-0.35692E-01	0.66452E-01
313	0.08781	-0.61850E-03	0.11408	0.10177	0.22665E-01
314	0.08024	-0.27799E-03	0.40333E-01	0.13272	0.75904E-08
315	0.06840	0.86120E-04	-0.52853E-06	0.92575E-01	0.75904E-08
316	0.06051	0.25046E-03	-0.24727E-06	0.93027E-01	-0.22665E-01
317	0.04861	0.65126E-03	-0.40475E-01	0.13380	-0.66452E-01
318	0.04100	0.82991E-03	-0.11459	0.10299	-0.10571
319	0.03031	0.96445E-03	-0.16068	0.37239E-01	-0.13776
320	0.02433	0.11228E-02	-0.16169	-0.50351E-01	-0.16043
321	0.01809	0.12225E-02	-0.12169	-0.12324	-0.17216
322	0.01586	0.13312E-02	-0.41605E-01	-0.16817	

(l) Pages 33 through 38
Figure 20.- Continued.

(alpha=0)*cos(alphac) source strengths

The page presents a dense numerical table (Figure 20, pages 38 and 39) of source‑strength values. The two leftmost columns are index pairs, followed by value columns. The right‑hand block of six columns could be read reliably and is reproduced below.

i	j						
1	14	0.01284	0.01279	0.01267	0.01267	0.01279	0.01284
15	28	0.02547	0.02538	0.02526	0.02526	0.02538	0.02547
29	42	0.03777	0.03505	0.03505	0.03505	0.03505	0.03777
43	56	0.04303	0.04056	0.03961	0.03961	0.04056	0.04303
57	70	0.04920	0.04630	0.04476	0.04476	0.04630	0.04920
71	84	0.05066	0.05081	0.04972	0.04972	0.05081	0.05066
85	98	0.05313	0.05284	0.05302	0.05303	0.05283	0.05314
99	112	0.04905	0.04674	0.05001	0.04605	0.05095	0.04760
113	126	0.04939	0.04664	0.05035	0.04769	0.05301	0.05257
127	140	0.04959	0.04980	0.05124	0.05251	0.05417	0.05522
141	154	0.04832	0.05416	0.04795	0.05763	0.04893	0.05904
155	168	0.04584	0.04487	0.04726	0.04542	0.04885	0.04579
169	182	0.04433	0.04817	0.04384	0.04965	0.04337	0.04850
183	196	0.04591	0.04678	0.04554	0.04656	0.04322	0.04445
197	210	0.04592	0.04564	0.04543	0.04419	0.04402	0.04194
211	224	0.04381	0.04552	0.04375	0.04449	0.04289	0.04427
225	238	0.04464	0.04413	0.04425	0.04375	0.04381	0.04358
239	252	0.06638	0.06537	0.06655	0.06517	0.06617	0.06553
253	266	0.06490	0.06614	0.06512	0.06656	0.06532	0.06654
267	280	0.06440	0.06366	0.06491	0.06389	0.06530	0.06453
281	294	0.06343	0.06453	0.06379	0.06502	0.06431	0.06532
295	308	0.06420	0.06372	0.06463	0.06416	0.06505	0.06467
309	322	0.06368	0.06432	0.06400	0.06475	0.06446	0.06503

(m) Pages 38 and 39
Figure 20.- Continued.

x = 1.0000 r = 0.2445 dr/dx = 0.2343 1.6000 m

body surface pressure distribution

j	y	z	beta	u/v0	v/v0	w/v0	vt/v0	cp(m)	dphi/dt	cpz	cp(i)	vcp/v0
1	0.0000	-0.2444	0.000	0.6998	0.0000	-0.2829	0.2829	0.5622	0.0000	0.4303	0.4303	0.0000
2	0.0213	-0.2435	5.001	0.6998	0.0438	-0.2833	0.2867	0.5587	0.0000	0.4282	0.4282	0.0302
3	0.0425	-0.2407	10.009	0.7007	0.0877	-0.2751	0.2887	0.5546	0.0000	0.4257	0.4257	0.0603
4	0.0633	-0.2361	15.008	0.7026	0.1304	-0.2588	0.2898	0.5493	0.0000	0.4224	0.4224	0.0900
5	0.0836	-0.2296	20.013	0.7045	0.1736	-0.2431	0.2988	0.5364	0.0000	0.4145	0.4145	0.1186
6	0.1034	-0.2215	25.020	0.7072	0.2113	-0.2205	0.3054	0.5236	0.0000	0.4066	0.4066	0.1469
7	0.1223	-0.2116	30.017	0.7109	0.2426	-0.1925	0.3097	0.5112	0.0000	0.3988	0.3988	0.1737
8	0.1403	-0.2001	35.026	0.7145	0.2749	-0.1645	0.3204	0.4923	0.0000	0.3868	0.3868	0.1989
9	0.1572	-0.1872	40.027	0.7189	0.3010	-0.1310	0.3283	0.4745	0.0000	0.3754	0.3754	0.2236
10	0.1729	-0.1728	45.027	0.7240	0.3215	-0.0938	0.3349	0.4563	0.0000	0.3636	0.3636	0.2452
11	0.1874	-0.1570	50.039	0.7292	0.3429	-0.0559	0.3474	0.4320	0.0000	0.3476	0.3476	0.2658
12	0.2003	-0.1401	55.036	0.7349	0.3550	-0.0177	0.3554	0.4110	0.0000	0.3336	0.3336	0.2849
13	0.2118	-0.1221	60.043	0.7412	0.3601	0.0194	0.3606	0.3919	0.0000	0.3206	0.3206	0.2997
14	0.2217	-0.1031	65.059	0.7475	0.3657	0.0581	0.3703	0.3680	0.0000	0.3041	0.3041	0.3148
15	0.2298	-0.0834	70.052	0.7540	0.3640	0.0965	0.3766	0.3475	0.0000	0.2897	0.2897	0.3263
16	0.2362	-0.0629	75.087	0.7607	0.3595	0.1338	0.3836	0.3258	0.0000	0.2742	0.2742	0.3314
17	0.2411	-0.0419	80.138	0.7674	0.3567	0.1747	0.3972	0.2971	0.0000	0.2533	0.2533	0.3406
18	0.2442	-0.0209	85.105	0.7756	0.3407	0.2184	0.4047	0.2720	0.0000	0.2347	0.2347	0.3504
19	0.2452	0.0001	90.014	0.7817	0.3260	0.2366	0.4028	0.2616	0.0000	0.2268	0.2268	0.3532
20	0.2442	0.0210	94.923	0.7882	0.3066	0.2499	0.3955	0.2557	0.0000	0.2222	0.2222	0.3504
21	0.2411	0.0420	99.889	0.7970	0.2823	0.2789	0.3969	0.2363	0.0000	0.2073	0.2073	0.3406
22	0.2362	0.0635	104.940	0.8040	0.2631	0.2952	0.3954	0.2233	0.0000	0.1972	0.1972	0.3314
23	0.2298	0.0835	109.974	0.8110	0.2422	0.3149	0.3973	0.2072	0.0000	0.1844	0.1844	0.3263
24	0.2217	0.1032	114.966	0.8177	0.2184	0.3293	0.3951	0.1959	0.0000	0.1753	0.1753	0.3148
25	0.2118	0.1202	119.981	0.8240	0.1957	0.3397	0.3920	0.1861	0.0000	0.1674	0.1674	0.2997
26	0.2003	0.1402	124.987	0.8302	0.1724	0.3517	0.3917	0.1738	0.0000	0.1573	0.1573	0.2849
27	0.1874	0.1571	129.982	0.8360	0.1507	0.3578	0.3882	0.1655	0.0000	0.1505	0.1505	0.2658
28	0.1729	0.1729	134.993	0.8411	0.1324	0.3596	0.3832	0.1598	0.0000	0.1457	0.1457	0.2452
29	0.1572	0.1873	139.991	0.8462	0.1132	0.3621	0.3793	0.1530	0.0000	0.1400	0.1400	0.2236
30	0.1403	0.2003	144.997	0.8506	0.0950	0.3626	0.3748	0.1482	0.0000	0.1360	0.1360	0.1989
31	0.1223	0.2118	149.997	0.8543	0.0783	0.3629	0.3713	0.1440	0.0000	0.1324	0.1324	0.1737
32	0.1034	0.2216	154.992	0.8579	0.0606	0.3632	0.3682	0.1394	0.0000	0.1285	0.1285	0.1469
33	0.0836	0.2298	159.996	0.8606	0.0467	0.3620	0.3650	0.1366	0.0000	0.1261	0.1261	0.1186
34	0.0633	0.2362	164.999	0.8625	0.0358	0.3609	0.3626	0.1348	0.0000	0.1245	0.1245	0.0900
35	0.0425	0.2408	169.995	0.8644	0.0243	0.3591	0.3599	0.1333	0.0000	0.1232	0.1232	0.0603
36	0.0213	0.2436	175.001	0.8653	0.0128	0.3582	0.3584	0.1327	0.0000	0.1227	0.1227	0.0302
37	0.0000	0.2445	180.000	0.8653	0.0000	0.3586	0.3586	0.1325	0.0000	0.1226	0.1226	0.0000
. . .												
69	-0.0836	-0.2296	339.987	0.7045	-0.1736	-0.2431	-0.2988	0.5364	0.0000	0.4145	0.4145	-0.1186
70	-0.0633	-0.2361	344.992	0.7026	-0.1304	-0.2588	-0.2898	0.5493	0.0000	0.4224	0.4224	-0.0900
71	-0.0425	-0.2407	349.991	0.7007	-0.0877	-0.2751	-0.2887	0.5546	0.0000	0.4257	0.4257	-0.0603
72	-0.0213	-0.2435	354.999	0.6998	-0.0438	-0.2833	-0.2867	0.5587	0.0000	0.4282	0.4282	-0.0302
73	0.0000	-0.2444	360.000	0.6998	0.0000	-0.2829	-0.2829	0.5622	0.0000	0.4303	0.4303	0.0000

force and moment coefficients - pressure integration

bernoulli pressures

x	cn(x)	cy(x)	cn	ca	cy	cm	cln	csl	xcpn	xcpy
1.00000	1.8115E-02	-3.2937E-08	3.3965E-04	9.4296E-04	-6.1758E-10	9.2908E-04	-1.6916E-09	0.0000E+00	0.050	0.016

(n) Pages 40 and 41

Figure 20.- Continued.

-111-

stratford separation criterion (laminar)   f(s) =0.01511

summary of pressure distribution and separation points on body ...   x =   1.00

+y side:

	y	z	beta	arc	cp	cp'	dcp'/dx
stagnation pt.	0.000	-0.244	0.000	0.430	0.562		
min. pressure	0.000	0.245	180.000	0.768	0.133	0.000	0.000
separation	0.000	0.000	0.000	0.000	0.000	0.000	0.000

-y side:

	y	z	beta	arc	cp	cp'	dcp'/dx
stagnation pt.	-0.021	0.244	184.999	0.430	0.133		
min. pressure	0.000	0.000	0.000	0.000	0.000	0.000	0.000
separation	0.000	0.000	0.000	0.000	0.000	0.000	0.000

separation not found at x =   1.000

(o) Page 42

Figure 20.- Continued.

x = 7.0000   r = 1.1528   dr/dx = 0.1034   m = 1.6000

body surface pressure distribution

j	y	z	beta	u/v0	v/v0	w/v0	vt/v0	cp(m)	dphi/dt	cpz	cp(i)	vcp/v0
1	0.0000	-1.2301	0.000	0.9117	0.0000	-0.1017	0.1017	0.1752	0.0000	0.1584	0.1584	0.0000
2	0.0954	-1.2257	4.453	0.9117	0.0215	-0.1019	0.1041	0.1745	0.0000	0.1579	0.1579	0.0318
3	0.1902	-1.2123	8.914	0.9139	0.0640	-0.0868	0.1078	0.1687	0.0000	0.1531	0.1531	0.0634
4	0.2832	-1.1903	13.384	0.9179	0.1221	-0.0601	0.1361	0.1518	0.0000	0.1390	0.1390	0.0945
5	0.3740	-1.1595	17.875	0.9218	0.1807	-0.0336	0.1838	0.1254	0.0000	0.1165	0.1165	0.1245
6	0.4616	-1.1205	22.390	0.9266	0.2034	-0.0050	0.2034	0.1067	0.0000	0.1001	0.1001	0.1538
7	0.5453	-1.0732	26.934	0.9317	0.2104	0.0242	0.2118	0.0921	0.0000	0.0871	0.0871	0.1814
8	0.6245	-1.0182	31.522	0.9369	0.2179	0.0535	0.2244	0.0753	0.0000	0.0719	0.0719	0.2074
9	0.6983	-0.9558	36.154	0.9443	0.2279	0.1039	0.2505	0.0468	0.0000	0.0455	0.0455	0.2318
10	0.7662	-0.8863	40.842	0.9522	0.2384	0.1578	0.2859	0.0116	0.0000	0.0115	0.0115	0.2535
11	0.8275	-0.8102	45.605	0.9602	0.2475	0.2113	0.3254	-0.0273	0.0000	-0.0278	-0.0278	0.2731
12	0.8816	-0.7282	50.443	0.9654	0.2180	0.2387	0.3233	-0.0358	0.0000	-0.0366	-0.0366	0.2901
13	0.9278	-0.6404	55.385	0.9708	0.1881	0.2658	0.3256	-0.0471	0.0000	-0.0486	-0.0486	0.3029
14	0.9658	-0.5474	60.455	0.9761	0.1550	0.2926	0.3311	-0.0600	0.0000	-0.0624	-0.0624	0.3133
15	0.9945	-0.4496	65.672	0.9809	0.1135	0.3156	0.3354	-0.0711	0.0000	-0.0746	-0.0746	0.3180
16	1.0135	-0.3459	71.156	0.9859	0.0724	0.3363	0.3440	-0.0852	0.0000	-0.0903	-0.0903	0.3121
17	1.0245	-0.2353	77.063	0.9853	0.0430	0.3073	0.3103	-0.0642	0.0000	-0.0670	-0.0670	0.3019
18	1.0300	-0.1192	83.401	0.9831	0.0167	0.2671	0.2676	-0.0371	0.0000	-0.0380	-0.0380	0.2943
19	1.0316	0.0001	90.006	0.9817	0.0207	0.2513	0.2521	-0.0268	0.0000	-0.0273	-0.0273	0.2916
20	1.0300	0.1194	96.611	0.9805	0.0273	0.2448	0.2463	-0.0218	0.0000	-0.0221	-0.0221	0.2943
21	1.0245	0.2355	102.949	0.9800	0.0207	0.2577	0.2586	-0.0268	0.0000	-0.0273	-0.0273	0.3019
22	1.0135	0.3461	108.855	0.9802	0.0120	0.2679	0.2682	-0.0321	0.0000	-0.0328	-0.0328	0.3121
23	0.9945	0.4498	114.338	0.9831	-0.0001	0.2570	0.2570	-0.0320	0.0000	-0.0327	-0.0327	0.3180
24	0.9658	0.5476	119.555	0.9859	-0.0140	0.2433	0.2437	-0.0308	0.0000	-0.0315	-0.0315	0.3133
25	0.9278	0.6406	124.625	0.9876	-0.0285	0.2380	0.2397	-0.0322	0.0000	-0.0329	-0.0329	0.3029
26	0.8816	0.7284	129.566	0.9889	-0.0437	0.2372	0.2412	-0.0352	0.0000	-0.0361	-0.0361	0.2901
27	0.8275	0.8105	134.404	0.9901	-0.0588	0.2354	0.2426	-0.0382	0.0000	-0.0392	-0.0392	0.2731
28	0.7661	0.8865	139.166	0.9933	-0.0497	0.2125	0.2183	-0.0335	0.0000	-0.0343	-0.0343	0.2535
29	0.6983	0.9560	143.853	0.9965	-0.0400	0.1892	0.1933	-0.0298	0.0000	-0.0304	-0.0304	0.2318
30	0.6244	1.0184	148.485	0.9993	-0.0335	0.1687	0.1720	-0.0277	0.0000	-0.0282	-0.0282	0.2074
31	0.5453	1.0735	153.072	1.0000	-0.0460	0.1679	0.1741	-0.0297	0.0000	-0.0303	-0.0303	0.1814
32	0.4616	1.1207	157.615	1.0007	-0.0587	0.1670	0.1770	-0.0320	0.0000	-0.0327	-0.0327	0.1538
33	0.3739	1.1598	162.130	1.0016	-0.0581	0.1627	0.1728	-0.0323	0.0000	-0.0330	-0.0330	0.1245
34	0.2832	1.1905	166.620	1.0034	-0.0273	0.1515	0.1539	-0.0291	0.0000	-0.0297	-0.0297	0.0945
35	0.1901	1.2126	171.089	1.0044	0.0031	0.1400	0.1400	-0.0278	0.0000	-0.0284	-0.0284	0.0634
36	0.0954	1.2259	175.549	1.0051	0.0143	0.1335	0.1343	-0.0277	0.0000	-0.0283	-0.0283	0.0318
37	0.0000	1.2304	180.000	1.0051	0.0000	0.1337	0.1337	-0.0277	0.0000	-0.0282	-0.0282	0.0000
. . .												
69	-0.3740	-1.1595	342.125	0.9218	-0.1807	-0.0336	-0.1838	0.1254	0.0000	0.1165	0.1165	-0.1245
70	-0.2832	-1.1903	346.616	0.9179	-0.1221	-0.0601	-0.1361	0.1518	0.0000	0.1390	0.1390	-0.0945
71	-0.1902	-1.2123	351.085	0.9139	-0.0640	-0.0868	-0.1078	0.1687	0.0000	0.1531	0.1531	-0.0634
72	-0.0954	-1.2257	355.547	0.9117	-0.0215	-0.1019	-0.1041	0.1745	0.0000	0.1579	0.1579	-0.0318
73	0.0000	-1.2301	360.000	0.9117	0.0000	-0.1017	-0.1017	0.1752	0.0000	0.1584	0.1584	0.0000

force and moment coefficients - pressure integration

bernoulli pressures

x	cn(x)	cy(x)	ca	cn	cy	cm	csl	cln	xcpn	xcpy
7.00000	9.5719E-02	1.1758E-08	4.1173E-03	1.2853E-02	3.3604E-10	2.9718E-02	9.4112E-12	5.7763E-10	3.934	40.923

(p) Pages 52 and 53
Figure 20.- Continued.

stratford separation criterion (laminar) f(s) =0.01511

summary of pressure distribution and separation points on body ...   x =   7.00

+y side:

	y	z	beta	arc	cp	cp'	dcp'/dx
stagnation pt.	0.000	-1.230	0.000	0.158	0.175	0.000	0.000
min. pressure	1.013	-0.346	71.156	1.468	-0.085	0.016	0.166
separation	1.023	-0.254	76.065	1.560	-0.068		

-y side:

	y	z	beta	arc	cp	cp'	dcp'/dx
stagnation pt.	0.000	1.230	180.000	0.158	-0.028	0.000	0.000
min. pressure	-1.013	-0.346	288.844	1.468	-0.085	0.016	0.166
separation	-1.023	-0.254	283.935	1.560	-0.068		

initial positions and strengths of shed, vorticity at x =   7.000

	nv	gam/v	m(k)	y	z	beta	vt/v	yc	zc	rg/r
+y side:	1	0.0760	0.0792	1.1003	-0.2730	76.0652	0.3159	1.1999	-0.2403	1.0615
-y side:	2	-0.0760	0.0792	-1.1003	-0.2730	283.9348	0.3159	-1.1999	-0.2403	1.0615

(q) Page 54

Figure 20.- Continued.

summary of vortex field at x = 18.784   h = 1.28400

nv	gam/v	y	z	xshed	beta	yc	zc	rg	rg/r
1	0.07598	1.52244	1.84515	7.00000	140.474	1.50748	1.40613	2.06148	1.10004
2	0.06696	1.58985	1.32580	8.50000	129.825	1.79016	0.85512	1.98391	1.05865
3	0.06992	1.59573	0.84098	10.00000	117.790	1.91456	0.46909	1.97119	1.05186
4	0.02430	0.38612	2.07295	11.50000	169.331	0.30857	1.94335	1.96770	1.05000
5	0.05399	1.62695	0.49243	13.00000	106.840	1.97939	0.20981	1.99048	1.06215
6	0.07315	0.77378	2.20681	14.50000	160.678	0.66407	1.99631	2.10386	1.12266
7	0.10473	1.24962	2.22813	16.00000	150.715	1.16578	1.91471	2.24169	1.19621
8	0.05480	1.41426	2.03604	17.50000	145.216	1.35131	1.65485	2.13649	1.14007
9	-0.07598	-1.52244	1.84515	7.00000	219.526	-1.50748	1.40613	2.06148	1.10004
10	-0.06696	-1.58985	1.32580	8.50000	230.175	-1.79016	0.85512	1.98391	1.05865
11	-0.06992	-1.59573	0.84098	10.00000	242.210	-1.91456	0.46909	1.97119	1.05186
12	-0.02430	-0.38612	2.07295	11.50000	190.669	-0.30857	1.94335	1.96770	1.05000
13	-0.05399	-1.62695	0.49243	13.00000	253.160	-1.97939	0.20981	1.99048	1.06215
14	-0.07315	-0.77378	2.20681	14.50000	199.322	-0.66407	1.99631	2.10386	1.12266
15	-0.10473	-1.24962	2.22813	16.00000	209.285	-1.16578	1.91471	2.24169	1.19621
16	-0.05480	-1.41426	2.03604	17.50000	214.784	-1.35131	1.65485	2.13649	1.14007

centroid of vorticity

	gam/v	y	z
+y body:	0.52383	1.32848	-1.66293
-y body:	-0.52383	-1.32848	1.66293

(r) Page 90
Figure 20.- Continued.

```
 x        r       dr/dx       m
18.7840  1.8740   0.0000    1.6000
body surface pressure distribution
```

j	z	y	beta	u/vo	v/vo	w/vo	vt/vo	cp(m)	dphi/dt	cpz	cp(i)	vcp/vo
1	-1.9517	0.0000	0.000	0.9899	0.0000	0.0331	0.0331	0.0200	-0.0008	0.0189	0.0197	0.0000
2	-1.9448	0.1469	4.320	0.9899	0.0818	0.0345	0.0345	0.0131	-0.0008	0.0122	0.0122	0.0336
3	-1.9227	0.2917	8.627	0.9899	0.0876	0.0355	0.0946	0.0120	-0.0008	0.0111	0.0119	0.0666
4	-1.8858	0.4347	12.982	0.9899	0.0645	0.0372	0.0745	0.0155	-0.0008	0.0145	0.0153	0.0987
5	-1.8355	0.5733	17.347	0.9899	0.0478	0.0459	0.0663	0.0168	-0.0008	0.0158	0.0166	0.1309
6	-1.7702	0.7062	21.749	0.9896	0.1059	0.0974	0.1438	0.0009	-0.0008	0.0001	0.0009	0.1597
7	-1.6917	0.8334	26.228	0.9892	0.1670	0.1518	0.2257	-0.0282	-0.0008	-0.0295	-0.0287	0.1885
8	-1.6007	0.9519	30.740	0.9885	0.1716	0.1735	0.2440	-0.0350	-0.0008	-0.0366	-0.0358	0.2153
9	-1.4962	1.0614	35.352	0.9872	0.1311	0.1644	0.2103	-0.0178	-0.0008	-0.0188	-0.0180	0.2369
10	-1.3803	1.1612	40.073	0.9860	0.0899	0.1586	0.1823	-0.0046	-0.0008	-0.0054	-0.0046	0.2594
11	-1.2531	1.2484	44.892	0.9867	0.0935	0.2241	0.2428	-0.0311	-0.0008	-0.0325	-0.0317	0.2756
12	-1.1141	1.3233	49.907	0.9873	0.1003	0.2921	0.3088	-0.0664	-0.0007	-0.0702	-0.0695	0.2878
13	-0.9657	1.3845	55.106	0.9877	0.0755	0.2979	0.3073	-0.0663	-0.0006	-0.0700	-0.0693	0.2984
14	-0.8063	1.4289	60.564	0.9879	0.0275	0.2490	0.2505	-0.0371	-0.0006	-0.0386	-0.0381	0.2980
15	-0.6344	1.4567	66.468	0.9884	-0.0112	0.2144	0.2147	-0.0223	-0.0004	-0.0230	-0.0226	0.2898
16	-0.4467	1.4673	73.066	0.9899	-0.0203	0.2281	0.2290	-0.0317	-0.0008	-0.0323	-0.0323	0.2687
17	-0.2385	1.4677	80.772	0.9917	-0.0229	0.2462	0.2473	-0.0440	-0.0008	-0.0445	-0.0453	0.2455
18	-0.0158	1.4683	89.383	0.9929	-0.0105	0.1829	0.1832	-0.0217	0.0027	-0.0193	-0.0220	0.2318
19	0.2122	1.4681	98.223	0.9941	-0.0004	0.1053	0.1053	-0.0086	-0.0093	-0.0007	-0.0086	0.2069
20	0.4436	1.4677	106.819	0.9956	-0.0009	0.0807	0.0813	-0.0363	-0.0393	0.0022	-0.0371	0.1332
21	0.6717	1.4688	114.576	0.9970	0.0202	0.1310	0.1325	-0.0489	-0.0390	-0.0116	-0.0506	0.1271
22	0.8929	1.4678	121.314	0.9982	0.0302	0.0432	0.0527	-0.0532	-0.0560	0.0009	-0.0551	0.0955
23	1.1060	1.4681	126.992	0.9991	0.0424	0.0543	0.0689	-0.0292	-0.0267	-0.0030	-0.0297	0.1652
24	1.3011	1.4692	131.526	1.0010	0.0568	0.0342	0.0662	-0.0657	-0.0623	-0.0063	-0.0687	0.0963
25	1.4784	1.4707	135.224	1.0025	0.0734	0.1553	0.1718	-0.0635	-0.0317	-0.0345	-0.0662	0.1770
26	1.6279	1.4587	137.903	1.0036	0.1200	0.2107	0.2425	-0.0878	-0.0272	-0.0660	-0.0932	0.2431
27	1.7234	1.4587	139.755	1.0032	0.1759	0.1656	0.2416	-0.1133	-0.0578	-0.0647	-0.1226	0.2031
28	1.7939	1.3917	142.195	1.0022	0.0850	0.0906	0.1242	-0.1013	-0.0888	-0.0199	-0.1087	0.0487
29	1.8817	1.3040	145.278	1.0010	0.0110	-0.0115	0.0159	-0.0766	-0.0783	0.0023	-0.0807	0.0462
30	1.9472	1.2342	147.631	1.0001	0.0106	0.0630	0.0638	-0.0729	-0.0723	-0.0043	-0.0766	0.0409
31	1.9579	1.1389	149.814	0.9997	-0.2027	0.0227	0.2040	-0.0979	-0.0638	-0.0410	-0.1048	0.0146
32	1.9544	0.9911	153.109	1.0015	-0.1006	-0.0235	-0.1033	-0.0636	-0.0528	-0.0136	-0.0664	0.0011
33	1.9569	0.8186	157.299	1.0038	-0.0716	-0.0311	-0.0781	-0.0573	-0.0459	-0.0136	-0.0595	-0.0355
34	1.9554	0.6296	162.152	1.0064	0.2265	-0.0403	-0.2301	-0.0983	-0.0394	-0.0658	-0.1052	-0.0307
35	1.9557	0.4251	167.736	1.0111	0.0111	-0.0427	-0.0582	-0.0554	-0.0317	-0.0258	-0.0575	-0.0381
36	1.9564	0.2154	173.716	1.0163	-0.2186	-0.0403	-0.2223	-0.1032	-0.0285	-0.0824	-0.1109	-0.0113
37	1.9551	0.0000	180.000	1.0168	0.0000	-0.0428	0.0428	-0.0608	-0.0276	-0.0357	-0.0634	0.0000
⋯												
69	-1.8355	-0.5733	342.653	0.9899	-0.0478	0.0459	-0.0663	0.0168	-0.0008	0.0158	0.0166	-0.1309
70	-1.8858	-0.4347	347.018	0.9899	-0.0645	0.0372	-0.0745	0.0155	-0.0008	0.0145	0.0153	-0.0987
71	-1.9227	-0.2917	351.373	0.9899	-0.0876	0.0355	-0.0946	0.0120	-0.0008	0.0111	0.0119	-0.0666
72	-1.9448	-0.1469	355.680	0.9899	-0.0818	0.0345	-0.0888	0.0131	-0.0008	0.0122	0.0129	-0.0336
73	-1.9517	0.0000	360.000	0.9899	0.0000	0.0331	-0.0331	0.0200	-0.0008	0.0189	0.0197	0.0000

force and moment coefficients - pressure integration

x	cn(x)	cy(x)	ca	cn	cy	cm	cln	csl
18.78400	6.8482E-02	7.7234E-09	2.3419E-03	2.0464E-02	-6.0386E-10	3.9660E-02	-1.4077E-09	-3.7268E-10

xcpn	xcpy
7.367	46.540

bernoulli pressures

(s) Pages 91 and 92

Figure 20.- Continued.
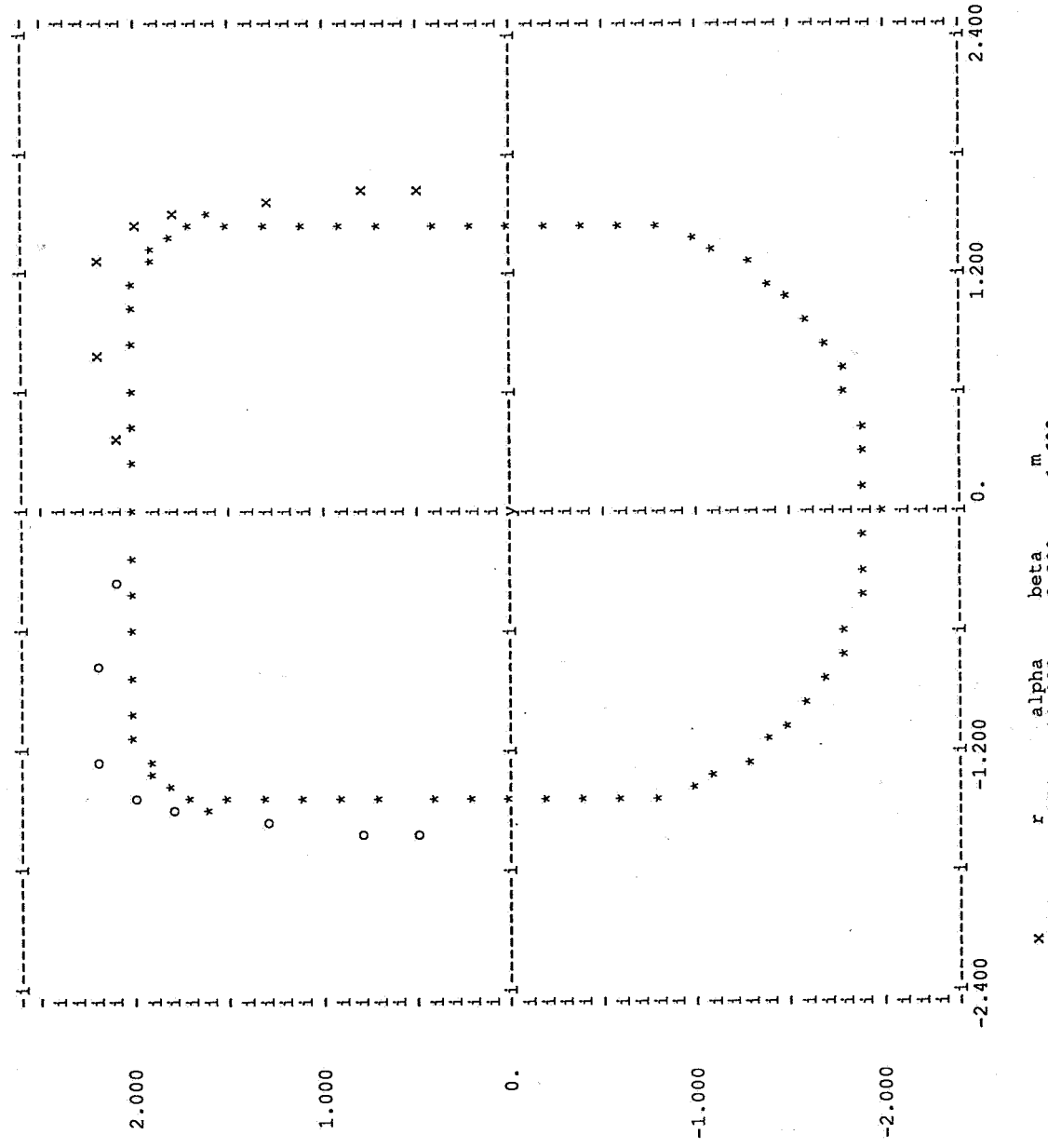
(t) Page 93
Figure 20.- Continued.

```
stratford separation criterion (laminar)  f(s) =0.01511

summary of pressure distribution and separation points on body ...    x =  18.78
```

+y side:

	y	z	beta	arc	cp	cp'	dcp'/dx
stagnation pt.	0.000	-1.952	0.000	0.019	0.020		
min. pressure	1.323	-1.114	49.907	1.652	-0.066	0.000	0.000
separation	1.411	-0.872	58.302	1.909	-0.049	0.016	0.106

-y side:

	y	z	beta	arc	cp	cp'	dcp'/dx
stagnation pt.	0.000	1.955	180.000	0.019	-0.061		
min. pressure	-1.323	-1.114	310.093	1.652	-0.066	0.000	0.000
separation	-1.411	-0.872	301.698	1.909	-0.049	0.016	0.106

```
initial positions and strengths of shed, vorticity at x =  18.784
```

	nv	gam/v	m(k)	y	z	beta	vt/v	yc	zc	rg/r
+y side:	17	0.0487	0.0576	1.4833	-0.9160	58.3022	0.2734	1.7286	-0.9072	1.0417
-y side:	18	-0.0487	0.0576	-1.4833	-0.9160	301.6978	0.2734	-1.7286	-0.9072	1.0417

```
centroid of vorticity
            gam/v       y         z
+y body:   0.57255   1.34165   1.44348
-y body:  -0.57255  -1.34165   1.44348
```

(u) Page 94

Figure 20.- Continued.

-118-

```
************************************  contribution of nose section to total loads  ************************************

    strengths and positions of vortices at end of nose section

                a =   1.5000
            gamma/2piva      y0/a      z0/a
    1         0.06075       0.8944    0.9623
    2        -0.06075      -0.8944    0.9623


            force and moment coefficients

                bernoulli loading pressure

        unrolled body coordinates    rolled body coordinates

    cx          0.00234                  0.00234
    cz          0.02046                  0.02046
    cy          0.00000                  0.00000
    cm          0.03966                  0.03966
    cln         0.00000                  0.00000
    cll         0.00000                  0.00000


vortex information written to tape11

         y              z            gamma/v
18
 1   0.15224E+01   0.18452E+01    0.75975E-01
 2   0.15899E+01   0.13258E+01    0.66962E-01
 3   0.15957E+01   0.84098E+00    0.69915E-01
 4   0.38612E+00   0.20730E+01    0.24304E-01
 5   0.16269E+01   0.49243E+00    0.53390E-01
 6   0.77378E+00   0.22068E+01    0.73153E-01
 7   0.12496E+01   0.22281E+01    0.10473E+00
 8   0.14143E+01   0.20360E+01    0.54797E-01
 9   0.14833E+01  -0.91602E+00    0.48719E-01
10  -0.15224E+01   0.18452E+01   -0.75976E-01
11  -0.15899E+01   0.13258E+01   -0.66962E-01
12  -0.15957E+01   0.84098E+00   -0.69915E-01
13  -0.38612E+00   0.20730E+01   -0.24304E-01
14  -0.16269E+01   0.49243E+00   -0.53390E-01
15  -0.77378E+00   0.22068E+01   -0.73153E-01
16  -0.12496E+01   0.22281E+01   -0.10473E+00
17  -0.14143E+01   0.20360E+01   -0.54797E-01
18  -0.14833E+01  -0.91602E+00   -0.48719E-01
```

(v) Pages 94 and 95

Figure 20.- Continued.

step 2   loads on forward-finned section with effects of forebody vorticity

```
$input  b2=      8.50000,  b2v=  0.,  crp=    11.7320,  crpv=  0.,  delr=  0.,  dell=
0., delu=   0., deld=   0., fac=    0.950000, fkle=   0.500000, fkse=  0.500000
, lvswp= 0., mswr=  6, mswl=  0, mswu=  0, mswd=  0, ncw=  6, ncwt=  0, nout=
0   0 0   0   1, npr=  0, ntdat=   0, ntpr=  0, n2dprf=   0, phidih=  0., phifr=
0., phifl=  0., phifu=   90.0000, phifd=   90.0000, swlep=   44.0000
, swlev= 0., swtep= -5.76000, swtev=  0., thetit=   0., thetr=  0., thetl=
0., thetu=   90.0000, thetd=   90.0000, tolfac=   1.00000, xlebip=   18.7840
, ybod=   1.50000  -1.50000  0.    0., zbod=  0.  0.    0.
$end
```

(w) Page 96

Figure 20.- Continued.

fin section input geometry description

fin property		fin 1 or r	fin 2 or 1	fin 3 or u	fin 4 or d
no. of panels - spanwise	(msw) =	6	0	0	0
root chord	(cr) =	11.732	11.732	0.000	0.000
leading edge sweep	(swle) =	44.000	44.000	0.000	0.000
trailing edge sweep	(swte) =	-5.760	-5.760	0.000	0.000
exposed semispan	(b2) =	8.500	8.500	0.000	0.000
fin dihedral	(phif) =	0.000	0.000	90.000	90.000
body angle of fin attachment	(thet) =	0.000	0.000	90.000	90.000
fin deflection	(del) =	0.000	0.000	0.000	0.000
y-intersection of fin to body	(ybod) =	1.500	-1.500	0.000	0.000
z-intersection of fin to body	(zbod) =	0.000	0.000	0.000	0.000
axial location of section le	(xwle) =	18.784			

interdigitated fin angles
phidih   thetit
   0.   0.

(x) Page 97

Figure 20.- Continued.

```
length of body influenced by fins

x of wing leading-edge                          (xlebip)  =   18.784
x of wing trailing-edge                         (xtebip)  =   30.516
length of interference shell                       (bil)  =   11.732
ring of corner coordinates at  leading edge     (ircle)   =   12
ring of corner coordinates at  trailing edge    (ircte)   =   18
ring of panels behind leading edge              (irple)   =   12
ring of panels ahead of trailing edge           (irpte)   =   17
first panel in interference shell               (ipanle)  =  155
last panel in interference shell                (ipante)  =  238
body segment containing leading-edge            (isecle)  =    1
body segment containing trailing-edge           (isecte)  =    1
```

(y) Page 98

Figure 20.- Continued.

triplet-induced velocities at fin control points

	x	y	z	bdu	bdv	bdw
1	2.43493	2.22458	0.00000	0.00642	0.00788	0.06506
2	4.26146	2.22458	0.00000	0.01701	0.00118	0.08104
3	6.08799	2.22458	0.00000	-0.00234	0.00627	0.07267
4	7.91452	2.22458	0.00000	-0.00472	0.00071	0.06872
5	9.74105	2.22458	0.00000	-0.00351	-0.00200	0.06574
6	11.56758	2.22458	0.00000	-0.00311	-0.00022	0.06731
7	3.56582	3.64384	0.00000	0.00187	0.00920	0.03059
8	5.14006	3.64384	0.00000	0.04222	0.03642	0.05685
9	6.71431	3.64384	0.00000	-0.01208	0.02033	0.03588
10	8.28855	3.64384	0.00000	-0.00795	0.01196	0.03666
11	9.86279	3.64384	0.00000	-0.00284	-0.00186	0.02533
12	11.43704	3.64384	0.00000	-0.00360	0.00000	0.02657
13	4.69749	5.06409	0.00000	0.00722	0.00046	0.01962
14	6.01928	5.06409	0.00000	0.00659	0.00019	0.02277
15	7.34106	5.06409	0.00000	0.01864	-0.01859	0.02273
16	8.66284	5.06409	0.00000	-0.02334	-0.02854	0.00492
17	9.98462	5.06409	0.00000	-0.00739	-0.01172	0.01575
18	11.30640	5.06409	0.00000	-0.00645	-0.00353	0.00681
19	5.83051	6.48602	0.00000	0.00104	-0.00621	0.01292
20	6.89953	6.48602	0.00000	0.00508	-0.00022	0.01165
21	7.96855	6.48602	0.00000	0.00201	-0.00333	0.01359
22	9.03757	6.48602	0.00000	0.01768	-0.01933	0.01215
23	10.10659	6.48602	0.00000	0.01241	-0.01335	0.01619
24	11.17561	6.48602	0.00000	0.00763	-0.01173	0.01048
25	6.96609	7.91116	0.00000	0.00320	-0.00241	0.00243
26	7.78177	7.91116	0.00000	0.00300	-0.00229	0.01009
27	8.59746	7.91116	0.00000	0.00507	-0.00149	0.00750
28	9.41315	7.91116	0.00000	0.00594	-0.00260	0.01054
29	10.22883	7.91116	0.00000	-0.04406	-0.05655	-0.01048
30	11.04451	7.91116	0.00000	0.01627	-0.01841	0.00843
31	8.10764	9.34380	0.00000	0.01403	-0.01164	0.00919
32	8.66866	9.34380	0.00000	0.00282	-0.00182	0.00813
33	9.22968	9.34380	0.00000	-0.00077	-0.00600	0.00704
34	9.79070	9.34380	0.00000	-0.00373	0.00032	0.00840
35	10.35172	9.34380	0.00000	0.00550	-0.00285	0.00524
36	10.91274	9.34380	0.00000	0.00842	-0.00640	0.00825

(z) Page 99

Figure 20.- Continued.

vortex-induced velocities at fin control points

	x	y	z	v	w
1	2.43493	2.22458	0.00000	0.01567	-0.00363
2	4.26146	2.22458	0.00000	0.01567	-0.00363
3	6.08799	2.22458	0.00000	0.01567	-0.00363
4	7.91452	2.22458	0.00000	0.01567	-0.00363
5	9.74105	2.22458	0.00000	0.01567	-0.00363
6	11.56758	2.22458	0.00000	0.01567	-0.00363
7	3.56582	3.64384	0.00000	0.00273	0.00118
8	5.14006	3.64384	0.00000	0.00273	0.00118
9	6.71431	3.64384	0.00000	0.00273	0.00118
10	8.28855	3.64384	0.00000	0.00273	0.00118
11	9.86279	3.64384	0.00000	0.00273	0.00118
12	11.43704	3.64384	0.00000	0.00273	0.00118
13	4.69749	5.06409	0.00000	0.00118	0.00102
14	6.01928	5.06409	0.00000	0.00118	0.00102
15	7.34106	5.06409	0.00000	0.00118	0.00102
16	8.66284	5.06409	0.00000	0.00118	0.00102
17	9.98462	5.06409	0.00000	0.00118	0.00102
18	11.30640	5.06409	0.00000	0.00118	0.00102
19	5.83051	6.48602	0.00000	0.00060	0.00075
20	6.89953	6.48602	0.00000	0.00060	0.00075
21	7.96855	6.48602	0.00000	0.00060	0.00075
22	9.03757	6.48602	0.00000	0.00060	0.00075
23	10.10659	6.48602	0.00000	0.00060	0.00075
24	11.17561	6.48602	0.00000	0.00060	0.00075
25	6.96609	7.91116	0.00000	0.00034	0.00055
26	7.78177	7.91116	0.00000	0.00034	0.00055
27	8.59746	7.91116	0.00000	0.00034	0.00055
28	9.41315	7.91116	0.00000	0.00034	0.00055
29	10.22883	7.91116	0.00000	0.00034	0.00055
30	11.04451	7.91116	0.00000	0.00034	0.00055
31	8.10764	9.34380	0.00000	0.00021	0.00042
32	8.66866	9.34380	0.00000	0.00021	0.00042
33	9.22968	9.34380	0.00000	0.00021	0.00042
34	9.79070	9.34380	0.00000	0.00021	0.00042
35	10.35172	9.34380	0.00000	0.00021	0.00042
36	10.91274	9.34380	0.00000	0.00021	0.00042

(aa) Page 100

Figure 20.- Continued.

velocities from constant-u panels

i	fu	fv	fw
1	0.18225	-0.17576	-0.23508
2	0.17375	-0.14015	-0.25105
3	0.08343	-0.07653	-0.24269
4	0.08761	-0.05637	-0.23873
5	0.08570	-0.02587	-0.23576
6	0.11024	-0.01465	-0.23733
7	0.21122	-0.20499	-0.20541
8	0.19400	-0.15941	-0.23167
9	0.11046	-0.07606	-0.21070
10	0.11684	-0.06814	-0.21149
11	0.08539	-0.03637	-0.20015
12	0.09961	-0.01149	-0.20139
13	0.23280	-0.22617	-0.19430
14	0.14369	-0.13247	-0.19744
15	0.17255	-0.11204	-0.19740
16	0.10421	-0.04937	-0.17960
17	0.12594	-0.04659	-0.19043
18	0.09372	-0.01676	-0.18148
19	0.23182	-0.22386	-0.18732
20	0.20436	-0.16217	-0.18606
21	0.17422	-0.10715	-0.18799
22	0.16306	-0.07723	-0.18655
23	0.12390	-0.03255	-0.19059
24	0.11166	-0.01869	-0.17683
25	0.23266	-0.22468	-0.18468
26	0.22497	-0.17726	-0.18430
27	0.20519	-0.12656	-0.18170
28	0.18195	-0.07953	-0.18474
29	0.16441	-0.05536	-0.16372
30	0.14562	-0.01831	-0.18263
31	0.23160	-0.22365	-0.18325
32	0.23035	-0.18150	-0.18220
33	0.22189	-0.13539	-0.18111
34	0.18839	-0.08146	-0.18247
35	0.14467	-0.03862	-0.17930
36	0.10302	-0.00891	-0.18231

(ab) Page 102

Figure 20.- Continued.

aft of leading edge of finned section

j	theta, deg.	xw	yw	zw	utot	vtot	wtot	cp bern.	p/pinf. bern.
1	281.26617	1.85756	0.19411	-1.97444	0.00219	0.11353	-0.15890	0.01283	1.02299
2	292.63074	1.85756	0.56911	-1.87396	0.00303	0.05183	-0.15232	0.02132	1.03821
3	304.20093	1.85756	0.90533	-1.67985	0.00645	0.21670	-0.00729	-0.05515	0.90116
4	316.10214	1.85756	1.17985	-1.40533	-0.01310	0.10909	-0.03012	0.02362	1.04233
5	328.48996	1.85756	1.37397	-1.06912	-0.05376	0.10222	0.09447	0.05249	1.09406
6	341.56506	1.85756	1.47444	-0.69412	-0.08522	0.02587	-0.03627	0.19078	1.34187
7	360.00000	1.85756	1.50000	-0.25000	-0.12952	-0.00211	-0.03197	0.29045	1.52049
8	18.43495	1.85756	1.47444	0.25000	-0.15768	-0.00647	-0.14886	0.25064	1.55086
9	31.01765	1.85756	1.49850	0.70056	0.03663	-0.01183	-0.06930	0.09595	0.82807
10	42.32370	1.85756	1.49260	1.13017	0.03106	-0.00031	-0.25058	-0.03700	0.93370
11	53.13010	1.85756	1.48132	1.66683	0.00397	-0.00667	-0.23377	-0.13098	0.76529
12	66.58666	1.85756	1.16683	1.98132	-0.00831	-0.47035	-0.21991	-0.15778	0.71725
13	78.63718	1.85756	0.63017	1.99260	0.00147	0.23834	-0.25293	-0.03502	0.93724
14	90.00000	1.85756	0.20056	1.99850	0.00189	0.26648	-0.20612	-0.04432	0.92057
. . .									
57	281.26617	9.67890	0.19411	-1.97444	-0.07049	0.03227	-0.16960	0.18069	1.32379
58	292.63074	9.67890	0.56911	-1.87396	-0.06650	0.10911	-0.12859	0.15629	1.28008
59	304.20093	9.67890	0.90533	-1.67985	-0.07582	0.10706	-0.09141	0.17161	1.30753
60	316.10214	9.67890	1.17985	-1.40533	-0.08152	0.11526	-0.02207	0.16232	1.29088
61	328.48996	9.67890	1.37397	-1.06912	-0.10849	0.05623	-0.01656	0.23233	1.41634
62	341.56506	9.67890	1.47444	-0.69412	-0.12123	0.02937	-0.00970	0.26126	1.46818
63	360.00000	9.67890	1.50000	-0.25000	-0.12577	-0.00211	-0.07498	0.29573	1.52994
64	18.43495	9.67890	1.47444	0.25000	-0.14433	-0.00647	-0.04210	0.24164	1.56699
65	31.51003	9.67890	1.47396	0.69412	0.09741	-0.03268	0.05344	-0.19359	0.65309
66	43.89785	9.67890	1.37396	1.06912	0.09670	-0.33652	0.08662	-0.27885	0.50030
67	55.79908	9.67890	1.17985	1.40533	0.07280	-0.00894	-0.19113	-0.11014	0.80263
68	67.36928	9.67890	0.90533	1.67985	0.05046	-0.02592	-0.02695	-0.08845	0.84150
69	78.73383	9.67890	0.56911	1.87397	0.04786	-0.04153	-0.13146	-0.06684	0.88023
70	90.00000	9.67890	0.19411	1.97444	0.05062	-0.01055	-0.20013	-0.06959	0.87530
71	281.26617	11.63423	0.19411	-1.97444	-0.08303	0.05433	-0.16669	0.20644	1.36995
72	292.63074	11.63423	0.56911	-1.87396	-0.08422	0.07511	-0.14268	0.20462	1.36668
73	304.20093	11.63423	0.90533	-1.67985	-0.09092	0.08145	-0.11106	0.21475	1.38484
74	316.10214	11.63423	1.17985	-1.40533	-0.09762	0.07961	-0.06854	0.22121	1.39640
75	328.48996	11.63423	1.37397	-1.06912	-0.10562	0.04244	-0.04987	0.23964	1.42944
76	341.56506	11.63423	1.47444	-0.69412	-0.10705	0.02700	-0.02764	0.23653	1.42387
77	360.00000	11.63423	1.50000	-0.25000	-0.11176	-0.00211	-0.10134	0.26926	1.48252
78	18.43495	11.63423	1.47444	0.25000	-0.10955	-0.00647	-0.08306	0.18015	1.67716
79	31.51003	11.63423	1.47444	0.69412	0.11618	-0.03046	0.03657	-0.21767	0.60993
80	43.89785	11.63423	1.37396	1.06912	0.10802	-0.32555	0.06014	-0.28145	0.49563
81	55.79908	11.63423	1.17985	1.40533	0.08764	0.05257	-0.24799	-0.14302	0.74371
82	67.36928	11.63423	0.90533	1.67985	0.07069	-0.03399	-0.02076	-0.12673	0.77289
83	78.73383	11.63423	0.56911	1.87397	0.07337	-0.03541	-0.13400	-0.11325	0.79706
84	90.00000	11.63423	0.19411	1.97444	0.06757	-0.06528	-0.19292	-0.10432	0.81307

(ac) Pages 103 and 104

Figure 20.- Continued.

integration of the bernoulli pressure distribution

mach = 1.6000   alphac= 10.0000   phir= 0.0000

refs= 159.9984   refl=   9.1760

xm =   25.1500   zm =   0.0000

point	xb	yb	zb	cp	cx*sref	cy*sref	cz*sref	cm*sref*refl	cln*sref*refl	cll*sref*refl
1	19.76167	0.19411	-1.97444	0.01283	0.00000	-0.00128	0.00974	0.05247	-0.00691	0.00064
2	19.76167	0.56911	-1.87396	0.02132	0.00000	-0.00625	0.01508	0.08126	-0.03366	0.00312
3	19.76167	0.90533	-1.67985	-0.05515	0.00000	-0.02571	-0.03350	-0.18053	-0.13852	-0.01285
4	19.76167	1.17985	-1.40533	-0.02362	0.00000	-0.01435	0.01101	0.05933	-0.07732	0.00717
5	19.76167	1.37397	-1.06912	0.05249	0.00000	-0.03713	0.01538	0.08287	-0.20007	0.01856
6	19.76167	1.47444	-0.69412	0.29078	0.00000	-0.14482	0.01907	0.10273	-0.78035	0.07241
7	19.76167	1.50000	-0.25000	0.29045	0.00000	-0.28396	0.00000	0.00000	-1.53009	0.07099
8	19.76167	1.50000	0.25000	-0.25064	0.00000	0.24504	0.00000	0.00000	1.32036	-0.06126
9	19.76103	1.49850	0.70056	-0.09595	-0.00012	0.07525	-0.00056	-0.00312	0.40570	0.05187
10	19.75750	1.49260	1.13017	-0.03700	-0.00025	0.03314	-0.00064	-0.00373	0.17908	0.03650
11	19.75175	1.48132	1.66683	-0.13098	-0.00310	0.15748	-0.00360	-0.02458	0.85471	0.25717
12	19.75175	1.16683	1.98132	-0.15778	-0.00373	-0.00433	0.18971	1.03152	0.02775	-0.21278
13	19.75750	0.63017	1.99260	-0.03502	-0.00024	0.00061	0.03137	-0.16964	0.00341	-0.01856
14	19.76103	0.20056	1.99850	-0.04432	-0.00005	0.00026	0.03476	0.18745	0.00142	-0.00645
...										
57	27.58300	0.19411	-1.97444	0.18069	0.00000	-0.01806	0.13716	-0.33372	0.04393	0.00903
58	27.58300	0.56911	-1.87396	0.15629	0.00000	-0.04579	0.11056	-0.26899	0.11142	0.02290
59	27.58300	0.90533	-1.67985	0.17161	0.00000	-0.07999	0.10425	-0.25363	0.19462	0.04040
60	27.58300	1.17985	-1.40533	0.16232	0.00000	-0.09860	0.07566	-0.18408	0.23990	0.04930
61	27.58300	1.37397	-1.06912	0.23233	0.00000	-0.16435	0.06807	-0.16563	0.39986	0.08217
62	27.58300	1.47444	-0.69412	0.26126	0.00000	-0.19833	0.02611	-0.06352	0.48253	0.09917
63	27.58300	1.50000	-0.25000	0.29573	0.00000	-0.28912	0.00000	0.00000	0.70343	0.07228
64	27.58300	1.50000	0.25000	0.24164	0.00000	-0.23624	0.01935	-0.04707	0.57477	0.05906
65	27.58300	1.47444	0.69412	-0.19359	0.00000	0.14696	0.08171	-0.19879	-0.35754	-0.07348
66	27.58300	1.37396	1.06912	-0.27885	0.00000	0.19726	0.05134	-0.12491	-0.47992	-0.09863
67	27.58300	1.17985	1.40533	-0.11014	0.00000	0.06691	0.05373	-0.13072	-0.16278	-0.03345
68	27.58300	0.90533	1.67985	-0.08845	0.00000	0.04123	0.04728	-0.11503	-0.10030	-0.02061
69	27.58300	0.56911	1.87397	-0.06684	0.00000	0.01958	0.04765	-0.11503	-0.04765	-0.00979
70	27.58300	0.19411	1.97444	-0.06959	0.00000	0.00695	0.05283	-0.12853	-0.01692	-0.00348
71	29.53834	0.19411	-1.97444	0.20644	0.00000	-0.02063	0.15671	-0.68771	0.09054	0.01031
72	29.53834	0.56911	-1.87396	0.20462	0.00000	-0.05996	0.14475	0.63519	0.26311	0.02998
73	29.53834	0.90533	-1.67985	0.21475	0.00000	-0.10010	0.13045	0.57246	0.43927	0.05005
74	29.53834	1.17985	-1.40533	0.22121	0.00000	-0.13437	0.10311	0.45247	0.58967	0.06718
75	29.53834	1.37397	-1.06912	0.23964	0.00000	-0.16952	0.07022	-0.30813	0.74390	0.08476
76	29.53834	1.47444	-0.69412	0.23653	0.00000	-0.17956	0.02364	-0.10373	0.78795	0.08978
77	29.53834	1.50000	-0.25000	0.26926	0.00000	-0.26325	0.00000	0.00000	1.15523	0.06581
78	29.53834	1.50000	0.25000	-0.18015	0.00000	0.17613	0.02175	-0.09546	-0.77292	-0.04403
79	29.53834	1.47444	0.69412	-0.21767	0.00000	0.16524	0.08247	-0.36190	-0.72512	-0.08262
80	29.53834	1.37396	1.06912	-0.28145	0.00000	0.19909	0.06666	-0.29254	-0.87370	-0.09955
81	29.53834	1.17985	1.40533	-0.14302	0.00000	0.08688	0.07698	-0.33783	-0.38125	-0.04344
82	29.53834	0.90533	1.67985	-0.12673	0.00000	0.05907	0.08011	-0.35154	-0.25923	-0.02954
83	29.53834	0.56911	1.87397	-0.11325	0.00000	0.03318	0.08011	-0.34750	-0.14561	0.01659
84	29.53834	0.19411	1.97444	-0.10432	0.00000	0.01042	0.07919	-0.34750	-0.04575	0.00521

(ad) Pages 104 through 106

Figure 20.- Continued.

body loads on ring 12 at x= 19.76167

　　　　　　bernoulli loading

　rolled body-axis coordinates　　　unrolled body-axis coordinates

cx　　0.00009　　　　　　　　0.00009
cy　　0.00000　　　　　　　　0.00000
cz　　0.00372　　　　　　　　0.00372
cll　　0.00000　　　　　　　　0.00000
cm　　0.00220　　　　　　　　0.00218
cln　　0.00000　　　　　　　　0.00000

. . .

body loads on ring 17 at x= 29.53834

　　　　　　bernoulli loading

　rolled body-axis coordinates　　　unrolled body-axis coordinates

cx　　0.00000　　　　　　　　0.00000
cy　　0.00000　　　　　　　　0.00000
cz　　0.01295　　　　　　　　0.01295
cll　　0.00000　　　　　　　　0.00000
cm　　-0.00619　　　　　　　-0.00619
cln　　0.00000　　　　　　　　0.00000

cumulative body loads to this station

　　　　　　bernoulli loading

　rolled body-axis coordinates　　　unrolled body-axis coordinates

cx　　0.00007　　　　　　　　0.00007
cy　　0.00000　　　　　　　　0.00000
cz　　0.04094　　　　　　　　0.04094
cll　　0.00000　　　　　　　　0.00000
cm　　-0.00389　　　　　　　-0.00390
cln　　0.00000　　　　　　　　0.00000

(ae) Pages 106 and 107

Figure 20.- Continued.

- 128 -

velocities at fin panel centroid points

j	xbar(j)	ybar(j)	zbar(j)	uchk	vchk	wchk	bdv	bdw	vnor
1	1.61299	2.22458	0.00000	0.18162	-0.17546	-0.17288	0.02355	0.06143	-0.11144
2	3.43952	2.22458	0.00000	0.16930	-0.13758	-0.24255	0.01685	0.07741	-0.16514
3	5.26605	2.22458	0.00000	0.10617	-0.07286	-0.21862	0.02194	0.06904	-0.14958
4	7.09258	2.22458	0.00000	0.08425	-0.04674	-0.22864	0.01638	0.06509	-0.16356
5	8.91911	2.22458	0.00000	0.08008	-0.02336	-0.23950	0.01367	0.06211	-0.17738
6	10.74565	2.22458	0.00000	0.12278	-0.02930	-0.24487	0.01588	0.06368	-0.18118
7	2.85741	3.64384	0.00000	0.21143	-0.20536	-0.16732	0.01193	0.03176	-0.13555
8	4.43165	3.64384	0.00000	0.17238	-0.14459	-0.23500	-0.03369	0.05802	-0.17698
9	6.00590	3.64384	0.00000	0.09179	-0.07895	-0.20623	-0.02306	0.03706	-0.16918
10	7.58014	3.64384	0.00000	0.11631	-0.06553	-0.20760	-0.00923	0.03784	-0.16976
11	9.15438	3.64384	0.00000	0.08142	-0.03111	-0.20648	-0.00086	0.02650	-0.17998
12	10.72863	3.64384	0.00000	0.09828	-0.01053	-0.20605	0.00273	0.02774	-0.17830
13	4.10269	5.06409	0.00000	0.22755	-0.21974	-0.18639	0.00164	0.02065	-0.16574
14	5.42447	5.06409	0.00000	0.16599	-0.13195	-0.15851	0.00137	0.02379	-0.13472
15	6.74625	5.06409	0.00000	0.17801	-0.11788	-0.17302	-0.01741	0.02375	-0.14927
16	8.06804	5.06409	0.00000	0.11166	-0.05739	-0.15920	0.02972	0.00595	-0.15326
17	9.38982	5.06409	0.00000	0.12355	-0.04298	-0.18785	-0.01054	0.01678	-0.17107
18	10.71160	5.06409	0.00000	0.08797	-0.00961	-0.17949	0.00471	0.00783	-0.17166
19	5.34945	6.48602	0.00000	0.23182	-0.22386	-0.18447	0.00681	0.01367	-0.17080
20	6.41847	6.48602	0.00000	0.20780	-0.16621	-0.16401	0.00039	0.01241	-0.15161
21	7.48749	6.48602	0.00000	0.17435	-0.10727	-0.17808	0.00393	0.01434	-0.16374
22	8.55651	6.48602	0.00000	0.16914	-0.08411	-0.16924	-0.01873	0.01290	-0.15634
23	9.62553	6.48602	0.00000	0.13108	-0.04108	-0.17266	-0.01275	0.01694	-0.15573
24	10.69455	6.48602	0.00000	0.11391	-0.02107	-0.17401	0.01112	0.00318	-0.17083
25	6.59903	7.91116	0.00000	0.23266	-0.22468	-0.18439	0.00275	0.01065	-0.17335
26	7.41472	7.91116	0.00000	0.22497	-0.17726	-0.17856	0.00263	0.01065	-0.16791
27	8.23040	7.91116	0.00000	0.20848	-0.13050	-0.16760	0.00115	0.00805	-0.15954
28	9.04609	7.91116	0.00000	0.18213	-0.07972	-0.17283	-0.00225	0.01109	-0.16174
29	9.86177	7.91116	0.00000	0.15175	-0.03960	-0.15960	0.05689	-0.00993	-0.16953
30	10.67746	7.91116	0.00000	0.14668	-0.01942	-0.16607	-0.01807	0.00898	-0.15709
31	7.85518	9.34380	0.00000	0.22365	-0.22355	-0.18342	-0.01142	0.00961	-0.17382
32	8.41620	9.34380	0.00000	0.23035	-0.18150	-0.18186	-0.00203	0.00855	-0.17332
33	8.97722	9.34380	0.00000	0.22189	-0.13539	-0.17401	0.00622	0.00746	-0.16655
34	9.53824	9.34380	0.00000	0.18839	-0.08146	-0.16201	-0.00054	0.00882	-0.15319
35	10.09926	9.34380	0.00000	0.14781	-0.04242	-0.15292	-0.00264	0.00565	-0.14727
36	10.66028	9.34380	0.00000	0.10332	-0.00925	-0.15924	-0.00619	0.00866	-0.15058

(af) Page 108

Figure 20.- Continued.

velocities at fin panel outboard aft corners

j	xrb(j)	yrc(j)	zrb(j)	uchk	vchk	wchk	bdv	bdw	vnor
1	3.07157	2.91667	0.00000	0.00417	-0.03650	-0.18060	0.02355	0.06143	-0.11917
2	4.77507	2.91667	0.00000	0.01431	-0.04568	-0.17884	0.01685	0.07741	-0.10143
3	6.47858	2.91667	0.00000	0.00871	-0.03408	-0.18951	0.02194	0.06904	-0.12047
4	8.18209	2.91667	0.00000	-0.00224	-0.02897	-0.16062	0.01638	0.06509	-0.09553
5	9.88559	2.91667	0.00000	-0.00574	-0.02179	-0.15271	0.01367	0.06211	-0.09060
6	11.58910	2.91667	0.00000	-0.12582	-0.03705	-0.17516	0.01588	0.06368	-0.11148
7	4.18780	4.33333	0.00000	0.21115	-0.20503	-0.17150	-0.01193	0.03176	-0.13973
8	5.63948	4.33333	0.00000	0.19052	-0.15549	-0.16833	-0.03369	0.05802	-0.11031
9	7.09116	4.33333	0.00000	0.11255	-0.07709	-0.16000	-0.02306	0.03706	-0.12294
10	8.54284	4.33333	0.00000	0.00878	-0.03399	-0.17442	-0.00923	0.03784	-0.13658
11	9.99452	4.33333	0.00000	0.07929	-0.02646	-0.11633	0.00086	0.02650	-0.08982
12	11.44620	4.33333	0.00000	0.10083	-0.01126	-0.13468	0.00273	0.02774	-0.10694
13	5.30403	5.75000	0.00000	0.22755	-0.21974	-0.18710	0.00164	0.02065	-0.16645
14	6.50388	5.75000	0.00000	0.12776	-0.14286	-0.19723	0.00137	0.02379	-0.17343
15	7.70374	5.75000	0.00000	0.17690	-0.11652	-0.16818	0.01741	0.02375	-0.14443
16	8.90359	5.75000	0.00000	0.21190	-0.05605	-0.08884	0.02972	0.00595	-0.08290
17	10.10345	5.75000	0.00000	0.22448	-0.04204	-0.11405	-0.01054	0.01678	-0.09727
18	11.30330	5.75000	0.00000	0.18714	-0.00606	-0.09998	0.00471	0.00783	-0.09214
19	6.42026	7.16667	0.00000	0.23182	-0.22386	-0.18461	-0.00681	0.01367	-0.17094
20	7.36829	7.16667	0.00000	0.20711	-0.03210	-0.16244	0.00039	0.01241	-0.15003
21	8.31632	7.16667	0.00000	-0.00078	-0.04564	-0.17864	0.00393	0.01434	-0.16430
22	9.26434	7.16667	0.00000	0.01415	-0.04002	-0.12120	-0.01873	0.01290	-0.10830
23	10.21237	7.16667	0.00000	0.13051	-0.00773	-0.08379	-0.01275	0.01694	-0.06685
24	11.16040	7.16667	0.00000	0.10334	-0.04136	-0.15350	-0.01112	0.00318	-0.15032
25	7.53650	8.58333	0.00000	0.00000	-0.03999	-0.20253	0.00275	0.01103	-0.19149
26	8.23270	8.58333	0.00000	0.00620	-0.04385	-0.13082	-0.00263	0.01065	-0.12017
27	8.92890	8.58333	0.00000	0.18238	-0.07997	-0.18592	-0.00115	0.00805	-0.17787
28	9.62510	8.58333	0.00000	0.15173	-0.02790	-0.10025	-0.00225	0.01109	-0.08916
29	10.32130	8.58333	0.00000	0.15388	-0.03952	-0.15577	0.05689	-0.00993	-0.16570
30	11.01750	8.58333	0.00000	0.23160	-0.02365	-0.08718	-0.01807	-0.00898	-0.07820
31	8.65273	10.00000	0.00000	0.23035	-0.22365	-0.18345	-0.01142	-0.00961	-0.17384
32	9.09710	10.00000	0.00000	0.22189	-0.18150	-0.16971	-0.00203	-0.00855	-0.16117
33	9.54148	10.00000	0.00000	0.18839	-0.13539	-0.17305	-0.00622	-0.00746	-0.16559
34	9.98585	10.00000	0.00000	0.14298	-0.08146	-0.13479	-0.00054	-0.00882	-0.12597
35	10.43022	10.00000	0.00000	0.10735	-0.03641	-0.10478	-0.00264	-0.00565	-0.09912
36	10.87460	10.00000	0.00000	0.10735	-0.01412	-0.03579	-0.00619	0.00866	-0.02713

(ag) Page 109

Figure 20.- Continued.

velocities and bernoulli pressures at control points immediately above and below fin surface

j	x(j)	y(j)	z(j)	utota	vtota	wtota	pressa	utotb	vtotb	wtotb	pressb
1	2.434927	2.224584	0.000000	0.188672	-0.152216	-0.173648	-0.307937	-0.166239	0.190517	-0.173648	0.353060
2	4.261459	2.224584	0.000000	0.190755	-0.123303	-0.173648	-0.306201	-0.127869	0.127750	-0.173648	0.291704
3	6.087990	2.224584	0.000000	0.081091	-0.054592	-0.173648	-0.127171	-0.108209	0.060913	-0.173648	0.263062
4	7.914521	2.224584	0.000000	0.082888	-0.039986	-0.173648	-0.129206	-0.082768	0.031645	-0.173648	0.208358
5	9.741053	2.224584	0.000000	0.082185	-0.012193	-0.173648	-0.126756	-0.104892	0.035446	-0.173648	0.258626
6	11.567585	2.224584	0.000000	0.107136	-0.001231	-0.173648	-0.169817	-0.110110	0.017935	-0.173648	0.271947
7	3.565819	3.643845	0.000000	0.213086	-0.193055	-0.173648	-0.346223	-0.200045	0.205901	-0.173648	0.423181
8	5.140062	3.643845	0.000000	0.098377	-0.053000	-0.173648	-0.372942	-0.124458	0.091081	-0.173648	0.294633
9	6.714306	3.643845	0.000000	0.124795	-0.077371	-0.173648	-0.157136	-0.108165	0.073025	-0.173648	0.260824
10	8.288548	3.643845	0.000000	0.082548	-0.035507	-0.173648	-0.203347	-0.082134	0.012107	-0.173648	0.207995
11	9.862793	3.643845	0.000000	0.096009	-0.008763	-0.173648	-0.128324	-0.078123	0.005408	-0.173648	0.199079
12	11.437036	3.643845	0.000000	0.240024	-0.224533	-0.173648	-0.150898	-0.111456	0.007189	-0.173648	0.275435
13	4.697495	5.064091	0.000000	0.150277	-0.131102	-0.173648	-0.382945	-0.215080	0.214957	-0.173648	0.452767
14	6.019275	5.064091	0.000000	0.191189	-0.129450	-0.173648	-0.250415	-0.178185	0.127702	-0.173648	0.410222
15	7.341056	5.064091	0.000000	0.080869	-0.057127	-0.173648	-0.307656	-0.136807	0.070683	-0.173648	0.328117
16	8.662837	5.064091	0.000000	0.133332	-0.012046	-0.173648	-0.124615	-0.125643	0.069652	-0.173648	0.302076
17	9.984618	5.064091	0.000000	0.087267	-0.217051	-0.173648	-0.214997	-0.097931	0.001764	-0.173648	0.244220
18	11.306399	5.064091	0.000000	0.232855	-0.161780	-0.173648	-0.135729	-0.093095	0.001822	-0.173648	0.233207
19	5.830508	6.486016	0.000000	0.209441	-0.103223	-0.173648	-0.373680	-0.230782	0.230678	-0.173648	0.478867
20	6.899527	6.486016	0.000000	0.176229	-0.095960	-0.173648	-0.336136	-0.195068	0.156945	-0.173648	0.438118
21	7.968546	6.486016	0.000000	0.180743	-0.045300	-0.173648	-0.283716	-0.170764	0.108502	-0.173648	0.399163
22	9.037566	6.486016	0.000000	0.136311	-0.029813	-0.173648	-0.289130	-0.131363	0.038997	-0.173648	0.320089
23	10.106586	6.486016	0.000000	0.119286	-0.221928	-0.173648	-0.218838	-0.091009	0.018272	-0.173648	0.279435
24	11.175606	6.486016	0.000000	0.235864	-0.174630	-0.173648	-0.190679	-0.229456	0.013644	-0.173648	0.278124
25	6.966088	7.911162	0.000000	0.227963	-0.127709	-0.173648	-0.377942	-0.221973	0.227426	-0.173648	0.478070
26	7.781774	7.911162	0.000000	0.210263	-0.081780	-0.173648	-0.360431	-0.196276	0.179887	-0.173648	0.490574
27	8.597460	7.911162	0.000000	0.187890	0.001524	-0.173648	-0.332020	-0.174531	0.120348	-0.173648	0.456472
28	9.413145	7.911162	0.000000	0.120356	-0.036380	-0.173648	-0.297461	-0.181778	0.074934	-0.173648	0.417333
29	10.228830	7.911162	0.000000	0.161883	-0.235624	-0.173648	-0.191773	-0.188799	0.078462	-0.173648	0.434050
30	11.044515	7.911162	0.000000	0.245624	-0.179466	-0.173648	-0.257300	-0.217571	-0.014798	-0.173648	0.292344
31	8.107636	9.343798	0.000000	0.233174	-0.129173	-0.173648	-0.390935	-0.227528	0.212228	-0.173648	0.460421
32	8.668657	9.343798	0.000000	0.221122	-0.179466	-0.173648	-0.367196	-0.222655	0.183535	-0.173648	0.501788
33	9.229677	9.343798	0.000000	0.192117	-0.129173	-0.173648	-0.345588	-0.184657	0.141606	-0.173648	0.511669
34	9.790696	9.343798	0.000000	0.150166	-0.081997	-0.173648	-0.303101	-0.135797	0.081997	-0.173648	0.440169
35	10.351717	9.343798	0.000000	0.111443	-0.041262	-0.173648	-0.240008	-0.093220	0.031558	-0.173648	0.331302
36	10.912737	9.343798	0.000000	0.111443	-0.015094	-0.173648	-0.177213	-0.093220	0.000642	-0.173648	0.233417

(ah) Page 111

Figure 20.- Continued.

pressure loadings at control points

j	x(j)	y(j)	z(j)	deltp,lin.	deltp,bern.
1	2.434927	2.224584	0.000000	0.709820	0.660997
2	4.261459	2.224584	0.000000	0.637248	0.597906
3	6.087990	2.224584	0.000000	0.378601	0.390232
4	7.914521	2.224584	0.000000	0.331312	0.337564
5	9.741053	2.224584	0.000000	0.374154	0.385382
6	11.567585	2.224584	0.000000	0.434492	0.441764
7	3.565819	3.643845	0.000000	0.826262	0.769404
8	5.140062	3.643845	0.000000	0.721349	0.667575
9	6.714306	3.643845	0.000000	0.413085	0.417960
10	8.288548	3.643845	0.000000	0.413857	0.411342
11	9.862793	3.643845	0.000000	0.321342	0.327403
12	11.437036	3.643845	0.000000	0.414930	0.426333
13	4.697495	5.064091	0.000000	0.910209	0.835712
14	6.019275	5.064091	0.000000	0.656922	0.660637
15	7.341056	5.064091	0.000000	0.655992	0.635773
16	8.662837	5.064091	0.000000	0.413024	0.426691
17	9.984618	5.064091	0.000000	0.462526	0.459217
18	11.306399	5.064091	0.000000	0.360724	0.368856
19	5.830508	6.486016	0.000000	0.927274	0.852547
20	6.899527	6.486016	0.000000	0.809019	0.774253
21	7.968546	6.486016	0.000000	0.693987	0.682879
22	9.037566	6.486016	0.000000	0.624212	0.609219
23	10.106586	6.486016	0.000000	0.499293	0.498272
24	11.175606	6.486016	0.000000	0.420590	0.418802
25	6.966088	7.911162	0.000000	0.930640	0.856012
26	7.781774	7.911162	0.000000	0.899871	0.851005
27	8.597460	7.911162	0.000000	0.813078	0.788493
28	9.413145	7.911162	0.000000	0.724843	0.714794
29	10.228830	7.911162	0.000000	0.604267	0.625823
30	11.044515	7.911162	0.000000	0.561365	0.549644
31	8.107636	9.343798	0.000000	0.926389	0.851356
32	8.668657	9.343798	0.000000	0.921404	0.868985
33	9.229677	9.343798	0.000000	0.887554	0.857257
34	9.790696	9.343798	0.000000	0.753548	0.743270
35	10.351717	9.343798	0.000000	0.571926	0.571310
36	10.912737	9.343798	0.000000	0.409326	0.410630

(ai) Page 112

Figure 20.- Continued.

- 132 -

fin loading information

```
       mach number =  0.16000E+01
    angle of attack =  10.000 degrees
    side slip angle =   0.000 degrees
           fin area =  122.38508
     reference area =  159.99840
   reference length =    9.17600
exposed fin span b/2=    8.50000
   moment center: xm =   25.15000
               zm =     0.00000
```

linear pressure (u/vinf) loads in body system

	total	fin 1 or r	fin 2 or l	fin 3 or u	fin 4 or d
defl. angle deg. =		0.00000	0.00000	0.00000	0.00000
cthr =	0.59489E-02	0.29744E-02	0.29744E-02	0.	0.
cz =	0.44770	0.22385	0.22385	0.	0.
cy =	0.	0.	0.	0.	0.
cm =	-0.27700E-01	-0.13850E-01	-0.13850E-01	0.	0.
cln =	0.	0.	0.	0.	0.
cll =	0.	-0.12907	0.12907	0.	0.
czft =		0.22385	0.22385	0.	0.
cyft =		0.	0.	0.	0.
cmft =		-0.13850E-01	-0.13850E-01	-0.13850E-01	0.
clnft =		0.	0.	0.	0.
clft =		-0.12907	0.12907	0.	0.

following are in unrolled body-axis coordinate system

	total	fin 1 or r	fin 2 or l	fin 3 or u	fin 4 or d
czu =	0.44770	0.22385	0.22385	0.	0.
cyu =	0.	0.	0.	0.	0.
cmu =	-0.27700E-01	-0.13850E-01	-0.13850E-01	0.	0.
clnu =	0.	0.	0.	0.	0.
czftu =		0.	-0.13850E-01	-0.13850E-01	0.
cyftu =		0.	0.	0.	0.
cmftu =		0.	0.	0.	0.

note: l.e. of lead panel in first chordwise row is supersonic

(aj) Page 113

Figure 20.- Continued.

- 133 -

spanwise distributions

-----------------------------upper right or right horizontal fin-----------------------------

i	y/(b/2)	cn*c/(2*b)	ct*c/(2*b)	cyl*c/(2*b)	cytot*c/(2*b)	cs*c/(2*b)	csint	ybar	gamnet(i)	gamma,le/vinf	xle
1	0.08525	0.15419	0.00000	0.00000	0.00000	0.00000	0.00000	0.00000	-2.61708	0.00000	0.69972
2	0.25222	0.14434	0.00000	0.00000	0.00000	0.00000	0.00000	0.00000	0.00000	0.00000	2.07029
3	0.41930	0.13489	0.00000	0.00000	0.00000	0.00000	0.00000	0.00000	0.00000	0.00000	3.44180
4	0.58659	0.12554	0.00000	0.00000	0.00000	0.00000	0.00000	0.00000	0.00000	0.00000	4.81494
5	0.75425	0.10963	0.00000	0.00000	0.00000	0.00000	0.00000	0.00000	0.00000	0.00000	6.19119
6	0.92280	0.07498	0.00000	0.00000	0.00000	0.00000	0.00000	0.00000	1.25392	0.00000	7.57467
7	1.00000	0.00000	0.00000	0.00000	0.00000	0.00000	0.00000	0.00000			

thrust- and side-force coefficients in plane of the fin

sumfx =cx..acts on leading edge
sumfyl=cy..acts on leading edge
sumfy2=cy..acts on leading and side edge
sumft2=cy..acts on side edge

sumfx = 0.00000E+00
sumfyl = 0.00000E+00
sumfy2 = 0.00000E+00
sumft2 = 0.13110E-02

side edge distribution

jtip	jse	distance from le /tipchord	suction force per unit length /(q*tipchord)	gamma,se /vinf	ybar	xse
	1	0.16667	-0.00004	0.00000	0.00000	8.20835
	2	0.33333	0.00485	0.00000	0.00000	8.65273
	3	0.50000	0.00464	0.00000	0.00000	9.09710
	4	0.66667	0.03500	0.00000	0.00000	9.54148
	5	0.83333	0.06368	0.00000	0.00000	9.98585
	6	1.00000	0.06891	0.00608	8.50000	10.43022

(ak) Page 114

Figure 20.- Continued.

-134-

s.e. augmentation of fin normal force from suction conversion in proportion with factor
kvse = 0.500

(local fin)
cnadd = 0.00066

(rolled body-axis)
cyadd   =   0.00000
czadd   =   0.00066
cmadd   =   -0.00023
clnadd   =   0.00000
clladd   =   -0.00071
xcg   =   28.3255
ycg   =   10.0000
zcg   =   0.0000

(unrolled body-axis)
cyadd   =   0.00000
czadd   =   0.00066
cmadd   =   -0.00023
clnadd   =   0.00000
clladd   =   -0.00071
xcg   =   28.3255
ycg   =   10.0000
zcg   =   0.0000

***** t.e. fin vorticity due to side-edge force augmentation

ivrt	gamma/vinf	y,c.g. (local fin)	z,c.g.	y,c.g. (body axes)	z,c.g.
1	0.00608	8.50000	0.23327	10.00000	0.23327

(a1) Pages 114 and 115

Figure 20.- Continued.

fin panel forces

j	ycpt(j)	delta-cp	gamma/vinf	fx	fy1	fy2
1	2.22458	0.70982	0.64825	0.11425	0.10018	0.00000
2	2.22458	0.63725	0.58198	0.01403	0.00981	0.00000
3	2.22458	0.37860	0.34576	0.02357	0.01229	0.00000
4	2.22458	0.33131	0.30258	0.00865	-0.00297	0.00000
5	2.22458	0.37415	0.34170	-0.00362	-0.00060	0.00000
6	2.22458	0.43449	0.39681	-0.00847	0.00010	0.00000
7	3.64384	0.82626	0.65037	0.07020	0.06155	0.00000
8	3.64384	0.72135	0.56779	-0.00536	-0.00375	0.00000
9	3.64384	0.41308	0.32515	0.00412	0.00215	0.00000
10	3.64384	0.41386	0.32576	0.00359	0.00123	0.00000
11	3.64384	0.32134	0.25293	-0.00454	-0.00075	0.00000
12	3.64384	0.41493	0.32660	-0.00431	-0.00005	0.00000
13	5.06409	0.91021	0.60155	0.01348	0.01182	0.00000
14	5.06409	0.65692	0.43415	0.04789	0.03347	0.00000
15	5.06409	0.65599	0.43354	0.02995	0.01561	0.00000
16	5.06409	0.41302	0.27296	0.01577	0.00542	0.00000
17	5.06409	0.46253	0.30568	0.00223	-0.00037	0.00000
18	5.06409	0.36072	0.23840	0.00134	-0.00002	0.00000
19	6.48602	0.92727	0.49564	0.00400	-0.00350	0.00000
20	6.48602	0.80902	0.43243	0.02700	0.01888	0.00000
21	6.48602	0.69399	0.37094	0.01042	0.00543	0.00000
22	6.48602	0.62421	0.33365	0.01636	0.00562	0.00000
23	6.48602	0.49929	0.26688	0.01355	0.00225	0.00000
24	6.48602	0.42059	0.22481	0.00180	-0.00002	0.00000
25	7.91116	0.93064	0.37955	0.00032	-0.00028	0.00000
26	7.91116	0.89987	0.36701	0.00596	0.00417	0.00000
27	7.91116	0.81308	0.33161	0.01325	0.00691	0.00000
28	7.91116	0.72484	0.29562	0.00998	0.00343	0.00000
29	7.91116	0.60427	0.24645	0.00288	0.00048	0.00000
30	7.91116	0.56137	0.22895	0.01074	-0.00013	0.00000
31	9.34380	0.92639	0.25986	-0.00013	-0.00011	-0.00004
32	9.34380	0.92140	0.25846	0.00024	-0.00017	0.00575
33	9.34380	0.88755	0.24897	0.00500	0.00261	0.00549
34	9.34380	0.75355	0.21138	0.01225	0.00421	0.04147
35	9.34380	0.57193	0.16043	0.01199	0.00199	0.07545
36	9.34380	0.40933	0.11482	0.00750	-0.00009	0.08164

(am) Page 115

Figure 20.- Continued.

fin loading information

```
        mach number =   0.16000E+01
    angle of attack =  10.000 degrees
    side slip angle =   0.000 degrees
           fin area = 122.38508
     reference area = 159.99840
   reference length =   9.17600
exposed fin span b/2=   8.50000
      moment center:  xm =  25.15000
                      zm =   0.00000
```

bernoulli pressure loads in body system

	total	fin 1 or r	fin 2 or 1	fin 3 or u	fin 4 or d
defl. angle deg. =		0.00000	0.00000	0.00000	0.00000
cthr =	0.59489E-02	0.29744E-02	0.29744E-02	0.	0.
cz =	0.43530	0.21765	0.21765	0.	0.
cy =	0.	0.	0.	0.	0.
cm =	-0.30241E-01	-0.15121E-01	-0.15121E-01	0.	0.
cln =	0.	0.	0.	0.	0.
cll =	0.	-0.12517	0.12517	0.	0.
czft =		0.21831	0.21831	0.	0.
cyft =		0.	0.	0.	0.
cmft =		-0.15348E-01	-0.15348E-01	0.	0.
clnft =		0.	0.	0.	0.
cllft =		-0.12589	0.12589	0.	0.

following are in unrolled body-axis coordinate system

		fin 1 or r	fin 2 or 1	fin 3 or u	fin 4 or d
czu =	0.43530	0.21765	0.21765	0.	0.
cyu =	0.	0.	0.	0.	0.
cmu =	-0.30241E-01	-0.15121E-01	-0.15121E-01	0.	0.
clnu =	0.	0.	0.	0.	0.
czftu =		0.	-0.15348E-01	-0.15348E-01	0.
cyftu =		0.	0.	0.	0.
cmftu =		0.	0.	0.	0.

note: l.e. of lead panel in first chordwise row is supersonic

(an) Page 116

Figure 20.- Continued.

spanwise distributions

-----------------------------upper right or right horizontal fin---------------------------------

i	y/(b/2)	cn*c/(2*b)	ct*c/(2*b)	cyl*c/(2*b)	cytot*c/(2*b)	cs*c/(2*b)	csint	ybar	gamnet(i)	gamma,le/vinf	xle
1	0.08525	0.15140	0.00000	0.00000	0.00000	0.00000	0.00000	0.00000	-2.61708	0.00000	0.69972
2	0.25222	0.14013	0.00000	0.00000	0.00000	0.00000	0.00000	0.00000	0.00000	0.00000	2.07029
3	0.41930	0.13207	0.00000	0.00000	0.00000	0.00000	0.00000	0.00000	0.00000	0.00000	3.44180
4	0.58659	0.12116	0.00000	0.00000	0.00000	0.00000	0.00000	0.00000	0.00000	0.00000	4.81494
5	0.75425	0.10605	0.00000	0.00000	0.00000	0.00000	0.00000	0.00000	0.00000	0.00000	6.19119
6	0.92280	0.07217	0.00000	0.00000	0.00000	0.00000	0.00000	0.00000	1.25392		7.57467
7	1.00000	0.00000									

thrust- and side-force coefficients in plane of the fin

sumfx =cx..acts on leading edge
sumfy1=cy..acts on leading edge
sumfy2=cy..acts on leading and side edge
sumft2=cy..acts on side edge

sumfx = 0.00000E+00
sumfy1 = 0.00000E+00
sumfy2 = 0.00000E+00
sumft2 = 0.13110E-02

side edge distribution

jtip jse	distance from le /tipchord	suction force per unit length /(q*tipchord)	gamma,se /vinf	ybar	xse
1	0.16667	-0.00004	0.00000	0.00000	8.20835
2	0.33333	0.00485	0.00000	0.00000	8.65273
3	0.50000	0.00464	0.00000	0.00000	9.09710
4	0.66667	0.03500	0.00000	0.00000	9.54148
5	0.83333	0.06368	0.00000	0.00000	9.98585
6	1.00000	0.06891	0.00608	8.50000	10.43022

(ao) Page 117

Figure 20.- Continued.

fin panel forces

j	ycpt(j)	delta-cp	gamma/vinf	fx	fy1	fy2
1	2.22458	0.66100	0.64825	0.11425	0.10018	0.00000
2	2.22458	0.59791	0.58198	0.01403	0.00981	0.00000
3	2.22458	0.39023	0.34576	0.02357	0.01229	0.00000
4	2.22458	0.33756	0.30258	0.00865	0.00297	0.00000
5	2.22458	0.38538	0.34170	-0.00362	-0.00060	0.00000
6	2.22458	0.44176	0.39681	-0.00847	0.00010	0.00000
7	3.64384	0.76940	0.65037	-0.07020	0.06155	0.00000
8	3.64384	0.66758	0.56779	-0.00536	-0.00375	0.00000
9	3.64384	0.41796	0.32515	0.00412	0.00215	0.00000
10	3.64384	0.41134	0.32576	0.00359	0.00123	0.00000
11	3.64384	0.32740	0.25293	-0.00454	-0.00075	0.00000
12	3.64384	0.42633	0.32660	-0.00431	-0.00005	0.00000
13	5.06409	0.83571	0.60155	0.01348	0.01182	0.00000
14	5.06409	0.66064	0.43415	0.04789	0.03347	0.00000
15	5.06409	0.63577	0.43354	0.02995	0.01561	0.00000
16	5.06409	0.42669	0.27296	0.01577	0.00542	0.00000
17	5.06409	0.45922	0.30568	0.00223	0.00037	0.00000
18	5.06409	0.36886	0.23840	0.00134	-0.00002	0.00000
19	6.48602	0.85255	0.49564	0.00400	0.00350	0.00000
20	6.48602	0.77425	0.43243	0.02700	0.01888	0.00000
21	6.48602	0.68288	0.37094	0.01042	0.00543	0.00000
22	6.48602	0.60922	0.33365	0.01636	0.00562	0.00000
23	6.48602	0.49827	0.26688	0.01355	0.00225	0.00000
24	6.48602	0.41880	0.22481	0.00180	-0.00002	0.00000
25	7.91116	0.85601	0.37955	0.00032	0.00028	0.00000
26	7.91116	0.85101	0.36701	0.00596	0.00417	0.00000
27	7.91116	0.78849	0.33161	0.01325	0.00691	0.00000
28	7.91116	0.71479	0.29562	0.00998	0.00343	0.00000
29	7.91116	0.62582	0.24645	0.00288	0.00048	0.00000
30	7.91116	0.54964	0.22895	0.01074	-0.00013	-0.00004
31	9.34380	0.85136	0.25986	-0.00013	-0.00011	-0.00575
32	9.34380	0.86898	0.25846	0.00024	0.00017	-0.00549
33	9.34380	0.85726	0.24897	0.00500	0.00261	0.04147
34	9.34380	0.74327	0.21138	0.01225	0.00421	0.07545
35	9.34380	0.57131	0.16043	0.01199	0.00199	0.08164
36	9.34380	0.41063	0.11482	0.00750	-0.00009	

(ap) Pages 117 and 118
Figure 20.- Continued.

*****t.e. fin vorticity due to attached flow*****

ivrt	gamma/vinf	y,c.g. (local fin)	y,c.g. (body axes)	z,c.g.
2	2.57385	6.62574	8.12574	0.00000

vortex information written on tapell from subroutine spnld

i	y	z	gamma
22			
1	0.15224E+01	0.18452E+01	0.75975E-01
2	0.15899E+01	0.13258E+01	0.66962E-01
3	0.15957E+01	0.84098E+00	0.69915E-01
4	0.38612E+00	0.20730E+01	0.24304E-01
5	0.16269E+01	0.49243E+00	0.53990E-01
6	0.77378E+00	0.22068E+01	0.73153E-01
7	0.12496E+01	0.22281E+01	0.10473E+00
8	0.14143E+01	0.20360E+01	0.54797E-01
9	0.14833E+01	-0.91602E+00	0.48719E-01
10	-0.15224E+01	0.18452E+01	-0.75976E-01
11	-0.15899E+01	0.13258E+01	-0.66962E-01
12	-0.15957E+01	0.84098E+00	-0.69915E-01
13	-0.38612E+00	0.20730E+01	-0.24304E-01
14	-0.16269E+01	0.49243E+00	-0.53990E-01
15	-0.77378E+00	0.22068E+01	-0.73153E-01
16	-0.12496E+01	0.22281E+01	-0.10473E+00
17	-0.14143E+01	0.20360E+01	-0.54797E-01
18	-0.14833E+01	-0.91602E+00	-0.48719E-01
19	0.10000E+02	0.23327E+00	0.60783E-02
20	0.81257E+01	0.00000E+00	0.25739E+01
21	-0.10000E+02	0.23327E+00	-0.60783E-02
22	-0.81257E+01	0.00000E+00	-0.25739E+01

(aq) Pages 118 and 119

Figure 20.- Continued.

step 3   vortex tracking over afterbody   afterbody loads with vortex effects

SAMPLE DEMON3 RUN FOR NONCIRCULAR NASA MODEL: TR 2434 -- DIMENSIONS IN INCHES

initial conditions

xi	xf	dx	tol	emkf	rgam	fdx
30.516	33.130	1.500	0.05000	1.050	0.000	0.000

options...

nclr	ncf	isym	nblsep	nsepr	nsmoth	ndfus	ndphi	lnp	nxfv	nfv	nvp	nvr	nvm	nva	nasym
3	1	0	1	0	0	1	1	1	1	0	0	0	0	0	0

nprntp	nprnts	nprntv	nprntvl	nplotv	nplota	nprtvl	ncntr	ncore	nvtrns	nrstrt	n2dprb
1	1	1	1	3	2	0	0	0	1	1	0

initial bernoulli pressure coefficients

2.0644E-01	2.0644E-01	2.0462E-01	2.0462E-01	2.1475E-01
2.2121E-01	2.2121E-01	2.3964E-01	2.3653E-01	2.6926E-01
2.6926E-01	-1.8015E-01	-2.1767E-01	-2.1767E-01	-2.8145E-01
-1.4302E-01	-1.4302E-01	-1.2673E-01	-1.2673E-01	-1.2673E-01
-1.2673E-01	-1.1325E-01	-1.0432E-01	-1.1325E-01	-1.1325E-01
-1.2673E-01	-1.2673E-01	-1.4302E-01	-1.4302E-01	-1.4302E-01
-1.4302E-01	-2.8145E-01	-1.8015E-01	-1.8015E-01	-1.8015E-01
-2.8145E-01	2.3653E-01	2.3964E-01	2.3964E-01	2.2121E-01
2.6926E-01	2.1475E-01	2.0462E-01	2.0462E-01	2.0644E-01
2.2121E-01				
2.0644E-01				

initial vorticity distribution

gamma/v	y	z	xshed
0.07598	1.52240	1.84520	0.00000
0.06696	1.58990	1.32580	0.00000
0.06991	1.59570	0.84098	0.00000
0.02430	0.38612	2.07300	0.00000
0.05399	1.62690	0.49243	0.00000
0.07315	0.77378	2.20680	0.00000
0.10473	1.24960	2.22810	0.00000
0.05480	1.41430	2.03600	0.00000
0.04872	1.48330	-0.91602	0.00000
0.00608	10.00000	0.23327	0.00000
2.57390	8.12570	0.00000	0.00000
-0.07598	-1.52240	1.84520	0.00000
-0.06696	-1.58990	1.32580	0.00000
-0.06991	-1.59570	0.84098	0.00000
-0.02430	-0.38612	2.07300	0.00000
-0.05399	-1.62690	0.49243	0.00000
-0.07315	-0.77378	2.20680	0.00000
-0.10473	-1.24960	2.22810	0.00000
-0.05480	-1.41430	2.03600	0.00000
-0.04872	-1.48330	-0.91602	0.00000
-0.00608	-10.00000	0.23327	0.00000
-2.57390	-8.12570	0.00000	0.00000

(ar) Page 120

Figure 20.- Continued.

summary of vortex field at x = 33.130   h = 1.11400

	nv	gam/v	y	z	xshed	beta	yc	zc	rg	rg/r
1	1	0.05552	1.51522	-0.82475	30.51600	61.440	1.68889	-0.71478	1.83392	1.11046
1	2	0.07598	1.55777	2.10932	0.00000	143.553	1.63126	2.00351	2.58362	1.56441
2	3	0.06696	1.61718	1.44210	0.00000	131.725	1.73015	1.33168	2.18329	1.32201
3	4	0.06991	1.60314	0.90083	0.00000	119.332	1.76446	0.79747	1.93630	1.17245
4	5	0.02430	0.46953	1.95921	0.00000	166.523	0.50390	1.80101	1.87017	1.13241
5	6	0.05399	1.71545	0.61232	0.00000	109.644	1.89820	0.53795	1.97296	1.19465
6	7	0.07315	0.77876	2.11146	0.00000	159.755	0.82607	1.97241	2.13841	1.29483
7	8	0.10473	1.10867	2.25395	0.00000	153.808	1.16431	2.13313	2.43020	1.47151
8	9	0.05480	1.34124	2.22924	0.00000	148.967	1.40482	2.11683	2.54056	1.53834
9	10	0.04872	1.41200	-0.82164	0.00000	59.805	1.59055	-0.69839	1.73712	1.05184
10	11	0.00608	9.77806	1.16406	0.00000	96.789	9.81254	1.15995	9.88087	5.98296
11	12	2.57390	8.11155	0.39551	0.00000	92.791	8.15366	0.39346	8.16314	4.94287
1	13	-0.05552	-1.51522	-0.82475	30.51600	298.560	-1.68889	-0.71478	1.83392	1.11046
1	14	-0.07598	-1.55777	2.10932	0.00000	216.447	-1.63126	2.00351	2.58362	1.56441
2	15	-0.06696	-1.61718	1.44210	0.00000	228.275	-1.73015	1.33168	2.18329	1.32201
3	16	-0.06991	-1.60314	0.90083	0.00000	240.668	-1.76446	0.79747	1.93630	1.17245
4	17	-0.02430	-0.46953	1.95921	0.00000	193.477	-0.50390	1.80101	1.87017	1.13241
5	18	-0.05399	-1.71545	0.61232	0.00000	250.356	-1.89820	0.53795	1.97296	1.19465
6	19	-0.07315	-0.77876	2.11146	0.00000	206.245	-0.82607	1.97241	2.13841	1.29483
7	20	-0.10473	-1.10867	2.25395	0.00000	206.192	-1.16431	2.13313	2.43020	1.47151
8	21	-0.05480	-1.34124	2.22924	0.00000	211.033	-1.40482	2.11683	2.54056	1.53834
9	22	-0.04872	-1.41200	-0.82164	0.00000	300.195	-1.59055	-0.69839	1.73712	1.05184
10	23	-0.00608	-9.77806	1.16406	0.00000	263.211	-9.81254	1.15995	9.88087	5.98296
11	24	-2.57390	-8.11155	0.39551	0.00000	267.208	-8.15366	0.39346	8.16314	4.94287

centroid of vorticity

	gam/v	y	z
+y body:	0.05552	1.51522	-0.82475
-y body:	-0.05552	-1.51522	-0.82475

(as) Page 127
Figure 20.- Continued.

x = 33.1300 r = 1.6515 dr/dx = 0.0000 m = 1.6000

body surface pressure distribution

j	y	z	beta	u/v0	v/v0	w/v0	vt/v0	cp(m)	dphi/dt	cpz	cp(i)	vcp/v0
1	0.0000	-1.8274	0.000	0.9808	0.0000	0.0202	0.0202	0.0111	0.0265	0.0375	0.0110	0.0000
2	-0.1326	-1.8210	4.164	0.9808	0.0112	0.0185	0.0216	0.0110	0.0265	0.0375	0.0109	0.0156
3	-0.2640	-1.8017	8.335	0.9809	0.0217	0.0312	0.0322	0.0101	0.0267	0.0367	0.0100	0.0310
4	-0.3931	-1.7698	12.522	0.9811	0.0326	0.0312	0.0451	0.0086	0.0268	0.0354	0.0085	0.0457
5	-0.5187	-1.7254	16.732	0.9813	0.0450	0.0356	0.0573	0.0067	0.0271	0.0338	0.0067	0.0594
6	-0.6398	-1.6689	20.974	0.9816	0.0453	0.0466	0.0650	0.0048	0.0274	0.0322	0.0048	0.0719
7	-0.7551	-1.6006	25.257	0.9820	0.0475	0.0554	0.0730	0.0026	0.0278	0.0304	0.0026	0.0829
8	-0.8638	-1.5209	29.592	0.9823	0.0485	0.0633	0.0798	0.0005	0.0283	0.0288	0.0005	0.0918
9	-0.9646	-1.4305	33.992	0.9825	0.0425	0.0728	0.0843	-0.0013	0.0289	0.0276	-0.0013	0.0984
10	-1.0566	-1.3298	38.470	0.9827	0.0394	0.0803	0.0894	-0.0033	0.0297	0.0263	-0.0033	0.1017
11	-1.1389	-1.2193	43.046	0.9829	0.0273	0.0793	0.0838	-0.0039	0.0308	0.0269	-0.0039	0.0998
12	-1.2104	-1.0999	47.739	0.9832	0.0099	0.0681	0.0688	-0.0040	0.0327	0.0287	-0.0040	0.0877
13	-1.2701	-0.9718	52.580	0.9834	-0.0128	0.0301	0.0327	-0.0049	0.0368	0.0319	-0.0050	0.0447
14	-1.3172	-0.8355	57.613	0.9837	-0.0585	-0.1104	-0.1250	-0.0246	0.0416	0.0167	-0.0250	-0.0938
15	-1.3503	-0.6912	62.892	0.9841	-0.0368	-0.0510	-0.0629	-0.0127	0.0405	0.0276	-0.0128	-0.0296
16	-1.3682	-0.5367	68.580	0.9843	-0.0164	-0.0254	-0.0303	-0.0068	0.0370	0.0302	-0.0068	0.0549
17	-1.3740	-0.3687	74.978	0.9846	-0.0116	-0.0319	-0.0339	-0.0053	0.0348	0.0295	-0.0053	0.0708
18	-1.3742	-0.1879	82.213	0.9848	-0.0116	-0.0228	-0.0256	-0.0046	0.0341	0.0294	-0.0046	0.0693
19	-1.3738	0.0000	89.999	0.9852	0.0000	-0.0185	0.0185	-0.0049	0.0340	0.0290	-0.0049	0.0622
20	-1.3742	0.1879	97.784	0.9856	0.0115	-0.0042	0.0123	-0.0060	0.0345	0.0285	-0.0061	0.0493
21	-1.3740	0.3687	105.020	0.9855	0.0119	-0.0105	0.0159	-0.0077	0.0362	0.0285	-0.0077	0.0263
22	-1.3682	0.5367	111.107	0.9853	0.0204	-0.0340	0.0397	-0.0116	0.0392	0.0275	-0.0117	-0.0074
23	-1.3503	0.6912	117.107	0.9852	0.0378	-0.0572	0.0686	-0.0170	0.0418	0.0246	-0.0172	-0.0392
24	-1.3172	0.8355	122.385	0.9851	0.0467	-0.0697	0.0838	-0.0202	0.0429	0.0225	-0.0205	-0.0555
25	-1.2701	0.9717	127.419	0.9851	0.0440	-0.0643	0.0643	-0.0171	0.0429	0.0255	-0.0169	-0.0433
26	-1.2103	1.0998	132.261	0.9852	0.0451	-0.0357	0.0575	-0.0167	0.0430	0.0261	-0.0176	-0.0354
27	-1.1388	1.2193	136.954	0.9853	0.0458	-0.0300	0.0548	-0.0174	0.0437	0.0262	-0.0186	-0.0379
28	-1.0566	1.3297	141.530	0.9854	0.0494	-0.0274	0.0565	-0.0184	0.0445	0.0259	-0.0205	-0.0447
29	-0.9645	1.4305	146.008	0.9853	0.0620	-0.0308	0.0692	-0.0202	0.0449	0.0244	-0.0217	-0.0558
30	-0.8637	1.5209	150.409	0.9853	0.0720	-0.0345	0.0798	-0.0214	0.0447	0.0230	-0.0229	-0.0708
31	-0.7551	1.6006	154.745	0.9852	0.0883	-0.0342	0.0947	-0.0226	0.0434	0.0205	-0.0222	-0.0867
32	-0.6397	1.6689	159.028	0.9852	0.1002	-0.0301	0.1046	-0.0219	0.0408	0.0186	-0.0182	-0.0985
33	-0.5186	1.7254	163.270	0.9851	0.1010	-0.0241	0.1038	-0.0180	0.0370	0.0188	-0.0134	-0.1033
34	-0.3930	1.7698	167.480	0.9853	0.0970	-0.0073	0.0973	-0.0133	0.0330	0.0197	-0.0076	-0.0930
35	-0.2639	1.8018	171.667	0.9856	0.0610	0.0077	0.0615	-0.0075	0.0324	0.0248	-0.0056	-0.0552
36	-0.1325	1.8210	175.838	0.9858	0.0270	0.0149	0.0308	-0.0056	0.0329	0.0273	-0.0056	-0.0234
37	0.0000	1.8275	180.000	0.9858	0.0000	0.0204	0.0204	-0.0052	0.0331	0.0279	-0.0052	0.0000
. . .												
69	-0.5187	-1.7254	343.268	0.9813	-0.0450	0.0356	-0.0573	0.0067	0.0271	0.0338	0.0067	-0.0594
70	-0.3931	-1.7698	347.478	0.9811	-0.0326	0.0312	-0.0451	0.0086	0.0268	0.0354	0.0085	-0.0457
71	-0.2640	-1.8017	351.665	0.9809	-0.0217	0.0237	-0.0322	0.0101	0.0267	0.0367	0.0100	-0.0310
72	-0.1326	-1.8210	355.836	0.9808	-0.0112	0.0185	-0.0216	0.0110	0.0265	0.0375	0.0109	-0.0156
73	0.0000	-1.8274	360.000	0.9808	0.0000	0.0202	-0.0202	0.0111	0.0265	0.0375	0.0110	0.0000

force and moment coefficients – pressure integration

x	cn(x)	cy(x)	ca	cn	cy	cm	cln	csl	xcpn	xcpy
33.13000	1.6072E-02	3.1741E-09	0.0000E+00	5.0443E-03	2.5613E-09	-3.4099E-03	-1.7166E-09	-1.2675E-11	31.353	19.000

bernoulli pressures

(at) Pages 128 and 129

Figure 20.- Continued.

x 33.130 r 1.651 alpha 10.000 beta 0.000 m 1.600
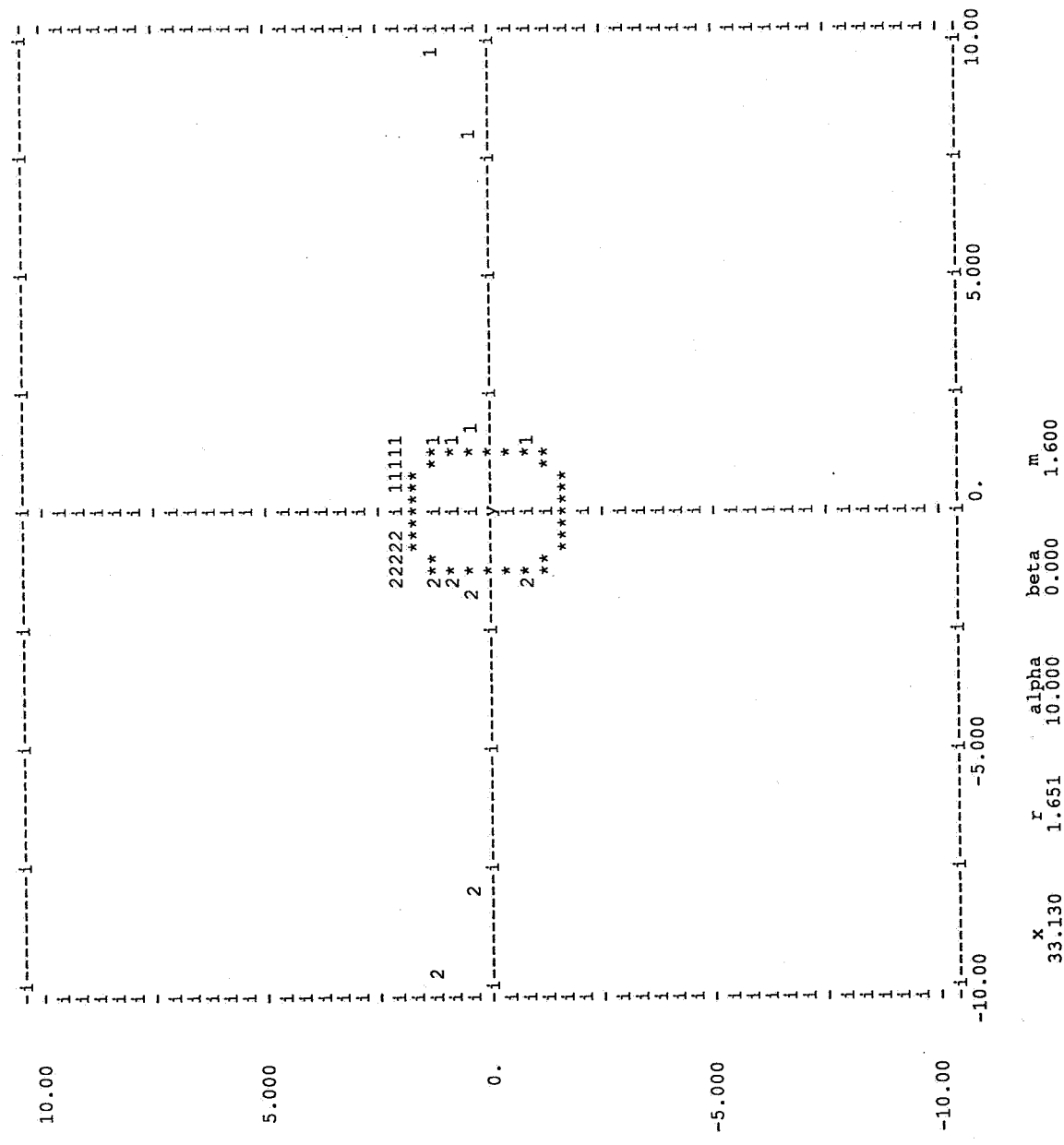
(au) Page 130

Figure 20.- Continued.

stratford separation criterion (laminar) f(s) =0.01511

summary of pressure distribution and separation points on body ...   x = 33.13

+y side:

	y	z	beta	arc	cp	cp'	dcp'/dx
stagnation pt.	0.000	-1.827	0.000	0.038	0.011		
min. pressure	0.000	0.000	0.000	0.000	0.000	0.000	0.000
separation	0.000	0.000	0.000	0.000	0.000	0.000	0.000

-y side:

	y	z	beta	arc	cp	cp'	dcp'/dx
stagnation pt.	-1.374	0.369	254.980	0.038	-0.008		
min. pressure	0.000	0.000	0.000	0.000	0.000	0.000	0.000
separation	0.000	0.000	0.000	0.000	0.000	0.000	0.000

separation not found at x = 33.130

centroid of vorticity

	gam/v	y	z
+y body:	0.05552	1.51522	-0.82475
-y body:	-0.05552	-1.51522	-0.82475

(av) Page 131

Figure 20.- Continued.

```
************************************** contribution of afterbody section to total loads ****************************************************

strengths and positions of vortices at end of nose section

          a =  1.5000

            gamma/2piva      y0/a       z0/a
      1        0.00589       1.0101     -0.5498
      1       -0.00589      -1.0101     -0.5498


              force and moment coefficients

                 bernoulli loading pressure

         unrolled body coordinates      rolled body coordinates

   cx          0.00000                     0.00000
   cz          0.00504                     0.00504
   cy          0.00000                     0.00000
   cm         -0.00341                    -0.00341
   cln         0.00000                     0.00000
   cll         0.00000                     0.00000


              (aw) Page 131
         Figure 20.- Continued.
```

step 4   loads on tail-finned section with effects of upstream vorticity

```
$input  b2=    4.00000, b2v=  0.,  crp=    5.33200, crpv=   0., delr=   0., dell=
0., delu=   0., deld=  0.,  fac=    0.950000, fkle=    0.500000, fksc=   0., dell=  0.500000
, lvswp=  0,  mswr=  6,  mswl=  0,  mswu=  0,  mswd=  0,  ncw=  4, ncwt=   0, nout=
0    0    0   1,  npr=   0, ntdat=  0,  ntpr=    0, n2dprf=  0, phidih=  0., phifr=
0., phifl=   0.,  phifu=   90.0000, phifd=   90.0000, swlep=   44.0000
, swlev=  0.,  swtep= -5.76000, swtcv=  0., thetlt=  0., thetit=  0., thetr=   0., thetl=
0., thetu=   90.0000, thetd= -1.50000, tolfac=   90.0000, xlebip=   1.00000, thetl=   33.1300
, ybod=  1.50000  -1.50000  0.   0.,  zbod=  0.   0.   0.   0.
$end
```

(ax) Page 132

Figure 20.- Continued.

```
                 fin section input geometry description

           fin property                fin 1 or r    fin 2 or l    fin 3 or u    fin 4 or d

no. of panels - spanwise        (msw) =      6            0             0            0
root chord                       (cr) =    5.332        5.332        0.000        0.000
leading edge sweep             (swle) =   44.000       44.000        0.000        0.000
trailing edge sweep            (swte) =   -5.760       -5.760        0.000        0.000
exposed semispan                 (b2) =    4.000        4.000        0.000        0.000
fin dihedral                   (phif) =    0.000        0.000       90.000       90.000
body angle of fin attachment   (thet) =    0.000        0.000       90.000       90.000
fin deflection                  (del) =    0.000        0.000        0.000        0.000
y-intersection of fin to body (ybod) =    1.500       -1.500        0.000        0.000
z-intersection of fin to body (zbod) =    0.000        0.000        0.000        0.000
axial location of section le  (xwle) =   33.130        0.000

         interdigitated fin angles
        phidih       thetit
          0.           0.
```

(ay) Page 133

Figure 20.- Continued.

- 148 -

length of body influenced by fins

x of wing leading-edge   (xlebip) =   33.130
x of wing trailing-edge   (xtebip) =   38.462
length of interference shell   (bil)   =   5.332
ring of corner coordinates at leading edge   (ircle) = 20
ring of corner coordinates at trailing edge   (ircte) = 24
ring of panels behind leading edge   (irple) = 20
ring of panels ahead of trailing edge   (irpte) = 23
first panel in interference shell   (ipanle) =267
last panel in interference shell   (ipantc) =322
body segment containing leading-edge   (isecle) = 1
body segment containing trailing-edge   (isecte) = 1

(az) Page 134

Figure 20.- Continued.

- 149 -

triplet-induced velocities at fin control points

i	x	y	z	bdu	bdv	bdw
1	1.50946	1.84127	0.00000	0.00073	-0.00129	0.08162
2	2.75147	1.84127	0.00000	0.00033	-0.00013	0.08288
3	3.99347	1.84127	0.00000	0.00012	-0.00025	0.08365
4	5.23548	1.84127	0.00000	0.00028	-0.00016	0.08473
5	1.98533	2.50926	0.00000	0.00001	-0.00041	0.05724
6	3.04922	2.50926	0.00000	0.00046	-0.00073	0.05900
7	4.11311	2.50926	0.00000	0.00011	-0.00037	0.06012
8	5.17700	2.50926	0.00000	0.00045	-0.00066	0.06013
9	2.46157	3.17778	0.00000	-0.00024	-0.00024	0.03884
10	3.34721	3.17778	0.00000	-0.00066	-0.00122	0.03959
11	4.23284	3.17778	0.00000	0.00022	-0.00063	0.04044
12	5.11848	3.17778	0.00000	0.00004	-0.00034	0.04077
13	2.93847	3.84723	0.00000	0.00216	-0.00324	0.02714
14	3.64560	3.84723	0.00000	0.00034	-0.00084	0.02777
15	4.35274	3.84723	0.00000	0.00009	-0.00025	0.02807
16	5.05988	3.84723	0.00000	0.00031	-0.00075	0.02862
17	3.41669	4.51853	0.00000	-0.00016	-0.00048	0.01984
18	3.94483	4.51853	0.00000	-0.00011	-0.00040	0.01977
19	4.47297	4.51853	0.00000	0.00033	-0.00081	0.02019
20	5.00111	4.51853	0.00000	0.00060	-0.00117	0.02041
21	3.89821	5.19446	0.00000	0.00042	-0.00128	0.01522
22	4.24612	5.19446	0.00000	0.00000	-0.00061	0.01477
23	4.59403	5.19446	0.00000	0.00030	-0.00089	0.01457
24	4.94194	5.19446	0.00000	-0.00003	-0.00044	0.01474

(ba) Page 135

Figure 20.- Continued.

vortex-induced velocities at fin control points

	x	y	z	v	w
1	1.50946	1.84127	0.00000	0.01104	-0.19467
2	2.75147	1.84127	0.00000	0.01104	-0.19467
3	3.99347	1.84127	0.00000	0.01104	-0.19467
4	5.23548	1.84127	0.00000	0.01104	-0.19467
5	1.98533	2.50926	0.00000	0.01686	-0.14942
6	3.04922	2.50926	0.00000	0.01686	-0.14942
7	4.11311	2.50926	0.00000	0.01686	-0.14942
8	5.17700	2.50926	0.00000	0.01686	-0.14942
9	2.46157	3.17778	0.00000	0.01398	-0.13849
10	3.34721	3.17778	0.00000	0.01398	-0.13849
11	4.23284	3.17778	0.00000	0.01398	-0.13849
12	5.11848	3.17778	0.00000	0.01398	-0.13849
13	2.93847	3.84723	0.00000	0.01333	-0.14088
14	3.64560	3.84723	0.00000	0.01333	-0.14088
15	4.35274	3.84723	0.00000	0.01333	-0.14088
16	5.05988	3.84723	0.00000	0.01333	-0.14088
17	3.41669	4.51853	0.00000	0.01499	-0.15180
18	3.94483	4.51853	0.00000	0.01499	-0.15180
19	4.47297	4.51853	0.00000	0.01499	-0.15180
20	5.00111	4.51853	0.00000	0.01499	-0.15180
21	3.89821	5.19446	0.00000	0.01988	-0.17223
22	4.24612	5.19446	0.00000	0.01988	-0.17223
23	4.59403	5.19446	0.00000	0.01988	-0.17223
24	4.94194	5.19446	0.00000	0.01988	-0.17223

(bb) Page 136

Figure 20.- Continued.

velocities from constant-u panels

	fu	fv	fw
1	0.04231	-0.04086	-0.06060
1	0.04309	-0.03012	-0.06186
2	0.03770	-0.01630	-0.06263
3	0.03122	-0.00518	-0.06370
4	0.06288	-0.06072	-0.08147
5	0.04896	-0.03422	-0.08324
6	0.03914	-0.01692	-0.08435
7	0.03355	-0.00556	-0.08436
8	0.07304	-0.07053	-0.07400
9	0.05189	-0.03627	-0.07474
10	0.04389	-0.01898	-0.07559
11	0.03535	-0.00586	-0.07592
12	0.07319	-0.07068	-0.05991
13	0.05600	-0.03914	-0.06054
14	0.04600	-0.01989	-0.06084
15	0.03722	-0.00617	-0.06138
16	0.06087	-0.05878	-0.04169
17	0.05829	-0.04075	-0.04161
18	0.04495	-0.01944	-0.04204
19	0.03808	-0.00631	-0.04225
20	0.03183	-0.03074	-0.01663
21	0.04418	-0.03089	-0.01619
22	0.04532	-0.01960	-0.01599
23	0.03678	-0.00610	-0.01616

(bc) Page 138

Figure 20.- Continued.

****

aft of leading edge of finned section

j	theta, deg.	xw	yw	zw	utot	vtot	wtot	cp bern.	p/pinf. bern.
1	281.26617	1.26635	0.19411	-1.97444	-0.00357	0.02898	-0.19924	0.03651	1.06542
2	292.63074	1.26635	0.56911	-1.87396	-0.00362	0.08000	-0.16716	0.03145	1.05636
3	304.20093	1.26635	0.90533	-1.67985	-0.00302	0.09937	-0.11689	0.02333	1.04181
4	316.10214	1.26635	1.17985	-1.40533	-0.00235	0.08472	-0.06680	0.01635	1.02929
5	328.48996	1.26635	1.37397	-1.06912	-0.00275	0.03369	-0.05928	0.02163	1.03876
6	341.56506	1.26635	1.47444	-0.69412	-0.01787	-0.11863	-0.28288	0.04001	1.07169
7	360.00000	1.26635	1.50000	-0.25000	-0.03071	-0.01869	-0.14928	0.09391	1.16828
8	18.43495	1.26635	1.47444	0.25000	-0.03150	-0.04694	-0.19008	-0.03456	0.93807
9	31.51003	1.26635	1.37396	0.69412	0.01827	0.06851	-0.24523	-0.01581	0.97167
10	43.89785	1.26635	1.17985	1.06912	-0.00263	0.03644	-0.15818	-0.02376	1.04258
11	55.79908	1.26635	0.90533	1.40533	0.00164	0.01526	-0.15195	0.02665	1.04776
12	67.36928	1.26635	0.56911	1.67985	0.00113	0.03189	-0.18726	0.02719	1.04873
13	78.73383	1.26635	0.56911	1.87397	0.00074	-0.03813	-0.24416	0.02258	1.04047
14	90.00000	1.26635	0.19411	1.97444	0.00121	-0.01569	-0.26248	0.01987	1.03561
...									
56	90.00000	5.26535	0.19411	1.97444	0.02163	-0.01057	-0.26316	-0.02076	0.96279

(bd) Pages 139 and 140
Figure 20.- Continued.

integration of the bernoulli pressure distribution

mach = 1.6000   alphac= 10.0000   phir= 0.0000

refs= 159.9984   refl= 9.1760

xm = 25.1500   zm = 0.0000

point	xb	yb	zb	cp	cx *sref	cy *sref	cz *sref	cm *sref*refl	cln *sref*refl	cll *sref*refl
1	33.79650	0.19411	-1.97444	0.03651	0.00000	-0.00249	0.01889	-0.16337	0.02151	0.00124
2	33.79650	0.56911	-1.87396	0.03145	0.00000	-0.00628	0.01517	-0.13113	0.05432	0.00314
3	33.79650	0.90533	-1.67985	0.02333	0.00000	-0.00741	0.00966	-0.08353	0.06410	0.00371
4	33.79650	1.17985	-1.40533	0.01635	0.00000	-0.00677	0.00519	-0.04491	0.05853	0.00338
5	33.79650	1.37397	-1.06912	0.02163	0.00000	-0.01043	0.00432	-0.03736	0.09019	0.00522
6	33.79650	1.47444	-0.69412	0.04001	0.00000	-0.02070	0.00273	-0.02357	0.17901	0.01035
7	33.79650	1.50000	-0.25000	0.09391	0.00000	-0.06259	0.00000	0.00000	0.54116	0.01565
8	33.79650	1.50000	0.25000	-0.03456	0.00000	0.02303	0.00000	0.00000	-0.19917	0.00576
9	33.79650	1.47444	0.69412	-0.01581	0.00000	0.00818	-0.00108	-0.00931	-0.07075	0.00409
10	33.79650	1.37396	1.06912	0.02376	0.00000	-0.01146	-0.00475	0.04104	0.09907	-0.00573
11	33.79650	1.17985	1.40533	0.02665	0.00000	-0.01104	-0.00847	0.07323	0.09543	-0.00552
12	33.79650	0.90533	1.67985	0.02719	0.00000	-0.00864	-0.01126	0.09737	0.07471	-0.00432
13	33.79650	0.56911	1.87397	0.02258	0.00000	-0.00451	-0.01089	0.09417	0.03901	-0.00226
14	33.79650	0.19411	1.97444	0.01987	0.00000	-0.00135	-0.01028	0.08893	0.01171	-0.00068
. . .										
56	37.79550	0.19411	1.97444	-0.02076	0.00000	0.00141	0.01075	-0.13589	-0.01789	0.00071

(be) Pages 140 and 141

Figure 20.- Continued.

```
body loads on ring   20   at x=  33.79650

                    bernoulli loading

   rolled body-axis coordinates      unrolled body-axis coordinates

cx      0.00000                         0.00000
cy      0.00000                         0.00000
cz      0.00014                         0.00014
cll     0.00000                         0.00000
cm     -0.00013                        -0.00013
cln     0.00000                         0.00000

. . .

body loads on ring   23   at x=  37.79550

                    bernoulli loading

   rolled body-axis coordinates      unrolled body-axis coordinates

cx      0.00000                         0.00000
cy      0.00000                         0.00000
cz      0.00246                         0.00246
cll     0.00000                         0.00000
cm     -0.00340                        -0.00340
cln     0.00000                         0.00000

cumulative body loads to this station

                    bernoulli loading

   rolled body-axis coordinates      unrolled body-axis coordinates

cx      0.00000                         0.00000
cy      0.00000                         0.00000
cz      0.00512                         0.00512
cll     0.00000                         0.00000
cm     -0.00652                        -0.00652
cln     0.00000                         0.00000
```

(bf) Pages 141 and 142

Figure 20.- Continued.

velocities at fin panel centroid points

j	xbar(j)	ybar(j)	zbar(j)	uchk	vchk	wchk	bdv	bdw	vnor
1	0.95056	1.84127	0.00000	0.04231	-0.04086	-0.04650	0.00975	-0.11305	-0.15955
2	2.19257	1.84127	0.00000	0.04309	-0.03012	-0.06003	0.01091	-0.11178	-0.17181
3	3.43457	1.84127	0.00000	0.03770	-0.01630	-0.06017	0.01079	-0.11102	-0.17119
4	4.67657	1.84127	0.00000	0.03122	-0.00518	-0.06144	0.01088	-0.10994	-0.17139
5	1.50658	2.50926	0.00000	0.06288	-0.06072	-0.06186	0.01645	-0.09218	-0.15404
6	2.57047	2.50926	0.00000	0.04896	-0.03422	-0.08148	0.01613	-0.09041	-0.17189
7	3.63436	2.50926	0.00000	0.03914	-0.01692	-0.07980	0.01650	-0.08930	-0.16909
8	4.69825	2.50926	0.00000	0.03355	-0.00556	-0.07974	0.01620	-0.08929	-0.16903
9	2.06303	3.17778	0.00000	0.07304	-0.07053	-0.06376	0.01374	-0.09965	-0.16341
10	2.94867	3.17778	0.00000	0.05189	-0.03627	-0.06669	0.01276	-0.09890	-0.16559
11	3.83431	3.17778	0.00000	0.04389	-0.01898	-0.06942	0.01336	-0.09805	-0.16747
12	4.71994	3.17778	0.00000	0.03535	-0.00586	-0.07216	0.01364	-0.09772	-0.16988
13	2.62026	3.84723	0.00000	0.07319	-0.07068	-0.05820	0.01009	-0.11374	-0.17194
14	3.32739	3.84723	0.00000	0.05600	-0.03914	-0.05059	0.01249	-0.11311	-0.16370
15	4.03453	3.84723	0.00000	0.04600	-0.01989	-0.05731	0.01308	-0.11281	-0.17011
16	4.74166	3.84723	0.00000	0.03722	-0.00617	-0.05578	0.01258	-0.11226	-0.16804
17	3.17903	4.51853	0.00000	0.06087	-0.05878	-0.04562	0.01451	-0.13196	-0.17759
18	3.70717	4.51853	0.00000	0.05829	-0.04075	-0.03696	0.01459	-0.13203	-0.16899
19	4.23531	4.51853	0.00000	0.04495	-0.01944	-0.03541	0.01418	-0.13161	-0.16702
20	4.76345	4.51853	0.00000	0.03808	-0.00631	-0.03905	0.01382	-0.13140	-0.17045
21	3.74165	5.19446	0.00000	0.03183	-0.03074	-0.02299	0.01860	-0.15701	-0.18000
22	4.08956	5.19446	0.00000	0.04418	-0.03089	-0.02117	0.01927	-0.15746	-0.17863
23	4.43747	5.19446	0.00000	0.04532	-0.01960	-0.01533	0.01899	-0.15766	-0.17299
24	4.78538	5.19446	0.00000	0.03678	-0.00610	-0.00987	0.01944	-0.15749	-0.16736

(bg) Page 143

Figure 20.- Continued.

velocities at fin panel outboard aft corners

j	xrb(j)	yrc(j)	zrb(j)	uchk	vchk	wchk	bdv	bdw	vnor
1	1.79903	2.16667	0.00000	0.04231	-0.04086	-0.05090	0.00975	-0.11305	-0.16395
2	2.95427	2.16667	0.00000	0.04309	-0.03012	-0.06334	0.01091	-0.11178	-0.17513
3	4.10951	2.16667	0.00000	0.03770	-0.01630	-0.06792	0.01079	-0.11102	-0.17894
4	5.26475	2.16667	0.00000	0.03122	-0.00518	-0.07114	0.01088	-0.10994	-0.18109
5	2.26507	2.83333	0.00000	0.06288	-0.06072	-0.06611	0.01645	-0.09218	-0.15828
6	3.24255	2.83333	0.00000	0.04896	-0.03422	-0.06981	0.01613	-0.09041	-0.16023
7	4.22003	2.83333	0.00000	0.00000	-0.01044	-0.07082	0.01650	-0.08930	-0.16012
8	5.19750	2.83333	0.00000	0.03355	-0.00556	-0.07293	0.01620	-0.08929	-0.16222
9	2.73110	3.50000	0.00000	0.00000	-0.01947	-0.05360	0.01374	-0.09965	-0.15325
10	3.53082	3.50000	0.00000	0.00000	-0.01384	-0.05923	0.01276	-0.09890	-0.15813
11	4.33054	3.50000	0.00000	0.00000	-0.01170	-0.05704	0.01336	-0.09805	-0.15510
12	5.13026	3.50000	0.00000	0.03535	-0.00586	-0.06250	0.01364	-0.09772	-0.16022
13	3.19713	4.16667	0.00000	0.07319	-0.07068	-0.05883	0.01009	-0.11374	-0.17257
14	3.81909	4.16667	0.00000	0.05600	-0.03914	-0.04836	0.01249	-0.11311	-0.16147
15	4.44105	4.16667	0.00000	0.00000	-0.01227	-0.04377	0.01308	-0.11281	-0.15658
16	5.06301	4.16667	0.00000	0.03722	-0.00617	-0.02386	0.01258	-0.11226	-0.13612
17	3.66316	4.83333	0.00000	0.00000	-0.01623	-0.01591	0.01451	-0.13196	-0.14787
18	4.10736	4.83333	0.00000	0.00000	-0.01554	-0.03874	0.01459	-0.13203	-0.17078
19	4.55156	4.83333	0.00000	0.00000	-0.01199	-0.02402	0.01418	-0.13161	-0.15563
20	4.99576	4.83333	0.00000	0.03808	-0.00631	-0.00400	0.01382	-0.13140	-0.15540
21	4.12920	5.50000	0.00000	0.00000	-0.00849	-0.00159	0.01860	-0.15701	-0.15860
22	4.39564	5.50000	0.00000	0.04418	-0.03089	-0.02396	0.01927	-0.15746	-0.18142
23	4.66208	5.50000	0.00000	0.04532	-0.01960	-0.02492	0.01899	-0.15766	-0.18258
24	4.92852	5.50000	0.00000	0.03678	-0.00610	-0.01188	0.01944	-0.15749	-0.16937

(bh) Page 144
Figure 20.- Continued.

velocities and bernoulli pressures at control points immediately above and below fin surface

j	x(j)	y(j)	z(j)	utota	vtota	wtota	pressa	utotb	vtotb	wtotb	pressb
1	1.509465	1.841271	0.000000	0.043041	-0.031107	-0.173648	-0.055360	-0.041581	0.050612	-0.173648	0.115399
2	2.751468	1.841271	0.000000	0.043416	-0.019213	-0.173648	-0.055521	-0.042761	0.041029	-0.173648	0.118955
3	3.993472	1.841271	0.000000	0.037824	-0.005516	-0.173648	-0.044479	-0.037585	0.027092	-0.173648	0.108874
4	5.235476	1.841271	0.000000	0.031503	-0.005704	-0.173648	-0.032233	-0.030937	0.016055	-0.173648	0.095162
5	1.985328	2.509261	0.000000	0.062887	-0.044265	-0.173648	-0.093432	-0.062866	0.077174	-0.173648	0.157846
6	3.049219	2.509261	0.000000	0.049420	-0.018091	-0.173648	-0.066878	-0.048491	0.050353	-0.173648	0.130401
7	4.113109	2.509261	0.000000	0.039250	-0.000429	-0.173648	-0.047195	-0.039029	0.033420	-0.173648	0.111546
8	5.177000	2.509261	0.000000	0.034008	-0.010636	-0.173648	-0.037178	-0.033100	0.021761	-0.173648	0.099542
9	2.461568	3.177780	0.000000	0.072793	-0.056790	-0.173648	-0.112552	-0.073279	0.084270	-0.173648	0.179517
10	3.347205	3.177780	0.000000	0.052544	-0.023510	-0.173648	-0.072965	-0.051232	0.049034	-0.173648	0.136529
11	4.232841	3.177780	0.000000	0.044113	-0.005625	-0.173648	-0.056537	-0.043675	0.032336	-0.173648	0.121669
12	5.118478	3.177780	0.000000	0.035387	-0.007780	-0.173648	-0.039800	-0.035304	0.019498	-0.173648	0.104372
13	2.938469	3.847226	0.000000	0.075347	-0.060586	-0.173648	-0.117517	-0.071029	0.080767	-0.173648	0.175218
14	3.645605	3.847226	0.000000	0.056338	-0.026653	-0.173648	-0.080203	-0.055654	0.051634	-0.173648	0.145897
15	4.352740	3.847226	0.000000	0.045905	-0.006808	-0.173648	-0.059962	-0.046095	0.032973	-0.173648	0.126871
16	5.059875	3.847226	0.000000	0.037526	-0.006415	-0.173648	-0.043914	-0.036912	0.018754	-0.173648	0.107859
17	3.416690	4.518526	0.000000	0.060712	-0.044270	-0.173648	-0.089427	-0.061029	0.073294	-0.173648	0.154497
18	3.944830	4.518526	0.000000	0.058186	-0.026155	-0.173648	-0.083618	-0.058397	0.055342	-0.173648	0.151453
19	4.472970	4.518526	0.000000	0.045284	-0.005262	-0.173648	-0.058763	-0.044625	0.033615	-0.173648	0.123629
20	5.001111	4.518526	0.000000	0.038681	-0.007507	-0.173648	-0.046154	-0.037479	0.020132	-0.173648	0.109019
21	3.898213	5.194460	0.000000	0.032255	-0.012137	-0.173648	-0.033805	-0.031411	0.049345	-0.173648	0.093739
22	4.246122	5.194460	0.000000	0.044181	-0.011619	-0.173648	-0.056762	-0.044185	0.050152	-0.173648	0.121080
23	4.594031	5.194460	0.000000	0.045620	-0.000606	-0.173648	-0.059378	-0.045021	0.038589	-0.173648	0.124075
24	4.941941	5.194460	0.000000	0.036753	0.013344	-0.173648	-0.042553	-0.036806	0.025538	-0.173648	0.107290

(bi) Page 146

Figure 20.- Continued.

pressure loadings at control points

j	x(j)	y(j)	z(j)	deltp,lin.	deltp,bern.
1	1.509465	1.841271	0.000000	0.169244	0.170760
2	2.751468	1.841271	0.000000	0.172355	0.174476
3	3.993472	1.841271	0.000000	0.150818	0.153353
4	5.235476	1.841271	0.000000	0.124881	0.127396
5	1.985328	2.509261	0.000000	0.251506	0.251278
6	3.049219	2.509261	0.000000	0.195821	0.197279
7	4.113109	2.509261	0.000000	0.156557	0.158742
8	5.177000	2.509261	0.000000	0.134215	0.136721
9	2.461568	3.177780	0.000000	0.292145	0.292069
10	3.347205	3.177780	0.000000	0.207553	0.209494
11	4.232841	3.177780	0.000000	0.175577	0.178205
12	5.118478	3.177780	0.000000	0.141381	0.144172
13	2.938469	3.847226	0.000000	0.292751	0.292735
14	3.645605	3.847226	0.000000	0.223984	0.226100
15	4.352740	3.847226	0.000000	0.184000	0.186833
16	5.059875	3.847226	0.000000	0.148875	0.151773
17	3.416690	4.518526	0.000000	0.243482	0.243924
18	3.944830	4.518526	0.000000	0.231165	0.235070
19	4.472970	4.518526	0.000000	0.179817	0.182392
20	5.001111	4.518526	0.000000	0.152320	0.155173
21	3.898213	5.194460	0.000000	0.127332	0.127545
22	4.246122	5.194460	0.000000	0.176731	0.177842
23	4.594031	5.194460	0.000000	0.181283	0.183453
24	4.941941	5.194460	0.000000	0.147118	0.149843

(bj) Page 147
Figure 20.- Continued.

fin loading information

```
          mach number =  0.16000E+01
      angle of attack =  10.000 degrees
      side slip angle =   0.000 degrees
             fin area =  25.59104
       reference area = 159.99840
     reference length =   9.17600
   exposed fin span b/2=  4.00000
   moment center:  xm =  25.15000
                   zm =   0.00000
```

linear pressure (u/vinf) loads in body system

	total	fin 1 or r	fin 2 or l	fin 3 or u	fin 4 or d
defl. angle deg. =		0.00000	0.00000	0.00000	0.00000
cthr =	0.17057E-03	0.85287E-04	0.85287E-04	0.	0.
cz =	0.29505E-01	0.14752E-01	0.14752E-01	0.	0.
cy =	0.	0.	0.	0.	0.
cm =	-0.35890E-01	-0.17945E-01	-0.17945E-01	0.	0.
cln =	0.	0.	0.	0.	0.
cll =	0.	-0.50559E-02	0.50559E-02	0.	0.
czft =		0.14752E-01	0.14752E-01	0.	0.
cyft =		0.	0.	0.	0.
cmft =		-0.17945E-01	-0.17945E-01	0.	0.
clnft =		0.	0.	0.	0.
cllft =		-0.50559E-02	0.50559E-02	0.	0.

following are in unrolled body-axis coordinate system

	total	fin 1 or r	fin 2 or l	fin 3 or u	fin 4 or d
czu =	0.29505E-01	0.14752E-01	0.14752E-01	0.	0.
cyu =	0.	0.	0.	0.	0.
cmu =	-0.35890E-01	-0.17945E-01	-0.17945E-01	0.	0.
clnu =	0.	0.	0.	0.	0.
czftu =		0.	0.	0.	0.
cyftu =		0.	0.	0.	0.
cmftu =		-0.17945E-01	-0.17945E-01	-0.17945E-01	0.

note: l.e. of lead panel in first chordwise row is supersonic

(bk) Page 148
Figure 20.- Continued.

spanwise distributions

---------------------------upper right or right horizontal fin---------------------------

i	y/(b/2)	cn*c/(2*b)	ct*c/(2*b)	cyl*c/(2*b)	cytot*c/(2*b)	cs*c/(2*b)	csint	ybar	gamnet(i)	gamma,le/vinf	xle
1	0.08532	0.04800	0.00000	0.00000	0.00000	0.00000	0.00000	0.00000	-0.38334	0.00000	0.32956
2	0.25232	0.04919	0.00000	0.00000	0.00000	0.00000	0.00000	0.00000	0.00000	0.00000	0.97463
3	0.41945	0.04536	0.00000	0.00000	0.00000	0.00000	0.00000	0.00000	0.00000	0.00000	1.62021
4	0.58681	0.03775	0.00000	0.00000	0.00000	0.00000	0.00000	0.00000	0.00000	0.00000	2.26669
5	0.75463	0.02695	0.00000	0.00000	0.00000	0.00000	0.00000	0.00000	0.00000	0.00000	2.91496
6	0.92361	0.01405	0.00000	0.00000	0.00000	0.00000	0.00000	0.00000	-1.26377	0.00000	3.56770
7	1.00000	0.00000	0.00000	0.00000	0.00000	0.00000	0.00000	0.00000			

thrust- and side-force coefficients in plane of the fin

sumfx =cx..acts on leading edge
sumfy1=cy..acts on leading edge
sumfy2=cy..acts on leading and side edge
sumft2=cy..acts on side edge

sumfx = 0.00000E+00
sumfy1 = 0.00000E+00
sumfy2 = 0.00000E+00
sumft2 = 0.20585E-04

side edge distribution

jtip	jse	distance from le /tipchord	suction force per unit length /(q*tipchord)	gamma,se /vinf	ybar	xse
1	1	0.25000	-0.01009	0.00000	0.00000	3.86276
	2	0.50000	0.01011	0.00000	0.00000	4.12920
	3	0.75000	0.01666	0.00000	0.00000	4.39564
	4	1.00000	-0.00508	0.00000	0.00000	4.66208

(bl) Page 149

Figure 20.- Continued.

fin panel forces

j	ycpt(j)	delta-cp	gamma/vinf	fx	fy1	fy2
1	1.84127	0.16924	0.10510	0.00198	0.00164	0.00000
2	1.84127	0.17235	0.10703	0.00026	0.00015	0.00000
3	1.84127	0.15082	0.09366	0.00031	0.00009	0.00000
4	1.84127	0.12488	0.07755	0.00023	0.00001	0.00000
5	2.50926	0.25151	0.13379	0.00350	0.00291	0.00000
6	2.50926	0.19582	0.10417	0.00024	0.00014	0.00000
7	2.50926	0.15656	0.08328	0.00051	0.00015	0.00000
8	2.50926	0.13421	0.07139	0.00044	0.00001	0.00000
9	3.17778	0.29214	0.12937	0.00177	0.00147	0.00000
10	3.17778	0.20755	0.09191	0.00099	0.00056	0.00000
11	3.17778	0.17558	0.07775	0.00064	0.00019	0.00000
12	3.17778	0.14138	0.06261	0.00031	0.00001	0.00000
13	3.84723	0.29275	0.10351	0.00024	0.00020	0.00000
14	3.84723	0.22398	0.07919	0.00105	0.00059	0.00000
15	3.84723	0.18400	0.06506	0.00031	0.00009	0.00000
16	3.84723	0.14887	0.05264	0.00039	0.00001	0.00000
17	4.51853	0.24348	0.06430	-0.00034	-0.00028	0.00000
18	4.51853	0.23316	0.06157	0.00038	0.00022	0.00000
19	4.51853	0.17982	0.04748	0.00042	0.00013	0.00000
20	4.51853	0.15232	0.04022	0.00017	0.00001	0.00000
21	5.19446	0.12733	0.02215	-0.00019	-0.00016	-0.00287
22	5.19446	0.17673	0.03074	-0.00020	-0.00012	0.00287
23	5.19446	0.18128	0.03153	-0.00003	0.00001	-0.00473
24	5.19446	0.14712	0.02559	0.00021	0.00001	-0.00144

(bm) Pages 149 and 150

Figure 20.- Continued.

- 162 -

fin loading information

```
      mach number =  0.16000E+01
   angle of attack = 10.000 degrees
   side slip angle =  0.000 degrees
          fin area = 25.59104
    reference area = 159.99840
  reference length =  9.17600
exposed fin span b/2=  4.00000
moment center:  xm = 25.15000
                zm =  0.00000
```

bernoulli pressure loads in body system

	total	fin 1 or r	fin 2 or l	fin 3 or u	fin 4 or d
defl. angle deg. =		0.00000	0.00000	0.00000	0.00000
cthr =	0.17057E-03	0.85287E-04	0.85287E-04	0.	0.
cz =	0.29801E-01	0.14900E-01	0.14900E-01	0.	0.
cy =	0.	0.	0.	0.	0.
cm =	-0.36268E-01	-0.18134E-01	-0.18134E-01	0.	0.
cln =	0.	0.	0.	0.	0.
cll =	0.	-0.51049E-02	0.51049E-02	0.	0.
czft =	0.	0.14900E-01	0.14900E-01	0.	0.
cyft =	0.	0.	0.	0.	0.
cmft =	0.	-0.18134E-01	-0.18134E-01	0.	0.
clnft =	0.	0.	0.	0.	0.
cllft =	0.	-0.51049E-02	0.51049E-02	0.	0.

following are in unrolled body-axis coordinate system

	total	fin 1 or r	fin 2 or l	fin 3 or u	fin 4 or d
czu =	0.29801E-01	0.14900E-01	0.14900E-01	0.	0.
cyu =	0.	0.	0.	0.	0.
cmu =	-0.36268E-01	-0.18134E-01	-0.18134E-01	0.	0.
clnu =	0.	0.	0.	0.	0.
czftu =	0.	0.	0.	0.	0.
cyftu =	0.	0.	0.	-0.18134E-01	0.
cmftu =	0.	0.	0.	0.	0.

note: l.e. of lead panel in first chordwise row is supersonic

(bn) Page 151

Figure 20.- Continued.

spanwise distributions

-------------upper right or right horizontal fin-------------

i	y/(b/2)	cn*c/(2*b)	ct*c/(2*b)	cyl*c/(2*b)	cytot*c/(2*b)	cs*c/(2*b)	csint	ybar	gamnet(i)	gamma,le/vinf	xle
1	0.08532	0.04867	0.00000	0.00000	0.00000	0.00000	0.00000	0.00000	-0.38334	0.00000	0.32956
2	0.25232	0.04959	0.00000	0.00000	0.00000	0.00000	0.00000	0.00000	0.00000	0.00000	0.97463
3	0.41945	0.04576	0.00000	0.00000	0.00000	0.00000	0.00000	0.00000	0.00000	0.00000	1.62021
4	0.58681	0.03809	0.00000	0.00000	0.00000	0.00000	0.00000	0.00000	0.00000	0.00000	2.26669
5	0.75463	0.02721	0.00000	0.00000	0.00000	0.00000	0.00000	0.00000	0.00000	0.00000	2.91496
6	0.92361	0.01418							0.00000		3.56770
7	1.00000	0.00000							-1.26377		

thrust- and side-force coefficients in plane of the fin

sumfx =cx..acts on leading edge
sumfy1=cy..acts on leading edge
sumfy2=cy..acts on leading and side edge
sumft2=cy..acts on side edge

sumfx = 0.00000E+00
sumfy1 = 0.00000E+00
sumfy2 = 0.00000E+00
sumft2 = 0.20585E-04

side edge distribution

jtip	jse	distance from le /tipchord	suction force per unit length /(q*tipchord)	gamma,se /vinf	ybar	xse
1	1	0.25000	-0.01009	0.00000	0.00000	3.86276
	2	0.50000	0.01011	0.00000	0.00000	4.12920
	3	0.75000	0.01666	0.00000	0.00000	4.39564
	4	1.00000	-0.00508	0.00000		4.66208

(bo) Page 152
Figure 20.- Continued.

fin panel forces

j	ycpt(j)	delta-cp	gamma/vinf	fx	fy1	fy2
1	1.84127	0.17076	0.10510	0.00198	0.00164	0.00000
2	1.84127	0.17448	0.10703	0.00026	0.00015	0.00000
3	1.84127	0.15335	0.09366	0.00031	0.00009	0.00000
4	1.84127	0.12740	0.07755	0.00023	0.00001	0.00000
5	2.50926	0.25128	0.13379	0.00350	0.00291	0.00000
6	2.50926	0.19728	0.10417	0.00024	0.00014	0.00000
7	2.50926	0.15874	0.08328	0.00051	0.00015	0.00000
8	2.50926	0.13672	0.07139	0.00044	0.00001	0.00000
9	3.17778	0.29207	0.12937	0.00177	0.00147	0.00000
10	3.17778	0.20949	0.09191	0.00099	0.00056	0.00000
11	3.17778	0.17821	0.07775	0.00064	0.00019	0.00000
12	3.17778	0.14417	0.06261	0.00031	0.00001	0.00000
13	3.84723	0.29273	0.10351	0.00024	0.00020	0.00000
14	3.84723	0.22610	0.07919	0.00105	0.00059	0.00000
15	3.84723	0.18683	0.06506	0.00031	0.00009	0.00000
16	3.84723	0.15177	0.05264	0.00039	0.00001	0.00000
17	4.51853	0.24392	0.06430	-0.00034	-0.00028	0.00000
18	4.51853	0.23507	0.06157	0.00038	0.00022	0.00000
19	4.51853	0.18239	0.04748	0.00042	0.00013	0.00000
20	4.51853	0.15517	0.04022	0.00017	0.00001	0.00000
21	5.19446	0.12754	0.02215	-0.00019	-0.00016	-0.00287
22	5.19446	0.17784	0.03074	-0.00020	-0.00012	-0.00287
23	5.19446	0.18345	0.03153	0.00003	0.00001	0.00473
24	5.19446	0.14984	0.02559	0.00021	0.00001	-0.00144

*****t.e. fin vorticity due to attached flow*****

ivrt	gamma/vinf (local fin)	y,c.g. (local fin)	y,c.g. (body axes)	z,c.g.
1	-0.00730	0.67526	2.17526	0.00000
2	0.39670	2.98581	4.48581	0.00000

(bp) Pages 152 and 153

Figure 20.- Continued.

```
                ***** summary of total loads *****

   alpha c =  10.00 deg.   phi =   0.000 deg.   mach =   1.60

      reference area = 160.00   reference length =    9.18


             bernoulli and/or shock expansion loading
                            pressure

   rolled body-axis coordinates       **        unrolled body-axis coordinates

   cxb     0.2408E-02                                 0.2408E-02
   czb     0.5380E+00                                 0.5380E+00
   cyb     0.1957E-08                                 0.1957E-08
   cmb    -0.4112E-01                                -0.4114E-01
   clnb   -0.3124E-08                                -0.3124E-08
   cllb   -0.3619E-09                                -0.3619E-09
```

(bq) Page 154

Figure 20.- Concluded.

- 166 -

REPORT DOCUMENTATION PAGE

Public reporting burden for this collection of information is estimated to average 1 hour per response, including the time for reviewing instructions, searching existing data sources, gathering and maintaining the data needed, and completing and reviewing the collection of information. Send comments regarding this burden estimate or any other aspect of this collection of information, including suggestions for reducing this burden, to Washington Headquarters Services, Directorate for Information Operations and Reports, 1215 Jefferson Davis Highway, Suite 1204, Arlington, VA 22202-4302, and to the Office of Management and Budget, Paperwork Reduction Project (0704-0188), Washington, DC 20503.

1. AGENCY USE ONLY *(Leave blank)*	2. REPORT DATE	3. REPORT TYPE AND DATES COVERED
		Contractor Report

4. TITLE AND SUBTITLE	5. FUNDING NUMBERS
Improvements to the Missile Aerodynamic Code DEMON3	C NAS1-17077
6. AUTHOR(S) Marnix F. E. Dillenius, David L. Johnson, and Daniel J. Lesieutre	WU 505-59-30-01

7. PERFORMING ORGANIZATION NAME(S) AND ADDRESS(ES)	8. PERFORMING ORGANIZATION REPORT NUMBER
Nielsen Engineering & Research, Inc. 510 Clyde Avenue Mountain View, CA 94043-2287	NEAR TR 435

9. SPONSORING / MONITORING AGENCY NAME(S) AND ADDRESS(ES)	10. SPONSORING / MONITORING AGENCY REPORT NUMBER
National Aeronautics and Space Administration Langley Research Center Hampton, VA 23665-5225	NASA CR-4432

11. SUPPLEMENTARY NOTES

Langley Technical Monitor: Jerry M. Allen
Final Report

12a. DISTRIBUTION / AVAILABILITY STATEMENT	12b. DISTRIBUTION CODE
Unclassified - Unlimited Subject Category 02	

13. ABSTRACT *(Maximum 200 words)*

Computer program DEMON3 was developed for the aerodynamic analysis of nonconventional supersonic configurations comprising a body with noncircular cross section and up to two wing or fin sections. Within a wing or fin section, the lifting surfaces may be in cruciform, triform, planar, or low profile layouts, and the planforms of the lifting surfaces allow for breaks in sweep. The body and the fin sections are modeled by triplet and constant u-velocity panels, respectively, accounting for mutual body-fin interference. Fin thickness effects are included. One of the unique features of DEMON3 is the modeling of high angle of attack vortical effects associated with the lifting surfaces and the body. In addition, shock expansion and Newtonian pressure calculation methods can be optionally engaged. These two-dimensional nonlinear methods are augmented by aerodynamic interference determined from the linear panel methods. Depending on geometric details of the body, the DEMON3 program can be used to analyze nonconvential configurations at angles of attack up to 25 degrees for Mach numbers from 1.1 to 6. Calculative results and comparisons with experimental data demonstrate the capabilities of DEMON3. Limitations and defficiencies are listed.

14. SUBJECT TERMS		15. NUMBER OF PAGES
wing-body-tail configurations panel methods noncircular body cross sections supersonic flow aerodynamic load distributions		168
		16. PRICE CODE A08

17. SECURITY CLASSIFICATION OF REPORT	18. SECURITY CLASSIFICATION OF THIS PAGE	19. SECURITY CLASSIFICATION OF ABSTRACT	20. LIMITATION OF ABSTRACT
Unclassified	Unclassified		